Austrian Society for ASEM Electron Microscopy

JOHANNES KEPLER UNIVERSITY LINZ

12th ASEM workshop on

Advanced Electron Microscopy

21st - 22nd April 2022
JKU Linz

Imprint
Published by Center for Surface and Nanoanalytics, JKU Linz, Altenberger Str. 69, 4040 Linz, Austria;
printed in 2351 Wr. Neudorf, Austria by Online Druck GmbH, Brown-Boveri-Straße 8, 2351 Wr. Neudorf, Austria

Organizing committee

- Priv. Doz. DI Dr. Heiko Groiß
- Dr. Alexey Minenkov
- Dr. Philipp Kürnsteiner

Christian Doppler Laboratory for Nanoscale Phase Transformations,
Center for Surface and Nanoanalytics, Johannes Kepler University Linz

- Elisabeth Mayrhofer

Center for Surface and Nanoanalytics, Johannes Kepler University Linz

- Dr. Philip Steiner
- Prof. Dr.in Susanna Zierler

Institute of Pharmacology, Faculty of Medicine, Johannes Kepler University Linz

Original graphical design and the booklet layout: Dr. Alexey Minenkov

12th ASEM workshop on

ADVANCED

ELECTRON MICROSCOPY

21st – 22nd April 2022

Johannes Kepler University Linz

CONTENT

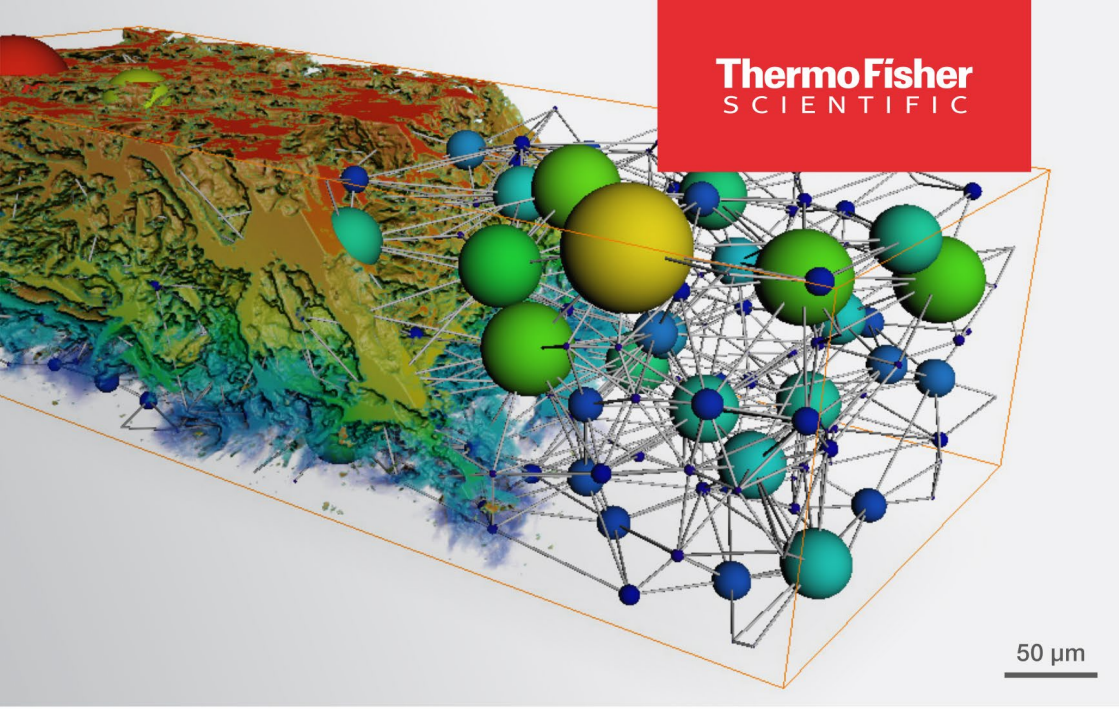

3D quantitative analysis of Li-ion battery graphite anode using the Helios 5 Laser PFIB and Avizo Software.

Helios 5 Laser PFIB

Fastest high-quality subsurface and 3D characterization at millimeter scale with nanometer resolution

The Thermo Scientific™ Helios™ 5 Laser PFIB delivers unmatched capabilities for extreme large-volume 3D analysis, Ga-free sample preparation, and precise micromachining.

Featuring an innovative, fully integrated femtosecond laser, it offers the fastest material removal rate with the highest cut face quality.

Learn more at **thermofisher.com/heliospfib**

thermo scientific

CONFERENCE INFORMATION

We welcome you for the first time to the **12th workshop of the Austrian Society for Electron Microscopy (ASEM)** at the **Johannes Kepler University (JKU) Linz**. Since the last ASEM workshop was held as an on-site event in 2019, everyone is surely happy that this year we can meet in the real world again. Let's take the chance to discuss a wide variety of electron microscopy topics during the talks and posters sessions, at the sponsors' booths, and, particularly, during the coffee breaks and the social events.

Here is some practical information:

Coronavirus Safety Protocols and Protective Measures at the JKU

Access to - and being present inside of - campus buildings is only permitted with proof of adherence to the "2.5G Rule" (PCR tested, vaccinated or recovered) which will be checked upon registration at the reception. **FFP2 (KN-95)** face masks are **mandatory** at the JKU inside the campus buildings. Detailed information can be found at https://www.jku.at/en/coronavirus-safety-protocols-and-protective-measures-at-the-jku/

Presenters' information

A Microsoft Windows laptop for PowerPoint and pdf-format will be provided. If you would like to use your own device, please make sure you carry the necessary adapters for VGA or HDMI. Laser pointer and microphones are available on-site. We kindly ask all presenters to upload and/or test their presentations/devices in the break prior to their time slot.

Poster presentation

Please mount your poster as soon as possible after your arrival and remove it only after the end of the workshop. Appropriate mounting material will be provided in the poster presenters hall and at the reception. A dedicated poster session is scheduled on Friday morning, but the posters are accessible during all coffee breaks.

Workshop Program

You can find all contributions to the workshop inside this booklet marked in the program with **orange** for **company contributions**, **green** for **life sciences** and **blue** for **materials science, physics and chemistry**.

The people at the reception will be happy to aid you with any further questions during the entire duration of the workshop.

Looking forward to fruitful discussions and a great 12th ASEM Workshop.

Your 12th ASEM Workshop 2022 Organization Team

JKU CAMPUS

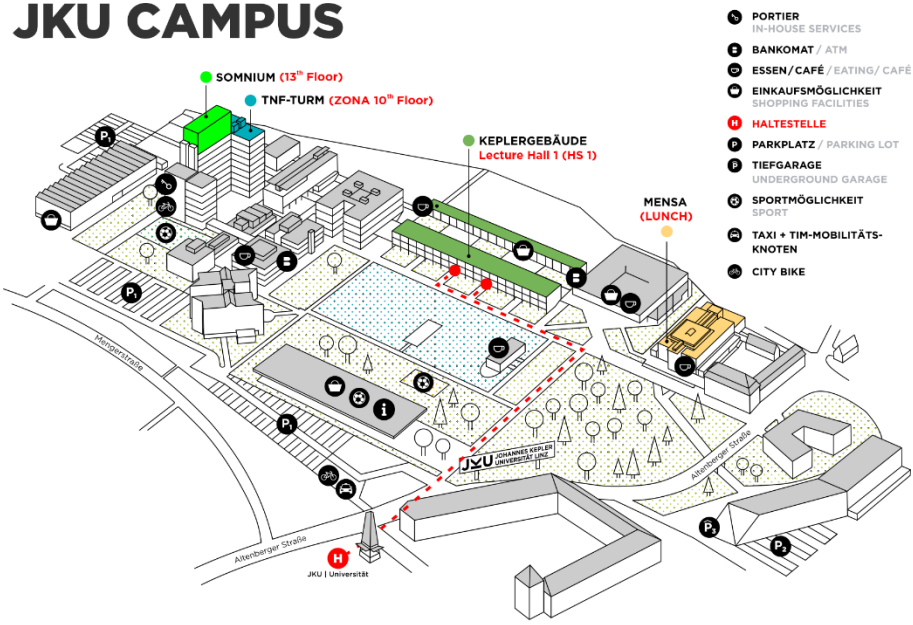

KEPLERGEBÄUDE

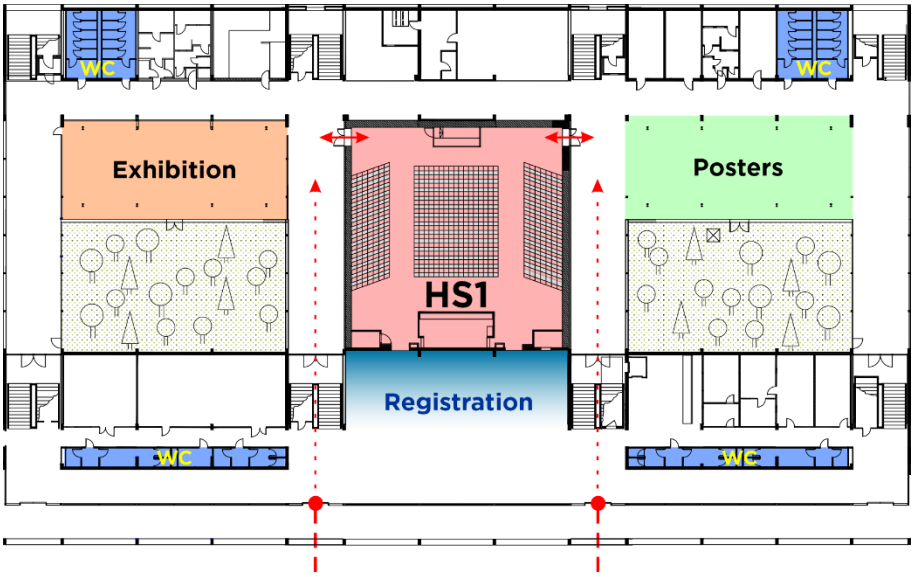

SOCIAL PROGRAM "VISITING MEDSPACE": Thursday 21st April

From the **green**-marked **Keplergebäude** where the **HS1** is located, follow the **red** line to the **„Universität" tram station**

Take the **tram (line 1 or 2)** to the **„Linke Brückenstraße"**tram station. From there you can continue by **bus (line 12 or 25)** to the **„Gruber-straße"** stop

The **bus stop** is on the right side of the **tram stop**. From the **„Gruberstraße"**bus stop you can walk to **Med Campus 1** in 2 minutes

PROGRAM

Thursday, April 21st, 2022

09:30		**REGISTRATION**	
12:30	SESSION 1	Opening ceremony	
12:45		**Lammer Judith** / FELMI-ZFE Graz *How an ASEM Workshop led to a successful quantification for atomic-scale EELS maps*	**8**
13:00		**Susi Toma** / Univerity of Vienna *abTEM: Transmission Electron Microscopy from First Principles*	**9**
13:15		**Steiner Philip** / Johannes Kepler University Linz *Pharmacological inhibition of TPC1 alters the ultrastructural basis for organellar interactions and plays an important role in allergic hypersensitivity*	**10**
13:30		**Käppeli Stephan** / Systron EMV GmbH *Magnetically Shielded Rooms for Electron Microscopy*	**11**
13:45		**Jäpel Tom** / TESCAN GmbH *High-performance laser-ablation/plasma-FIB large-scale cross-sectioning and 3D analysis*	**12**
14:00		**COFFEE BREAK**	
14:30	SESSION 2	**Radlinger Thomas** / FELMI-ZFE Graz *Imaging the magnetic domain structure of spinodal alloys using differential phase contrast STEM (DPC-STEM)*	**15**
14:45		**Chen Zhuo** / Erich Schmid Institute of Materials Science Leoben *TEM studies on intermixing of transition metal nitride superlattice triggered by nanoindentation*	**16**
15:00		**Seebauer Stefan** / TU Wien *Quantitative chemical analysis of the γ- and γ'-phases in nickel base superalloy PWA1483*	**17**
15:15		**Ploszczanski Leon** / University of Natural Resources and Life Sciences, BOKU *Why do Schwann cells like spider silk?*	**18**
15:30		**Bichler Bernhard** / VIDEKO GmbH *Broad Argon Ion Beam Milling Systems & SEM: A powerful alternative to FIB-SEM for wide cross sections and large-scale surface polishings*	**19**
15:45		**Phifer Daniel** / ThermoFisher Scientific *Swapping Ion Species with Plasma FIB to make better (S)TEM lamella*	**20**
16:00		**SHORT BREAK**	
16:15-17:00		**ASSEMBLY OF ASEM MEMBERS**	
17:30-18:30		**VISITING MEDSPACE**	
19:00		**CONFERENCE DINNER "STIEGL-KLOSTERHOF LINZ"**	

Friday, April 22nd, 2022

08:30		**EARLY MORNING COFFEE**	
09:00	SESSION 3	**Haselmann Ulrich** / Erich Schmid Institute of Materials Science Leoben *Defects and Dopant Gradients in Bismuth-Ferrite Thin Films*	24
09:15		**Sunkara Sowmya** / Medical University of Graz *Organotypic culture as an ex-vivo model to study Alzheimer's disease in brain*	25
09:30		**Grininger Christoph** / University of Graz *Electron crystallography – From small molecules to proteins*	26
09:45		**Smith Andrew Jonathan** / Kleindiek Nanotechnik GmbH *Enhanced in situ Applications using Micromanipulators and Nanopositioners*	27
10:00		**Schwinger Wolfgang** / Carl Zeiss GmbH *TEM-like Ultrastructure Imaging with a New Degree of Speed and Quality*	28
10:15		**POSTER SESSION**	
11:00	SESSION 4	*Invited Speaker*: **Minnich Bernd** / University of Salzburg *SEM & 3D-Morphometry in Vascular Biology: Vascular Corrosion Casting in Biomedicine and Zoology*	32
11:30		**Horák Michal** / University of Brno *Plasmon resonances in biocompatible nanoparticles*	34
11:45		**Joudi Wael** / University of Vienna *Correlated AFM/STEM study on the Mechanical Stiffness of Defect-Engineered Graphene*	35
12:00		**Frerichs Hajo** / Quantum Design Microscopy GmbH *Two Microscopes are better than One – In-situ Correlative Analysis by combination of AFM and SEM*	36
12:15		**LUNCH BREAK**	
13:15	SESSION 5	*Fritz Grasenick Laureate:* **Ederer Manuel** / TU Wien *Imaging the Spatial Distribution of Electronic States in Graphene Using Electron Energy-Loss Spectroscopy: Prospect of Orbital Mapping*	40
13:30		**Postl Andreas** / University of Vienna *Indirect measurement of the carbon adatom migration barrier on graphene*	42
13:45		**Preimesberger Alexander** / TU Wien *Discrimination of coherent and incoherent cathodoluminescence using temporal photon correlations*	43
14:00		**Kastenmüller Andreas** / AMETEK GmbH *Latest Development in EELS*	44
14:15		**Raggl Georg** / JEOL (Germany) GmbH *Integrated lasers and ultra-fast electrostatic beam blanking systems – Pathways to new experiments in modern transmission electron microscopy*	45
14:30		**COFFEE BREAK**	
14:45	SESSION 6	*Fritz Grasenick Laureate:* **Noisternig Stefan** / University of Vienna *In situ STEM analysis of electron beam induced chemical etching of an ultra-thin amorphous carbon foil by oxygen during high resolution scanning*	48
15:00		**Åhlgren E. Harriet** / University of Vienna *Electron microscopy in gas atmospheres: exploring the role of oxygen in the degradation of 2D materials*	50
15:15		**Šimić Nikola** / FELMI- ZFE Graz *Phase Analysis of (Li)FePO4 by Selected Area Electron Diffraction in Transmission Electron Microscopy*	51
15:30		**Huang Yong** / Erich Schmid Institute of Materials Science Leoben *Stacking faults dominant strengthening mechanism behind the anomalous hardness variation of TaN/TiN multilayer films*	52
15:45		Closing Ceremony and Farewell	

SYSTRON
MAGNETIC SHIELDING

Magnetically shielded TEM rooms

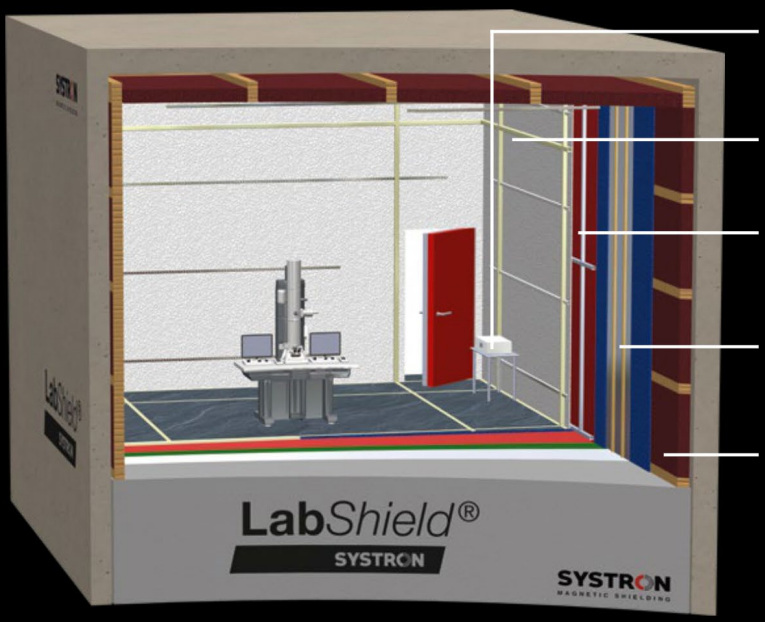

Active cancellation system

Inner room structure

DC Shielding & sub-construction

AC Shielding & sub-construction

Outer room structure

- Assessment of situation
- Development of concept with 3D FEM simulations
- Design and implementation of entire room
- Guaranteed performance

Systron EMV GmbH
CH-8635 Dürnten
D-91126 Schwabach
www.systronemv.com

Thursday, April 21st, 2022

SESSION 1

12:30	Opening Ceremony
12:45	**Lammer Judith** / FELMI-ZFE Graz *How an ASEM Workshop led to a successful quantification for atomic-scale EELS maps*
13:00	**Susi Toma** / Univerity of Vienna *abTEM: Transmission Electron Microscopy from First Principles*
13:15	**Steiner Philip** / Johannes Kepler University Linz *Pharmacological inhibition of TPC1 alters the ultrastructural basis for organellar interactions and plays an important role in allergic hypersensitivity*
13:30	**Käppeli Stephan** / Systron EMV GmbH *Magnetically Shielded Rooms for Electron Microscopy*
13:45	**Jäpel Tom** / TESCAN GmbH *High-performance laser-ablation/plasma-FIB large-scale cross-sectioning and 3D analysis*

How an ASEM Workshop led to a successful quantification for atomic-scale EELS maps

J. Lammer[1]*, S. Löffler[2], C. Berger[3], D. Knez[1], G. Haberfehlner[1], G. Kothleitner[1], F. Hofer[1], E. Bucher[3], W. Sitte[3], W. Grogger[1]

[1] *Graz Centre for Electron Microscopy (ZFE) & Institute of Electron Microscopy and Nanoanalysis (FELMI), Graz University of Technology*
[2] *University Service Centre for Transmission Electron Microscopy (USTEM), TU Wien*
[3] *Chair of Physical Chemistry, Montanuniversität Leoben*

With this abstract, we reflect on how ASEM workshops bring together researchers from different Austrian electron microscope facilities producing important scientific research results.

At the 9th ASEM workshop (2019) the corresponding author of this abstract, a dedicated PhD student, presented her work on elemental analyses at atomic resolution of the second order Ruddlesden-Popper ferrite $Ba_{1.1}La_{1.9}Fe_2O_7$. This ceramic exhibits promising properties for future applications in protonic ceramic fuel cells, electrolyser cells or membranes for hydrogen separation. Fundamental research on such materials is therefore needed in order to correlate mass and charge transport properties with the crystal structure of the material. At the particular time of the original presentation, we had already acquired high-resolution EDX and EELS maps of $Ba_{1.1}La_{1.9}Fe_2O_7$, which suggested that Ba and La were not equally distributed but have preferred crystal sites. Unfortunately, acquiring elemental maps at atomic-scale is always prone to channeling effects, which lead to additional intensity stemming from neighbouring atomic columns – a circumstance which renders a straightforward, reliable quantification impossible. After her presentation, an assistant professor and expert in EELS simulations from the USTEM (TU Wien) approached the speaker and offered to perform inelastic multislice simulations in order to overcome the problem with unknown neighbouring off-axis intensities. With sound knowledge of the channeling behavior, we then were able to paint a fuller picture, combining visually graspable, colourful EELS elemental maps and the actual composition of each atomic column. Through subtracting the additional off-axis intensity we successfully performed a column-by-column quantification for La and Ba [1]. The outcome of this collaboration will now be presented at this ASEM workshop.

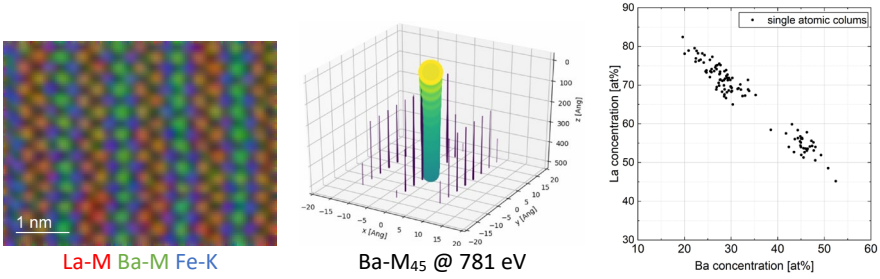

Figure 1. Left: Experimental EELS elemental map of barium lanthanum ferrate. Centre: simulated EELS Ba-M intensity showing contributions from on-axis atoms (green/yellow) and neighbouring atomic columns (blue/purple). Right: scatter plot of Ba and La concentrations per atomic column.

[1] J. Lammer, C. Berger, S. Löffler, et al., Ultramicroscopy, **234**, 11347 (2022)

*Corresponding author: judith.lammer@felmi-zfe.at

abTEM: Transmission Electron Microscopy from First Principles

J. Madsen, T. Susi*

University of Vienna, Faculty of Physics, Boltzmanngasse 5, 1090 Vienna, Austria

In many cases, the quantitative interpretation of TEM images requires simulations based on atomistic structure models. Image simulation has typically relied on the independent atom model (IAM) that neglects bonding effects, which are increasingly measurable and important [1]. Moreover, the recent rise in popularity of the four-dimensional (4D) scanning TEM has been partially due to promises of unprecedented sensitivity to electromagnetic fields [2]; however, such data call for rigorous theoretical interpretation through simulations.

Since all electrons and the nuclear cores contribute to the scattering potential, simulations that go beyond the IAM have relied on computationally highly demanding all-electron calculations. We have developed a method to generate *ab initio* electrostatic potentials when describing the core electrons by projector functions. Combined with an interface to quantitative image simulations, we can show an accuracy equivalent to earlier all-electron calculations at a much lower computational cost [3].

We have now implemented this method in a freely available open-source program based on Python, dubbed "abTEM" for *ab initio* Transmission Electron Microscopy [4]. abTEM integrates directly with two popular open-source Python codes: the Atomic Simulation Environment (ASE) for setting up atomistic models and GPAW for calculating electrostatic potentials based on the real-space projector-augmented wave density functional theory. Support for multiple GPUs and advanced parallelization has recently been added via dask [5].

We demonstrate the capabilities of our method by modeling twisted bilayer graphene for an interferometric 4D-STEM measurement [6]. This system requires on the order of a thousand atoms to represent in simulations, which, to our knowledge, is the largest system ever to be used in a quantitative electron microscopy image simulation that includes an accurate representation of bonding effects. Further, we show that abTEM simulations with a DFT potential can correctly describe experimental 4D-STEM ptychographic reconstructions of charge transfer effects in semiconducting WS2 and insulating hBN [7].

The abTEM code is freely available online at https://github.com/jacobjma/abTEM.

[1] J. Madsen, T.J. Pennycook, T. Susi, Ultramicroscopy, **231**, 113253 (2021)
[2] C. Ophus, Microscopy and Microanalysis, **25**, 563 (2017)
[3] T. Susi, et al., Ultramicroscopy, **197**, 16 (2019)
[4] J. Madsen and T. Susi, Open Res. Europe, **1**:24 (2021)
[5] Dask Development Team (2016). https://dask.org
[6] M.J. Zachman et al., Small, **17** (28), 2100388 (2021)
[7] J. Madsen, C. Hofer, T.C. Pekin, M. Schloz, T.A. Bui, C. Koch, T.J. Pennycook, T. Susi, *in preparation* (2022)

The authors acknowledge funding by the European Research Council (ERC) under the European Union's Horizon 2020 research and innovation programme (Grant agreement No. 756277-ATMEN), and computational resources by the Vienna Scientific Cluster (VSC).

* Corresponding author: toma.susi@univie.ac.at

Pharmacological inhibition of TPC1 alters the ultrastructural basis for organellar interactions and plays an important role in allergic hypersensitivity

P. Steiner[1*], A. Andosch[2], K. Oberascher[2], T. Gudermann[3], I. Boekhoff[3], H. Kerschbaum[2] and S. Zierler[1,3]

[1]*Institute of Pharmacology, Medical Faculty, Johannes Kepler University Linz, Austria*
[2]*Department of Biosciences, Paris Lodron University, Salzburg, Austria*
[3]*Walther Straub Institute of Pharmacology and Toxicology, Faculty of Medicine, Ludwig-Maximilians University Munich, Germany*

Basophilic granulocytes and primary mast cells are innate effector cells of allergic reactions. Previously, we reported that the two-pore channel, TPC1, plays an important role in the Ca^{2+} homeostasis of intracellular organelles, such as endolysosomes and the endoplasmic reticulum (ER) of rat basophilic leukemia cells (RBL-1) and murine mast cells [1]. Pharmacologic inhibition of TPC1 results in enhanced anaphylactic responses in mice. However, there is a lack of ultrastructural knowledge that underlies these processes. We have therefore implemented 2D and 3D transmission electron microscopic (TEM) methods to investigate the ultrastructure of RBL-1 controls in comparison to cells treated with the plant alkaloid tetrandrine. It was reported before that tetrandrine acts as an inhibitor of TPCs [2]. Our 2D TEM investigations with RBL-1 controls depicted that ER and endolysosomes form inter-organellar contact sites (**Figure 1**a; arrow). Moreover, 3D TEM tomography revealed the extent of the large contact surfaces between the two organelles (**Figure 1**b-c; arrows). In comparison, these contact surfaces decreased in cells, treated with tetrandrine. Moreover, it was observed that endolysosomes visibly enlarged after the tetrandrine treatment, which has recently been discussed in an osmotic context [3]. Here, we aim at a better understanding of the role of TPC channels in the regulation of the crosstalk between ER and endolysosomes at an ultrastructural level. Correlating our findings with analytical EM, as well as with molecular biological and immunological experiments could help clarify whether TPC channels are indeed promising pharmacological targets for the treatment of allergic hypersensitivity.

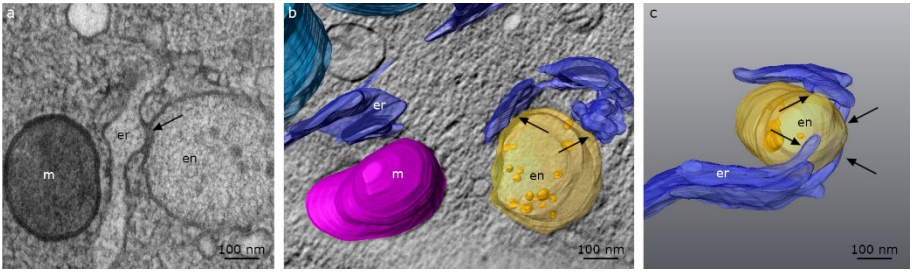

Figure 1. a) TEM micrograph of RBL-1 control. **b-c)** 3D TEM tomograms of RBL-1 controls. m: mitochondria; er: endoplasmic reticulum; en: endolysosomes; arrows: er and en contact sites / surfaces.

[1] E. Arlt, et al., PNAS, **117**, 18068 (2020)
[2] Y. Sakurai, et al., Science, **347**, 995 (2015)
[3] C. Chen, et al., BBA Mol Cell Res, **1868**, 118921 (2021)

* Corresponding author: philip.steiner@jku.at

Magnetically Shielded Rooms for Electron Microscopy

St. Kaeppeli*, B. de Boer

Systron EMV GmbH, Schoenbuehlstrasse 2, 8635 Duernten, Switzerland

High-resolution electron microscopes are very sensitive to interferences from environmental magnetic fields. Systron EMV GmbH provides with solutions to attenuate magnetic fields to acceptable levels even in magnetically challenging environments. Thus, best performance of the microscopes can be achieved. One project recently completed is the laboratory for a Krios G4 TEM at the Research Institute of Molecular Pathology (IMP) of the Vienna BioCenter.

The selected laboratory room was interfered by magnetic fields from various sources. Dominant were the DC-operated tramways and subways in close vicinity, causing slowly altering magnetic fields, so-called Near-DC fields. Sources inside the building (elevators and power supply) further increased the magnetic field levels. In total, the level of the varying fields added up to 1500 nT peak-to-peak measured prior to shielding. The aim for the microscope was to have a level of 10 nT peak-to-peak only.

The selected shielding concept Systron LabShield® combines two passive shielding layers with an active cancellation system. The purpose of the first passive shielding layer (Aluminum) is to reduce the 50 Hz magnetic fields and its harmonics, while the second consisting of Mu-metal is highly efficient against the Near-DC disturbances. The active cancellation system inside the room is reducing the residual magnetic field to its final level.

The concept was verified with aid of 3D-field simulations (Comsol Multiphysics) before implementation. For guaranteeing a smooth and timely assembly of the room interior, every detail was pre-designed with 3D CAD (SolidWorks) before the pre-fabrication in different workshops.

After proving that the remaining field variations were below 10 nT peak-to-peak, the microscope was released for installation (**Figure 1)**.

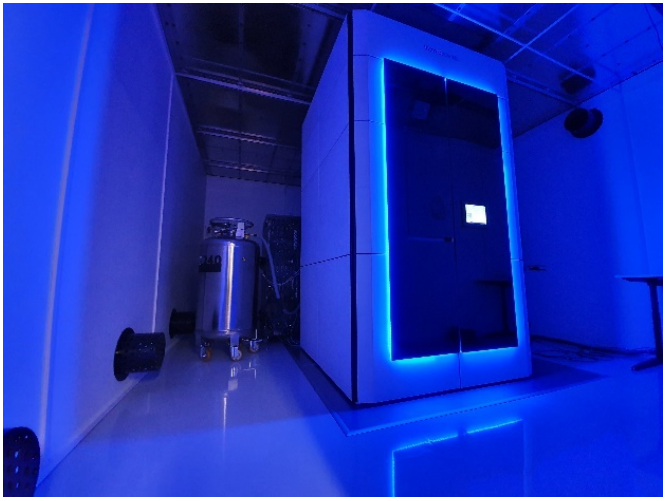

Figure 1. Magnetically shielded Krios G4 room at the Vienna BioCenter

* Corresponding author: stephan.kaeppeli@systronemv.com

High-performance laser-ablation/plasma-FIB large-scale cross-sectioning and 3D analysis

T. Jäpel[1*], R. D. Blando[2], T. Borůvka[3], J. Wissler[1], J. V. Oboňa[2], L. Hladík[2]

[1]*TESCAN GmbH, Zum Lonnenhohl 46, 44319 Dortmund, Germany*
[2]*TESCAN ORSAY HOLDING, a.s., Libušina třída 21, 623 00 Brno, Czech Republic*
[3]*TESCAN Brno s.r.o., Libušina třída 1, 623 00 Brno, Czech Republic*

TESCAN's Large Volume Workflow is a new high-throughput analysis method for synergetic parallel operation of tools with various analytical capabilities and processing speeds.
There are plenty of large-scale microstructure features in materials and high-volume components of modern semiconductors. Defects can happen in larger amounts for which microstructural failure analysis is needed. Features or defects can deeply be buried in the bulk material. An often-experienced commonality is that fast material removal is needed to reach deeply buried regions of interest.

The industrial-grade TESCAN **plasma-FIB** technology is a versatile, powerful large-scale tool. Still, large-scale FIB processes may take up to 20 hours. **Mechanical cutting** and polishing are hard to use for site specific preparation. It can still induce mechanical stresses or other defects. **Broad ion beam** treatment has been used for many years but lacks accurate site-specificity. Charging materials like **glass**, **polymers** or similar can also provide difficulties. Obtaining here good preparation results with a plasma-FIB in an acceptable timely fashion is challenging.

One way for improvement is the adjustment of plasma-FIB parameters. Increasing plasma beam currents is one of many possibilities for process acceleration; up to 3 µA for TESCAN. Another beneficial approach is laser ablation which provides vast-scale area ablation as separate process. In cooperation with 3D-Micromac laser ablation has been added to TESCANs plasma-FIB workflows. This lecture will show the benefits of the versatile, interoperable **standalone system-solution** combination for millimeter-wide vast and large-scale sample preparation and analysis in valuable synergy of plasma-FIB and laser ablation.

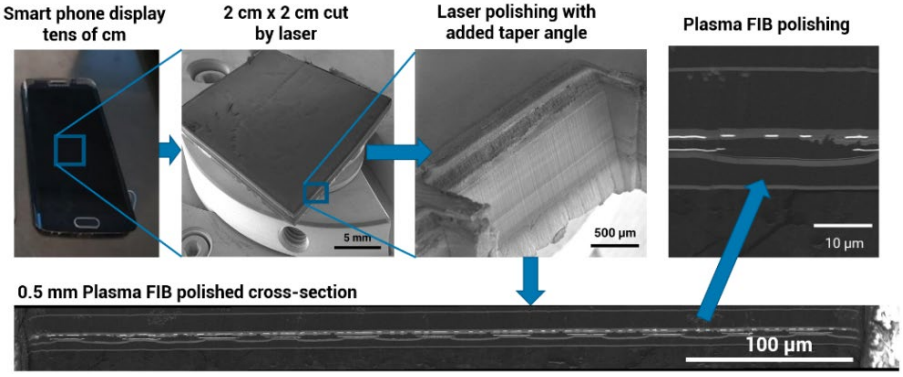

Figure 1. AMOLED display preparation example for a successful TESCAN Large Volume Workflow with more than 95% time saving compared to a sole plasma FIB preparation.

* Corresponding author: tom.jaepel@tescan.com

TESCAN Dynamic micro-CT

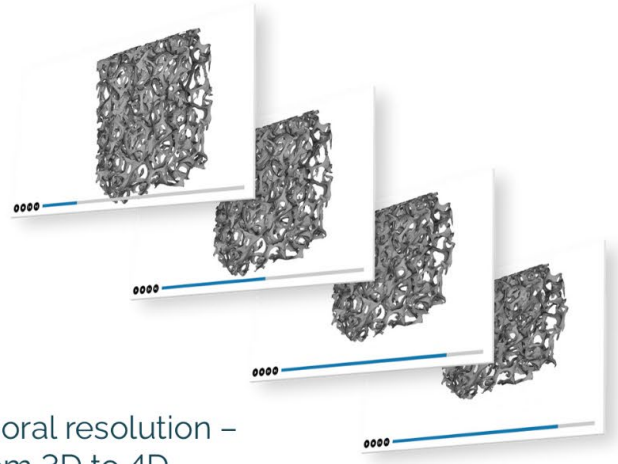

Leading the way in temporal resolution – shifting your research from 3D to 4D

Continuous Compression of 3D printed plastic parts – 5.9 sec/scan, 220 total scans

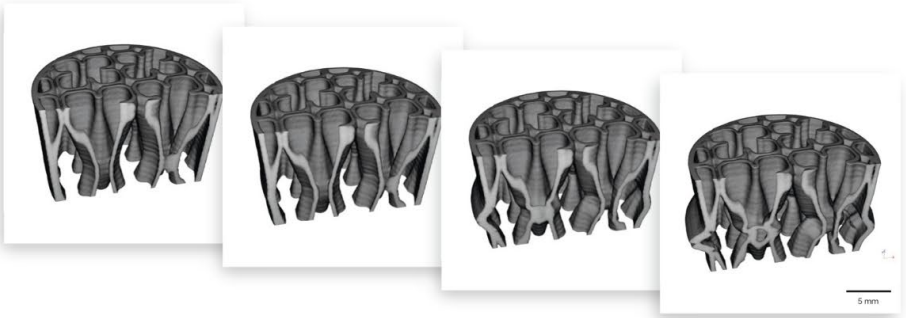

Dynamic Imaging of Dissolving Soap Bubbles - 30 sec/scan, 150 total scans

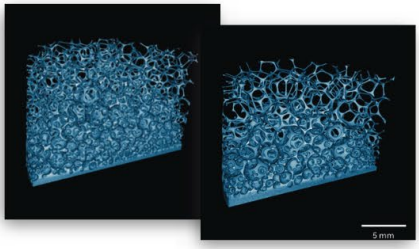

Analysis of Soap Bubble Coalescence

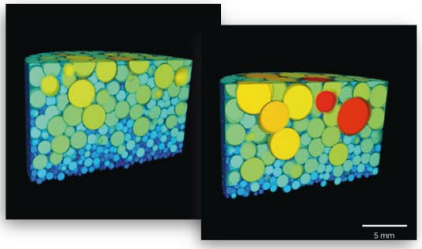

TESCAN

What can you do with Dynamic CT?
Contact us today to find out.

www.tescan.com

Thursday, April 21st, 2022

SESSION 2

14:30	**Radlinger Thomas** / FELMI-ZFE Graz *Imaging the magnetic domain structure of spinodal alloys using differential phase contrast STEM (DPC-STEM)*
14:45	**Chen Zhuo** / Erich Schmid Institute of Materials Science Leoben *TEM studies on intermixing of transition metal nitride superlattice triggered by nanoindentation*
15:00	**Seebauer Stefan** / TU Wien *Quantitative chemical analysis of the γ- and γ'-phases in nickel base superalloy PWA1483*
15:15	**Ploszczanski Leon** / University of Natural Resources and Life Sciences, BOKU *Why do Schwann cells like spider silk?*
15:30	**Bichler Bernhard** / VIDEKO GmbH *Broad Argon Ion Beam Milling Systems & SEM: A powerful alternative to FIB-SEM for wide cross sections and large-scale surface polishings*
15:45	**Phifer Daniel** / ThermoFisher Scientific *Swapping Ion Species with Plasma FIB to make better (S)TEM lamella*

Imaging the magnetic domain structure of spinodal alloys using differential phase contrast STEM (DPC-STEM)

T.Radlinger[1]*, F.Hofer[1,2], G.Kothleitner[1,2]

[1]*Institute of Electron Microscopy and Nanoanalysis, Graz University of Technology, Steyrergasse 17, 8020 Graz, Austria*
[2]*Graz Centre for Electron Microscopy (ZfE), Steyrergasse 17, 8020 Graz, Austria*

Spinodal alloys are intriguing and promising materials for exploring the relationship between the chemical and the magnetic microstructure of magnetic alloys. The spinodal decomposition of such alloys due to heating treatments within the miscibility gap results in a segregation of a magnetic phase embedded in a non-magnetic matrix and is well known [1]. Although the compositional evolution of the microstructure and its manipulation has been subject of studies, little is known about the magnetic microstructure evolution. Differential phase contrast (DPC) carried out in scanning transmission electron microscopy ((S)TEM) mode is capable of doing so [2,3].

In this study, we investigated the magnetic domain structure and the chemical microstructure of spinodally decomposed $Cu_{52}Ni_{34}Fe_{14}$ and $Fe_{54}Cr_{31}Co_{15}$ alloys. We were able to shed light on the material microstructures by combining high-angle annular dark field imaging (HAADF), energy-dispersive X-ray spectroscopy (EDXS) elemental mapping and DPC-STEM imaging, revealing interesting relationships between compositional and magnetic properties of these alloys.

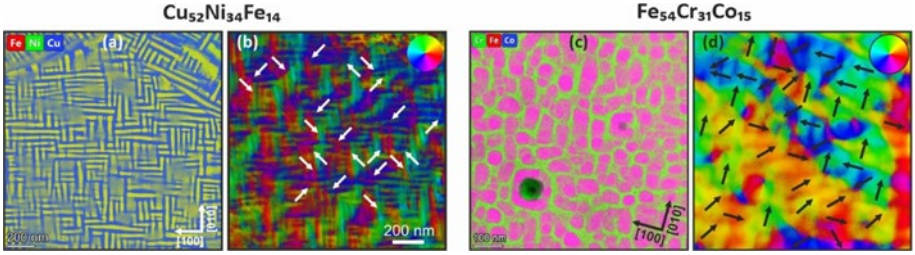

Figure 1. The Chemical microstructure and in-plane magnetic domain structure of spinodally decomposed $Cu_{52}Ni_{34}Fe_{14}$ and $Fe_{54}Cr_{31}Co_{15}$ alloys. The overlay of the EDXS elemental maps reveals the chemical microstructure, i.e. Ni-rich platelets embedded in Cu-rich matrix for CuNiFe (a) and FeCo-rich particles within a Cr-rich matrix for FeCrCo (c). The magnetic induction maps (b, d) display the in-plane magnetic domain structure where the direction of the magnetic vectors is a function of hue. A colorwheel within the image displays this relation. The white and dark arrows within the images reveal the direction of the magnetization vector for certain areas.

[1] F. Fehim, Materials and Design, **42**, 131 (2012)
[2] J. Zweck, J. Phys.: Condens. Matter, **28**, 403001 (2016)
[3] R. Nistico, F. Cesano, F. Garello, Inorganics, **8**, 6 (2020)

* Corresponding author: thomas.radlinger@felmi-zfe.at

TEM studies on intermixing of transition metal nitride superlattice triggered by nanoindentation

Z. Chen[1], Y. Zheng[1], L. Löfler[2], M. Bartosik[3], G. K. Nayak[2], O. Renk[1], D. Holec[2], Z. Zhang*

[1]*Erich Schmid Institute of Materials Science, Austrian Academy of Sciences, A-8700 Leoben, Austria*
[2]*Department of Materials Science, Montanuniversität Leoben, A-8700 Leoben, Austria*
[3]*Institute of Materials Science and Technology, TU Wien, A-1060 Vienna, Austria*

Mechanical properties of nanoscale multilayer coatings are to a large extent governed by the number of interfaces and their characteristics. In general, multilayer coatings with a bilayer-period thickness of just a few nanometers showed the highest hardness, toughness, and elastic modulus. However, the beneficial effect of reduced bilayer thicknesses on mechanical properties is not observed for any layer spacing. It has been reported that, similar to nanocrystalline metals, the hardness and toughness of the multilayer coating decrease again when the bilayer-period thickness is reduced below a certain critical value, being on the order of a few nanometers. For TMNs (transition metal nitride) multilayer, the current understanding for this degradation of properties is that component intermixing already occurs during the thin film deposition and annealing process.

Here [1], we report on a phenomenon occurring during the indentation of TMN multilayer, presumably explaining the degradation of hardness. Nanoindentation is found to disrupt and intermix the multilayer structure due to the deformation imposed (as seen in **Figure 1**). Detailed electron microscopy studies (HAADF HRTEM and EELS) and atomistic simulations provide evidence for intermixing in an epitaxial transition metal nitride superlattice thin film induced by nanoindentation. The formation of a solid solution reduces the interfacial density and leads to a sharp drop in the dislocation density. Our results confirm that plastic deformation causes the microstructure instability of nitride multilayer, which may further improve our understanding of multilayer strength mechanisms.

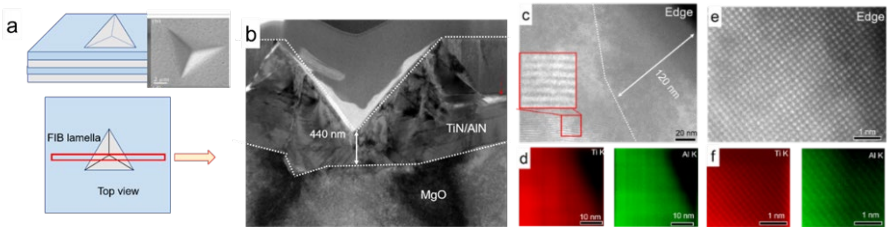

Figure 1. Experimental observation of nanoindentation induced superlattice alloying. a, Schematic diagram of preparation of indentation TEM samples b, Cross-sectional low magnification STEM HAADF image of the indented SL, with some cracks visible. c, Cross-sectional HAADF image of the indented SL. d, Overall EDXS mappings (Ti and Al K-peak signal) taken near the imprint surface. e f, Atomic-resolution HAADF and elemental mapping (EDXS) in the surface region of the imprint.

[1] Z. Chen, et al., Acta Materialia, **214**, 117004 (2021)

This work is supported by FWF P 33696 (Z.C and Z.Z.).

* Corresponding author: zaoli.zhang@oeaw.ac.at

Quantitative chemical analysis of the γ- and γ'-phases in nickel base superalloy PWA1483

S. Seebauer[1,2,3*], M. Stöger-Pollach[1,2], J. Bernardi[1,2], H. Cerva[2,3], O. Eibl[1,2]

[1]*USTEM Service Unit of University Service Centre for Transmission Electron Microscopy, TU Vienna*
[2]*Institute of Solid State Physics, TU Vienna, Wiedner Hauptstraße 8-10, 1040 Vienna, Austria*
[3]*Siemens AG, Otto-Ring-6, 81739 Munich, Germany*

Macroscopic physical properties are correlated to the microstructure in nickel base superalloys. In these materials mechanical properties are strongly influenced by the presence of sub-micrometer sized γ'-phase precipitates. In this presentation the detailed phase compositions of single crystalline superalloy PWA1483 (nominal composition $Ni_{60}Cr_{14}Co_9Al_8Ti_5Ta_1W_1Mo_1$) is elucidated. PWA1483 forms globular to cubical, 0.2 to 0.6 µm sized γ'-phases surrounded by 0.1 to 0.3 µm broad γ-matrix channels. The chemical compositions of the highly alloyed solid solutions determine the crystal structure and the γ and γ'-phase fractions formed during heat treatment [1]. The two phases γ (Cr,Co-rich) and γ' (Al,Ti-rich) are described in the literature as Ni (space group: Fm$\bar{3}$m) and as Ni_3Al (space group: Pm$\bar{3}$m) crystal structure, however, chemical and structural details are frequently not reported.

In transition metals X-ray absorption and overlapping X-ray lines are challenges for a quantitative analysis [2]. SEM-EDX and STEM-EDX were applied for a quantitative EDX analysis. The nominal composition of PWA1483 was measured and confirmed by SEM-EDX with an accuracy of up to 1.5 at.% using multiple scan areas of 0.25 mm². STEM-EDX spectra were acquired on the same sample on a Jeol 2200FS (EDX-detector: Jeol Centurio SSD) at Siemens and a Fei Tecnai F20 (EDX-detector: EDAX Apollo XLTW SSD) at the USTEM. Only FIB-prepared lamellae were used mounted on a Cu grid.

Tabulated k-factors of the standardless Cliff-Lorimer method were found to be inaccurate up to 20% [2]. Quantitative analysis of the nominal composition yielded modified k-factors using STEM-EDX mappings acquired over an 8 µm² wide area of the TEM lamellas. After recalibration of the k-factors the chemical composition of the individual phases were determined yielding $Ni_{54}Cr_{24}Co_{11}Al_5Ti_2Ta_1W_2Mo_1$ for the γ-matrix and $Ni_{67}Cr_4Co_5Al_{12}Ti_8Ta_2W_1Mo_1$ for the γ'-phases. Both TEM systems at USTEM and at Siemens yielded the same chemical composition for the two phases within the error bars, which proves the significance of EDX analysis for such complex materials. The chemical composition of the individual phases together with the nominal composition yielded the volume fraction of the γ-matrix and was calculated as of 48 ±5%. This result was confirmed by SEM secondary electron greyscale images.

The presented analysis of the γ and γ'-phases by STEM-EDX provides a unique and quick method for analyzing the chemical composition of the individual phases with high accuracy. From this data the phase fractions can be determined if the nominal composition of the superalloy was known.

[1] T. Pollock, S. Tin, Journal of Propulsion and Power, **22** (1) 361 (2006)
[2] D.B. Williams, C.B. Carter, Quantitative X-ray microanalysis. In: Transmission Electron Microscopy, Plenum Press, New York (1996)

* Corresponding author: stefan.seebauer@student.tuwien.ac.at

Why do Schwann cells like spider silk?

L. Ploszczanski[1*], K. Peter[1], G. Sinn[1], A. Naghilou[2], C. Radtke[2], H. Lichtenegger[1]

[1] *University of Natural Resources and Life Sciences, Institute of Physics and Materials Science, Vienna,*
[2] *Med Uni Vienna/Vienna General Hospital, Plastic and Reconstructive Surgery, Vienna, Austria*

Spider silk (SPSI) has been established as one of nature's most fascinating materials due to its unique properties. A remarkable application of the SPSI is its use in reconstructive medicine as nerve guidance structure/filament for nerve regeneration [1]. The Schwann cells (SCs), which are a crucial part of the nerve regeneration process adhere to SPSI and migrate along it to support axonal elongation [2]. SPSI degrades without inflammatory response or physiological pH changes. However, the interaction between the SCs and the silk and by that the SPSI properties, that promote SC adhesion are still unclear. The aim of this project is to elucidate material properties of SPSI, that are crucial for its unique performance in nerve regeneration. Not all spider silks show the same medical success, and we believe that properties such as composition, ultrastructure, and mechanical behaviour have a pronounced influence on the acceptance of SPSI by SCs. Therefore, by combining experiments consisting of in vitro studies and the material characterization of various SPSIs, the properties, which are responsible for the advanced success of SPSI in nerve regeneration, will be clarified.

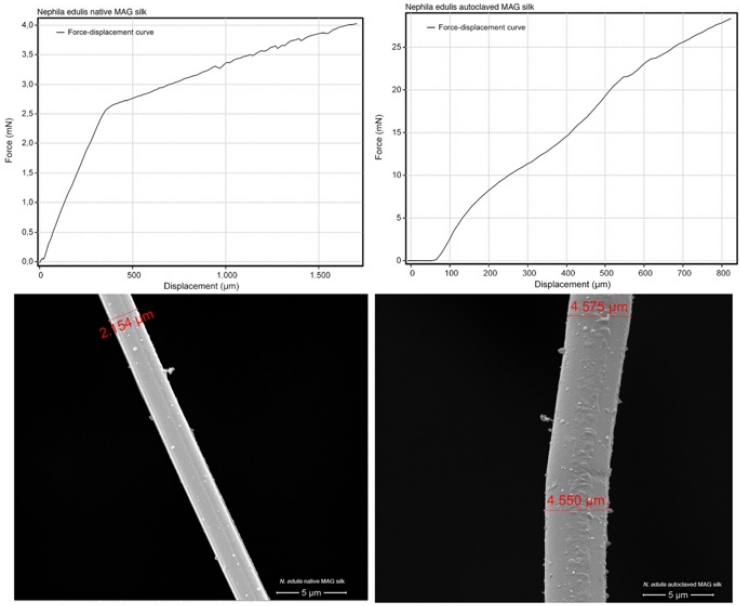

Figure 1. Force-displacement curves and SEM micrographs of the native and autoclaved *N. edulis* MAG SPSI

[1] Radtke, C., et al., PLOS ONE, **6**(2), e16990 (2011**)**
[2] Kornfeld T, et al., Biomaterials, doi: 10.1016/j.biomaterials.2021.120692.
[3] Riekel, C., et al., Frontiers in Materials, **6**:315 (2019)

* Corresponding author: leon.ploszczanski@boku.ac.at

Broad Argon Ion Beam Milling Systems & SEM:
A powerful alternative to FIB-SEM for wide cross sections and large-scale surface polishings

B. Bichler[1*], R. Steffen[2]

[1]*Videko GmbH, Offical Hitachi Distributor Austria, Handelsstraße 14, 2512 Tribuswinkel*
[2]*Hitachi High-Tech Europe GmbH, Europark Fichtenhain 12A, 47807 Krefeld*

Sample preparation like cross sectioning (embedding – polishing, Microtome) usually is an important step for material analysis in a scanning electron microscope. For air sensitive or brittle materials (e. g. for understanding battery materials), classic processes are not suitable. Therefore, ion beam processing is the method of choice.

FIB instrument may be used for cross sectioning. These instruments offer a good solution for high precision site-specific cross sectioning. However, they suffer drawbacks for milling wide areas due to limited speed and field of view. Other artefacts like curtaining and re-deposition in pores may also be present in FIB cuts.

An additional technique that is shown in this presentation is Broad Ion-beam Milling (BIB) that is more and more used for various applications. The Hitachi benchtop Ar+ ion milling system provides a versatile, cost-effective and consistent milling solution, which overcomes many of the challenges of other techniques. Hard, soft, mixed and sensitive (air and heat) materials can be sectioned with little or no preparation artefact, making BIB an ideal technique like for the complex set of materials used in LiBs.

In this presentation it is shown that BIB milling is a versatile tool for SEM sample preparation for all kinds of materials and that BIB-SEM is a smart and cost effective alternative to FIB-SEM systems.

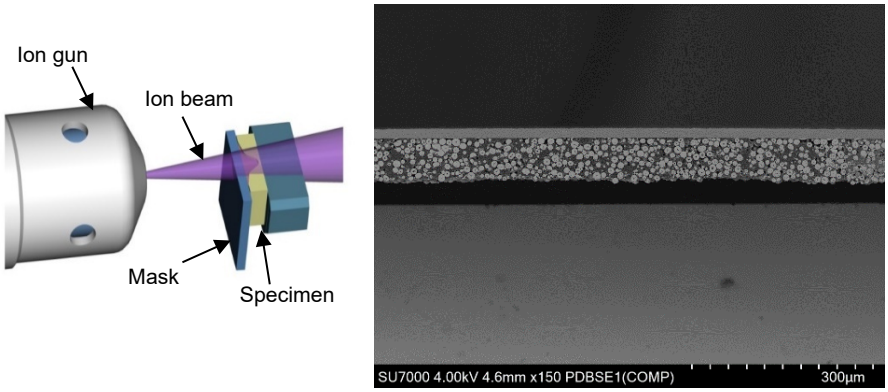

Figure 1. Cross-section of LiB cathode, process time < 1h using Hitachi IM5000 ion milling System.

[1] R. Steffen, M. Dixon, M. Eriksson; Combining SEM and broad ion beam milling to better understand LiB materials; Hitachi White paper https://go.hitachi-hightech.eu/l/343231/2021-04-09/4hfzb8

* Corresponding author: bernhard.bichler@videko.at

Swapping Ion Species with Plasma FIB to make better (S)TEM lamella

D. Phifer*

Thermo Fisher Scientific, Eindhoven, The Netherlands

Compared to Ga+ liquid metal ion source (LMIS) DualBeam FIB-SEMs, Xe+ inductively couple plasma (ICP) DualBeams add the benefit of completely Ga+ free sample preparation [1]. Until recently, only Ga+ and Xe+ source technologies have been commercially available. LMIS Ga+ FIB technology offers a ion beam that provides high resolution capability for nanoprototyping and offers enough current for S/TEM sample preparation of most samples in less than an hour as well as FIB serial sectioning tomography (SST) of volumes up to 40X40X40 µm3/hr (silicon using 30 kV-65 nA) with interslice distances as small as 3 nm [2,3]. On the other hand, Xe+ PFIB technology has a much larger beam current capability allowing researchers to investigate volumes up to 130X130X130 µm3/hr (silicon using 30 kV-2.5 µA). Additionally, xenon ions offer the user the ability to prepare gallium-free S/TEM samples or cross-sections [4,5]. However, for a number of applications, neither gallium nor xenon may provide the highest quality results because of their intrinsic properties.

In this paper, we present the latest generation of plasma FIB technology supporting multiple ion species as a primary ion beam on Thermo Scientific Helios Hydra DualBeam. Next to xenon, the Helios Hydra provides researchers with 3 additional ion species – argon, oxygen and nitrogen. A single ion source can deliver all 4 ion species independently with a patented, automated, fast and easy switching capability. Thermo Fisher has improved performance with access to multiple ion species “on-the-fly” to significantly providing advantages to various use cases such as fast removal with Xenon and lamella quality improvements with low voltage Argon final cleaning. For example, this new method of S/TEM sample preparation with Xe+ ions and a final low energy polish (<1.5kV) of Ar+ ions improves contrast in HR-STEM and avoids most of the sample damage in the final lamella. Supported with SRIM data, it is easy to see why fast removal is better with Xe+ and polishing with Ar+ reduces the amorphous region and induces less dislocations in materials.

The Helios Hydra PFIB is designed on an established high-performance platform, the Helios NanoLab, offering state-of-the-art SEM performance with sub-nm imaging at 1 keV and up. The multiple ion source technology allows for gas switching between species in less than 10 minutes without any degradation in performance for Xe+ PFIB. The system is fully compatible with the complete line up of automation from Thermo Fisher: AutoTEM 5, Auto Slice&View 5, AutoScript 4, Maps and iFAST.

[1] P. Tesch et al, Proceedings from the 34th International Symposium for Testing and Failure Analysis 6 (2008)
[2] C.A. Volkert and A.M. Minor, MRS Bulletin **32,** 389 (2007)
[3] J. Mayer et al, MRS Bulletin **32**, 400 (2007)
[4] L.A. Giannuzzi and N. Smith, Microscopy and Microanalysis **17**, 646 (2011)
[5] B. Van Leer and R. Passey, Microscopy and Microanalysis **23**, 272 (2017)

* Corresponding author: daniel.phifer@thermofisher.com

VIDEKO
our vision: your success.

HITACHI
Inspire the Next
Electron Microscopy

IM5000 Series
SAMPLE PREPARATION

- ☐ Cross-section milling rate: >1 mm/h
- ☐ Wide-area cross-section milling up to 10 mm
- ☐ Hybrid milling: cross-section/flat-milling
- ☐ Cooling temperature control between 0°C and -100°C (Optional)

SU8600
Scanning Electron Microscope

- ☐ Enhanced User-Experience with Advanced Automation
- ☐ Ultrahigh-Resolution and Comprehensive Analysis
- ☐ Enhanced Signal Detection Capabilities
- ☐ For oxygen and moisture-sensitive material: Air-Protection tansfer system between IM and SEM optional available

CONTACT ME!

Bernhard Bichler
VIDEKO GmbH
Tel.: +43 2252 93 1800-21
Mobil: +43/664/91 62 789
Mail: bernhard.bichler@videko.at
www.videko.at

Imaging the near-to-native state

ZEISS Correlative Cryo Workflow

Connect widefield, laser scanning, and FIB-SEM microscopes in a seamless and easy-to-use procedure. ZEISS Correlative Cryo Workflow provides hardware and software optimized for the needs of correlative cryogenic microscopy, from localization of fluorescent macromolecules to high-contrast volume imaging and on-grid lamella thinning for cryo electron tomography.

www.zeiss.at/mikroskopie

ZEISS

Friday, April 22nd, 2022

SESSION 3

09:00	**Haselmann Ulrich** / Erich Schmid Institute of Materials Science Leoben *Defects and Dopant Gradients in Bismuth-Ferrite Thin Films*
09:15	**Sunkara Sowmya** / Medical University of Graz *Organotypic culture as an ex-vivo model to study Alzheimer's disease in brain*
09:30	**Grininger Christoph** / University of Graz *Electron crystallography – From small molecules to proteins*
09:45	**Smith Andrew Jonathan** / Kleindiek Nanotechnik GmbH *Enhanced in situ Applications using Micromanipulators and Nanopositioners*
10:00	**Schwinger Wolfgang** / Carl Zeiss GmbH *TEM-like Ultrastructure Imaging with a New Degree of Speed and Quality*

Defects and Dopant Gradients in Bismuth-Ferrite Thin Films

U. Haselmann[1*], T. Radlinger[2], Y. E. Suyolcu[3], M. N. Popov[4], T. Spitaler[4], L. Romaner[4,5], D. Knez[6], Y. P. Ivanov[1], P. A. van Aken[3], G. Kothleitner[2,6] and Z. Zhang[1**]

[1]*Erich Schmid Institute of Materials Science, Austrian Academy of Sciences, 8700 Leoben, Austria*
[2]*Institute for Electron Microscopy and Nanoanalysis, Graz University of Technology,8010 Graz, Austria*
[3]*Max Planck Institute for Solid State Research, 70569 Stuttgart, Germany*
[4]*Materials Center Leoben Forschung GmbH, 8700 Leoben, Austria*
[5]*Department of Materials Science, Montanuniversität Leoben, 8700 Leoben, Austria*
[6]*Graz Centre for Electron Microscopy, Austrian Cooperative Research, 8010 Graz, Austria*

$BiFeO_3$ (BFO) is single-phase multiferroic material with a direct coupling between the electric polarization and magnetization and huge potential for various applications [1].

Stripes, which had a darker contrast in the HAADF image and showed no periodic spacing between each other, were investigated in a $Bi_{0.9}Ca_{0.1}FeO_3$ thin film. It could be shown (**Figure 1**a-d) that these defects are agglomerated O vacancies with a special ordering while simultaneously being negatively charged domain walls (NCDW) [1,2]. In another thin film ($Bi_{0.8}Ca_{0.2}Fe_{0.95}Co_{0.05}O_3$) it could be shown that the Ca solubility in the secondary Bi_2O_3 (BO) phase, which was present in this film sample, is much lower than in BFO (**Figure 1**e,f) providing novel insights into the relatively unknown ternary phase system of Bi_2O_3 – Fe_2O_3 – CaO [1,3].

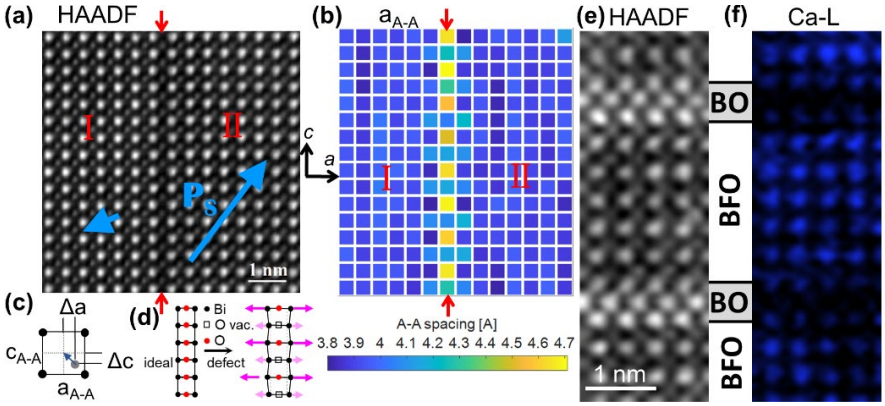

Figure 1. (a) HAADF image of an in-plane defect of agglomerated O vacancies which is simultaneously also a NCDW. **(b)** Distances between A-sites in *a* direction which shows an alternating elongation. **(c)** Schematic of A-site spacings and the polarization. **(d)** Illustration of A- and O sites in the ideal perovskite structure and in the defect. **(a)-(d)** adapted under the Creative Commons Attribution 4.0 License from ref. [2], ©2021, American Chemical Society. **(f)** HAADF image showing two BO plates in BFO matrix. **(g)** Ca-L EELS chemical map demonstrating that the BO plates are Ca poor. **(e),(f)** adapted from ref. [3]

[1] U. Haselmann, Atomic-Scale Study on Dopant- and Strain Effects in Bismuth-Ferrite Thin Films, PhD Thesis, Montanuniverstät Leoben (2022)
[2] U. Haselmann, Y. E. Suyolcu, P.-C. Wu, et al., ACS Appl. Electron. Mater., **3**, 4498 (2021)
[3] U. Haselmann, T. Radlinger, W. Pei, et al., Ca Solubility in a $BiFeO_3$ Based System with a Secondary Bi_2O_3 Phase on a Nanoscale, **in submission** at J. Phys. Chem. C

*Corresponding author: haselmann.ulrich@gmail.com
** Corresponding author: zaoli.zhang@oeaw.ac.at

Organotypic culture as an *ex-vivo* model to study Alzheimer's disease in brain

S. Sunkara[1], R. Megjidi[1], S. Patz[2], W. Sattler[3] and G. Leitinger[1*]

[1]*Division of Cell Biology, Histology and Embryology, Gottfried Schatz Research Center, Medical University of Graz, Austria*
[2]*Research unit for experimental traumatology, University clinic for neurosurgery, Medical University of Graz, Austria*
[3]*Division of Molecular biology and Biochemistry, Gottfried Schatz Research Center, Medical University of Graz, Austria*

Organotypic cultures (OTC) represents a promising method to study neurodegenerative diseases with the advantage of preservation of original architecture and connections. Counter to the classical slice cultures from model animals, we established Alzheimer's disease (AD) condition ex-vivo in hippocampus region of porcine brain for our initial trails. The three-dimensional tissue culture of thickness 160 microns was treated with amyloid beta oligomers ($A\beta O_{1\text{-}42}$) and incubated for 3-5 days against a control to simulate AD. We designed a simple protocol to generate oligomers from the amyloid beta peptide prior to our treatments. Using both light microscopy and electron microscopy, we observed that the 3D architecture and the neuronal connectivity of the porcine brain sample is well-maintained mimicking the in-vivo system. We compared the morphology of the samples obtained from post-mortem porcine samples with OTC samples and found that the cell-integrity and the neuronal connections are viable and the cells are in an active state. There was no sign of autolysis and no dark spots were observed in the slices indicating that the slices were healthy and without any contamination respectively. The slices exposed to $A\beta O_{1\text{-}42}$, polymerised and formed aggregates and displayed a mesh like appearance in the extracellular matrix and in axon terminals when observed in electron microscope. We observed a few fibrils inside axon terminal, which conforms to the studies that - Aβ enters inside the axon terminals as the disease progresses. From this, we conclude that OTC is a suitable and time saving model to study Alzheimer's disease, especially due to its preserved composition of diverse cell types including the blood brain barrier. Previous studies have shown that Aβ affect the neuronal connections via disturbing the synapses [1]. Our immediate follow-up studies include quantifying the synapses in $A\beta O_{1\text{-}42}$ treated slices to understand the effect of $A\beta O_{1\text{-}42}$ on neuronal communication in AD. We plan to switch to human brain samples and replicate the same, after establishing in porcine model.

[1] G. M. Shankar *et al.*, Nat. Med., **14 (**8), 837 (2008)

The project is funded by FWF – Austrian Science fund - P 29370.

* Corresponding author: gerd.leitinger@medunigraz.at

Electron crystallography – From small molecules to proteins

C. Grininger[1]*, G. Hofer[2], L. Schooltink[1], T. Pavkov-Keller[1]

[1] *Institute for Molecular Biosciences – Structural Biology, University of Graz, Humboldtstraße 50/3, 8010 Graz, Austria*
[2] *Department of Materials and Environmental Chemistry, Stockholm University, Svante Arrhenius väg 16C, SE-106 91 Stockholm, Sweden*

3D electron diffraction (ED) is an uprising method for the structural characterization of nanocrystalline materials. This also includes beam sensitive materials like protein crystals. Although there are also drawbacks for this method in protein crystallography, we used the spirit of the nanocrystallography revolution and started with first experiments on our transmission electron microscope.

A well-known bottleneck in the structural characterization of macromolecules with X-ray diffraction is crystallization. Often the needed crystal size cannot be achieved despite extensive optimization of crystallization conditions. Nevertheless, the yield of sea urchin like needle clusters, microcrystals and almost two-dimensional platelets is a silver lining. Those crystals – too small for X-ray crystallography – could be applied to microcrystal electron diffraction methods. Additionally, it is a fast method that could soon outperform X-ray crystallography for special cases like ligand screening.

So far, we were able to acquire knowledge for the basic workflow for data collection with our instrument setup, a Zeiss Libra 120 plus TEM with an OMEGA energy filter and a TVIPS TemCam-XF416(ES) detector. We collected continuous rotation electron diffraction data for the zeolite ZSM-5 and protein nanocrystals (lysozyme, der f 20 like) under cryo conditions.

With these fundamental achievements we are on track to apply ED to more challenging crystals and also solve novel protein structures in the future.

*Corresponding author: christoph.grininger@uni-graz.at

Enhanced *in situ* Applications using Micromanipulators and Nanopositioners

A. J. Smith*, K. Schock, A. Rummel, M. Kemmler, S. Kleindiek

Kleindiek Nanotechnik, Aspenhaustr. 25, 7270 Reutlingen

Utilizing a set of micromanipulators integrated into an SEM's or FIB/SEM's vacuum chamber yields access to a wide array of additional applications beyond the standard use-cases for such microscopes. These range from electrical and mechanical characterization of micro- to nano-scale objects (e.g. semiconductor devices, nanowires, and other microstructures) to complex manipulation and positioning tasks such as arranging nano dots or eucentric tilt/rotation about a chosen ROI on a given sample. … to name just a few.

Recent developments in the field of integrated micromanipulators and positioners include a set of piezo-actuated micro-tweezers suitable for use at LN_2 temperatures that can be used to transfer TEM lamella prepared in cryoFIB from the frozen sample bulk to suitable sample holders for cryoTEM.

Another application that is relevant to processing samples using FIB tools is the mitigation of unwanted milling artefacts ("curtains") that result when cross sectioning inhomogeneous materials. A miniature, four-axis eucentric tilt stage can be used to dynamically vary the ion beam's incident angle and thus minimize if not eliminate the bothersome "curtaining" effects. The same compact substage can also be used in SEM applications where there is a need to image a sample in various orientations that may not be attainable using the microscope's sample stage.

A rather recent application for a tool that has been available for quite some time is *in situ* X-ray diffraction. The referenced tool is a very precise rotation drive that allows the user to select the ROI to rotate around. The method utilizes a target material mounted to the tip of a micromanipulator that can thus be positioned at the desired location relative to a sample. The sample is in turn mounted to the abovementioned rotation drive. The entire setup us placed on the microscope's sample stage (**Figure 1**) and can be positioned so that the target is illuminated by the electron beam. A suitable detector is mounted opposite the target and the sample is rotated in small increments after recording each diffraction image.

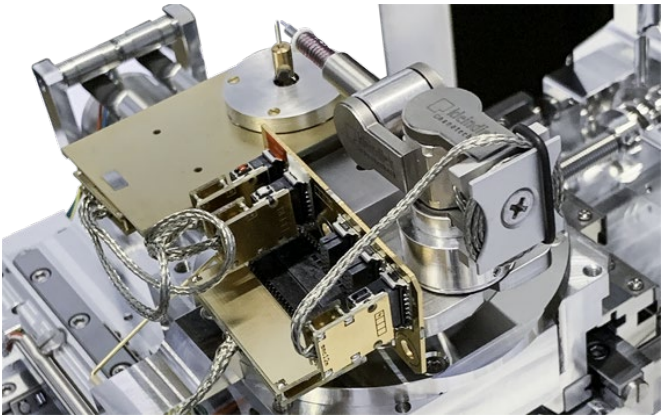

Figure 1. Combined micromanipulator and nanolathe platform installed on a Zeiss XB550.

* Corresponding author: andrew.smith@kleindiek.com

TEM-like Ultrastructure Imaging with a New Degree of Speed and Quality

W. Schwinger[1]*, R. Neujahr[2]

[1]*Carl Zeiss GmbH, Laxenburgerstr. 2, 1100 Wien*
[2]*Carl Zeiss Microscopy GmbH, Kistlerhofstrasse 75, 81379 München, Deutschland*

Electron microscopy is traditionally used for high resolution study of the subcellular structures of tissues and cells. Transmission electron microscopes (TEM) have been the preferred choice for ultrastructural imaging, although scanning electron microscopes (SEM) equipped with backscatter electron detectors also enable the acquisition of high-resolution, TEM-like images and in addition delivers some outstanding benefits TEM cannot provide – like automatic imaging of multiple samples.

With a new diode design and superior detector sensitivity, ZEISS Sense BSD can detect very small numbers of electrons and convert low signals into high-contrast images. Fast image acquisition with low acceleration voltages and low electron doses becomes possible. Especially biological samples can be imaged without damage and deterioration of the image quality induced by charging effects.

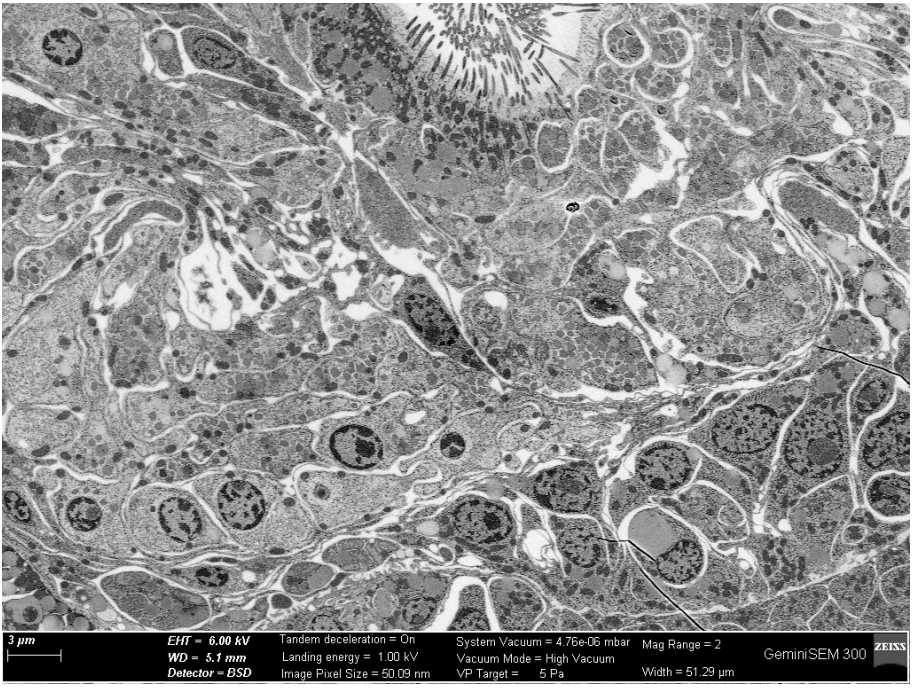

Figure 1. 50 nm thin section imaged with ZEISS Sense BSD detector at 1keV landing energy. Sample courtesy by Anna Seybold & Harald Hausen, Sars Centre for Marine Molecular Biology, University of Bergen, Norway.

*Corresponding author: wolfgang.schwinger@zeiss.com

kleindiek
nanotechnik

stable
versatile
reliable

Give your microscope a hand

www.kleindiek.com

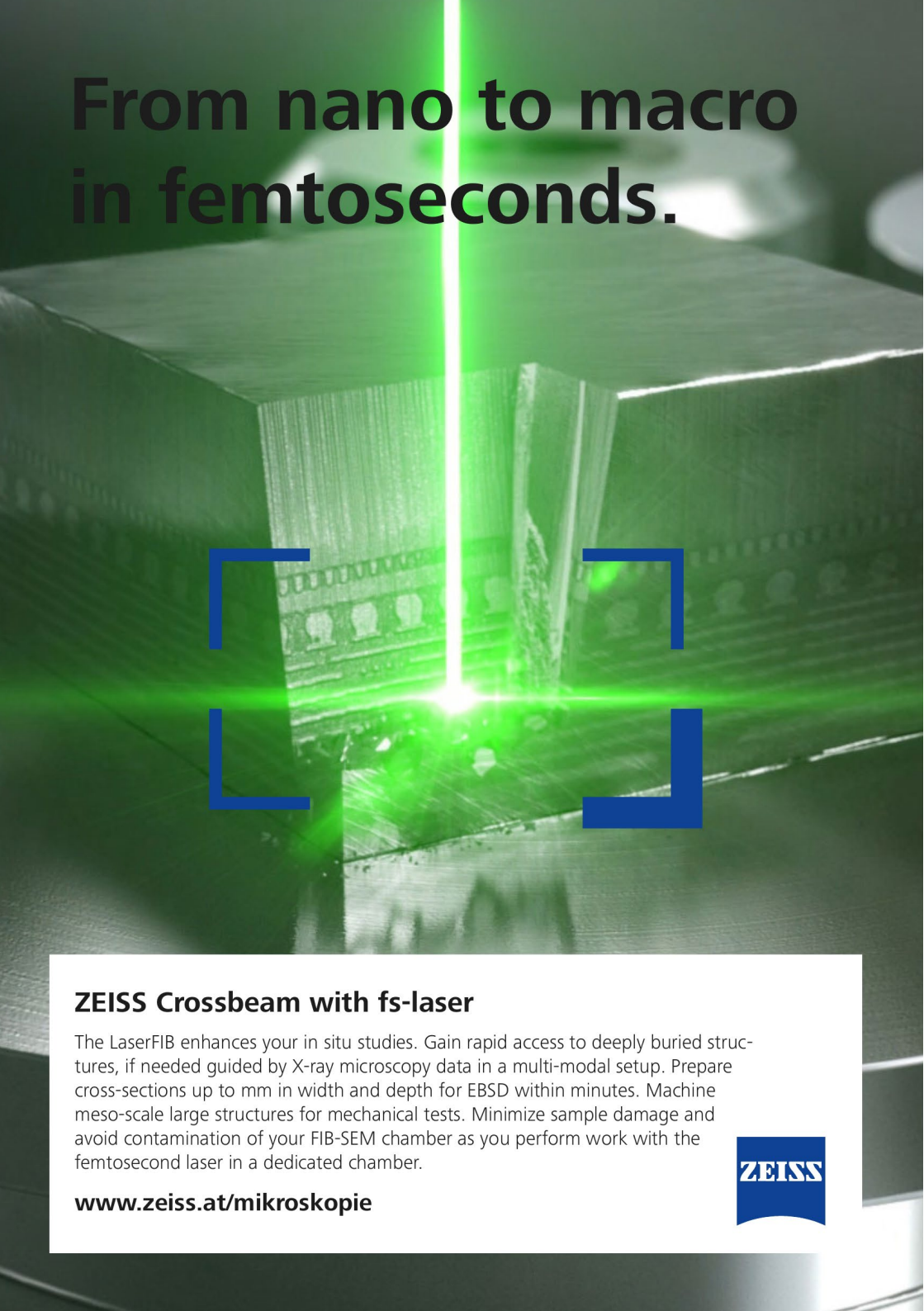

ZEISS Crossbeam with fs-laser

The LaserFIB enhances your in situ studies. Gain rapid access to deeply buried structures, if needed guided by X-ray microscopy data in a multi-modal setup. Prepare cross-sections up to mm in width and depth for EBSD within minutes. Machine meso-scale large structures for mechanical tests. Minimize sample damage and avoid contamination of your FIB-SEM chamber as you perform work with the femtosecond laser in a dedicated chamber.

www.zeiss.at/mikroskopie

ZEISS

Friday, April 22nd, 2022

SESSION 4

11:00	*Invited Speaker*: **Minnich Bernd** / University of Salzburg *SEM & 3D-Morphometry in Vascular Biology: Vascular Corrosion Casting in Biomedicine and Zoology*
11:30	**Horák Michal** / University of Brno *Plasmon resonances in biocompatible nanoparticles*
11:45	**Joudi Wael** / University of Vienna *Correlated AFM/STEM study on the Mechanical Stiffness of Defect-Engineered Graphene*
12:00	**Frerichs Hajo** / Quantum Design Microscopy GmbH *Two Microscopes are better than One – In-situ Correlative Analysis by combination of AFM and SEM*

SEM & 3D-Morphometry in Vascular Biology: Vascular Corrosion Casting in Biomedicine and Zoology

B. Minnich* and A. Lametschwandtner

Vascular Research Unit, Department of Environment & Biodiversity, University of Salzburg Hellbrunnerstr. 34, 5020 Salzburg, Austria

The vascular corrosion casting technique is a specific method to investigate the architecture of microvascular networks of normal and diseased tissues and organs in man and animals. By replacing blood by a polymerizing resin delicate vascular casts (= replicas) of the vessels' lumina can be obtained. Examination of vascular casts in the scanning electron microscope (SEM) enables to gain detailed information on (i) the luminal side of the vessel by means of imprints of endothelial cell nuclei, sphincters, intimal cushions, flow dividers and venous valves and (ii) on the geometry of vascular networks in terms of vessel diameters, intervascular- and interbranching distances as well as branching angles. Data can be used to test any vascular network for underlying optimality principles. Due to the high depth of focus of the SEM the three-dimensional arrangement of vascular trees and networks can be explored thoroughly. Thus, vascular relations between regions far remote from each other, yet functionally belonging together, can be pinpointed. In practice, these investigations are instrumental in developmental research, e.g. in the study of growth and regression of blood vessels in developing organs as well as in the study of normal healthy and pathologically changed blood vessels.

SEM holds great potential for morphological research, as applying it comes with great resolution and a high depth of focus, giving SEM micrographs pseudo three-dimensionality. Adversely, the high depth of focus prevents accurate dimensional or spatial measurements of imaged microstructures from either the SEM video-display, printed micrographs or from photo-negatives. Macroscopic objects are viewed close up using binocular vision. Binocular vision is also used in microscopy where stereophotogrammetry and related techniques applying stereo paired images, and a variety of hardware tools calculate the third dimension (z-coordinate) via the parallax.

A method for dimensional and angular measurements of microstructures imaged in the SEM (3D-morphometry - M3, ComServ, Austria) was first developed in our lab in 1999 [1]. It uses digitized stereo paired images, frame-grabbed (slow scan) directly from the SEM's photo-display, vector equation-based algorithms for the calculation of spatial coordinates (x/y/z) and derived distance - as well as angular measurements. It offers dynamic data exchange to open source software in combination with online graphing of frequency distributions of measured variables. Formulas for central perspective depth computation allow the overall error to be less than 1.0%.

Currently, this technique is used to examine developmental and regression processes of the microvasculature of different organs in various animals such as the South African clawed toad (*Xenopus laevis* Daudin) [2,3] and to explore the angioarchitecture of the human great saphenous vein (*Vena saphena* magna), which plays a critical role in bypass crafting during human coronary surgery [4]. Further research using these techniques has been conducted on diabetes melitus Type 2 induced mice. Here we investigated microvascular changes in the liver, the eyes and the penis causing dysfunction and proved the effectiveness of therapies

* Corresponding author: bernd.minnich@plus.ac.at

such as shock-waves or THCV administration. Another field of application is the study of compromised lung vascularization of COPD induced rats.

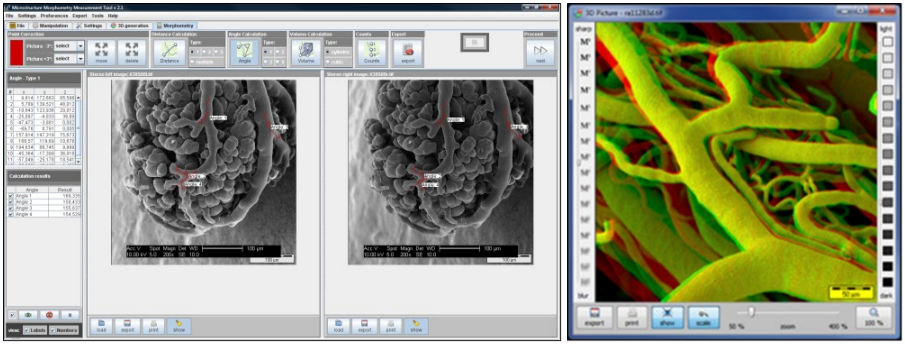

Figure 1. M3 graphical user interface (GUI) showing the morphometry screen while measuring branching angles of feeding arteries of the spleen of the adult *Xenopus laevis* Daudin.
Figure 2. Anaglyphic 3D image of a vascular corrosion cast.

[1] Minnich B. et al, Journal of Microsccopy **195**, 23-33 (1999)
[2] Lametschwandtner A. et al, Anatomical Sciences International **87**, 88-100 (2012)
[3] Lametschwandtner, A., Spornitz, U., & Minnich, B. The Anatomical Record, **305**, 243-253 (2021)
[4] Kachlik D. et al, Central European Journal of Medicine **3**(4), 475-481 (2008)

Short-CV

Ao. Univ.-Prof. Mag. Dr. Bernd Minnich, FRMS
Dept. of Environment & Biodiversity
Paris Lodron University of Salzburg

Membership Austrian Society for Electron Microscopy	1997 to date
Membership Microscopy Society of America	2000 - 2018
Membership European Microscopy Society	2002 to date
Watson Memorial Award - Microscopy Society of America	2002
Habilitation - Venia docendi „Gefäßbiologie und Elektronenmikroskopie“	2003
Professorship for Biostatistics at Paracelsus Medical University	2003 to date
Best Advanced Scientist Award – Microscience, Royal Microscopical Society	2004
Professorship at the Biology Department of the University of Salzburg	2004 to date
Head of Division “Integrative Animal Biology”	2011 - 2013
Fellow of the Royal Microscopical Society, Oxford, GB	2014 to date
Head of Division “Animal Structure & Function”	2016 - 2018
Board member of Austrian Society for Electron Microscopy	2018 to date
Head of the Vascular Biology Research Unit	2018 to date
Head of the Ethics Committee of the State of Salzburg	2019 to date

Plasmon resonances in biocompatible nanoparticles

M. Horák[1]*, F. Ligmajer[1], V. Čalkovský[1], A. Daňhel[2], J. Mach[1], T. Šikola[1]

[1]*Brno University of Technology, Brno, Czech Republic*
[2]*Institute of Biophysics of the Czech Academy of Sciences, Brno, Czech Republic*

We present a study of biocompatible nanoparticles made of silver amalgam and gallium using STEM-EELS on a single particle level.

Silver amalgam is one of the most suitable solid electrode materials in electroanalysis of various reducible organic and inorganic compounds. The main advantage of silver amalgam within this context is its wide cathodic potential window, high mechanical stability, adequate sensitivity, and advantageous strong interaction with biopolymers. Nanostructuring the amalgam promises improved electrochemical performance and brings along the prospect of plasmonic activity. Our results show that silver amalgam, apart from its proven usefulness in electroanalytic chemistry, can be also regarded as a novel plasmonic material with promising optical properties. Silver amalgam nano- and micro-particles exhibit strong plasmon resonances in ultraviolet to mid-infrared regions depending on the particle size, see **Figure 1**c. These findings establish silver amalgam nanoparticles as promising candidates for applications within photochemistry and spectroelectrochemistry, where the synergy between their plasmonic and electrochemical qualities can be fully utilized [1].

Gallium is commonly known as a metal with a melting temperature of 29.7 °C. It has several solid-state phases which enables a variety of phase-changing systems which are under investigation. Bulk plasmon energy of gallium is 13.7 eV and it has no strong interband transitions in a wide region from ultraviolet to infrared, which makes it an ideal plasmonic candidate. We have explored the plasmonic nature of its nanoparticles and shown that plasmon resonances can be tuned from ultraviolet to visible spectral region by changing the size of the nanoparticle, see **Figure 1**.

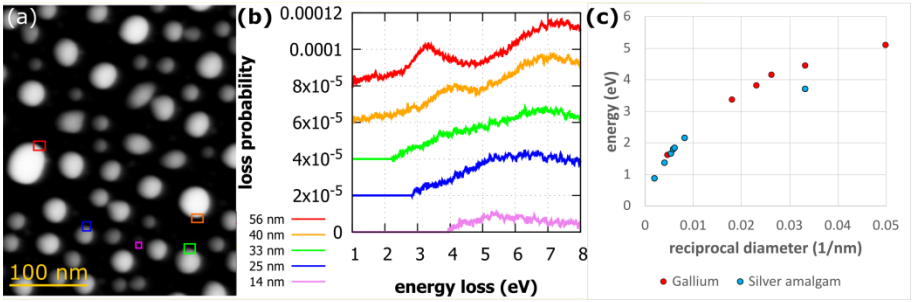

Figure 1. (a) STEM HAADF image of Ga nanoparticles on silicon nitride membrane, (b) EEL spectra showing the dipole plasmon resonance in individual Ga nanoparticles. (c) Dispersion relation of Ga and AgHg nanoparticles proving the wide range tunability of the dipole plasmon mode.

[1] F. Ligmajer, M. Horák, T. Šikola, et al., J. Phys. Chem. C, **123**, 16957 (2019)

* Corresponding author: michal.horak2@ceitec.vutbr.cz

Correlated AFM/STEM study on the Mechanical Stiffness of Defect-Engineered Graphene

W. Joudi*, A. Trentino, K. Mustonen, C. Mangler, J. Kotakoski

Faculty of Physics, University of Vienna, Boltzmanngasse 5, 1090 Vienna, Austria

The first isolation of a single layer graphene sheet from graphite via the adhesive tape method in 2004 [1] triggered an avalanche of experiments studying this two-dimensional (2D) material, including investigations on the unique electronic as well as mechanical properties. Since these macroscopically observed properties are a result of elemental composition and atomic structure, the 2D nature of graphene allows for a direct correlation by linking atomic resolution scanning transmission electron microscopy (STEM) images to the observed macroscopic properties. Moreover, this structure-to-property correlation permits investigations on alterations of material properties through defect-engineering. In this study, the in-plane mechanical stiffness of graphene in its pristine state is compared to a defective state in the form of vacancies by correlating atomic force microscopy (AFM) nano-indentation measurements to atomic resolution STEM images. Both instruments, as well as the target chamber where the vacancies are created, are part of the Controlled Alteration of Nano-materials in Vacuum down to the Atomic Scale (CANVAS) system at the University of Vienna, which provides an ultra-high vacuum environment permitting direct correlation. The vacancy density is precisely determined by 2D STEM scan maps, which combine individual small FOV atomic resolution images into one large area, followed by processing of the data set by a convolutional neural network [2]. With a vacancy density of around 1 x 10^{13} cm^{-2} the 2D elastic modulus decreases by approximately 40%. The STEM images reveal strain-induced surface corrugation caused by the vacancies [3], which might play a role in the weakening mechanism.

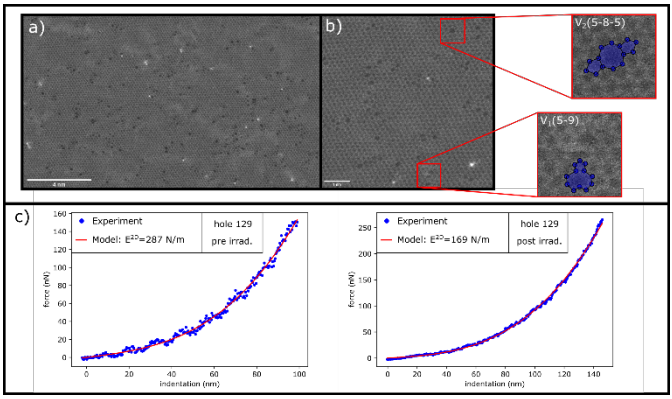

Figure 1. Atomic resolution STEM image (a) and corresponding magnification (b) revealing the introduced vacancies. AFM nano-indentation curves of the same graphene drumhead before and after irradiation (c).

[1] K. S. Novoselov et al., Science, **306** (5696), 666 (2004)
[2] A. Trentino et al., Nano Letters, **21** (12) 5179 (2021)
[3] J. Kotakoski, F. R. Eder, J. C. Meyer, Phys. Rev. B, **89** 201406 (2014)

* Corresponding author: wael.joudi@univie.ac.at

Two Microscopes are better than One – *In-situ* Correlative Analysis by combination of AFM and SEM

H. Frerichs*, S. Seibert, L. Stühn, M. Wolff, C.H. Schwalb

Quantum Design Microscopy GmbH, Im Tiefen See 60a, 64293 Darmstadt, Germany

Combining different analytical methods into one instrument is of great importance for the simultaneous acquisition of complementary information. Especially the *in-situ* combination of scanning electron microscopy (SEM) and atomic force microscopy (AFM) enables completely new insights in the micro and nano-world. In this work, we present the unique *in-situ* combination of scanning electron and ion microscopy (SEM/FIB) and atomic force microscopy (AFM) for nanoscale characterization [1-2].

We will present a variety of case studies to highlight the advantages of interactive correlative *in-situ* nanoscale characterization for different materials and nanostructures. We show results for *in-situ* electrical characterization by conductive AFM for 2D materials as well as electrostatic force microscopy (EFM) of piezoceramic films [3]. In addition, we will present results for the *in-situ* characterization of magnetic nanostructures by combination of SEM and high-vacuum magnetic force microscopy (MFM). SEM enables to identify grain boundaries in order to measure the magnetic properties directly via MFM with nanometer resolution (see **Figure 1**).

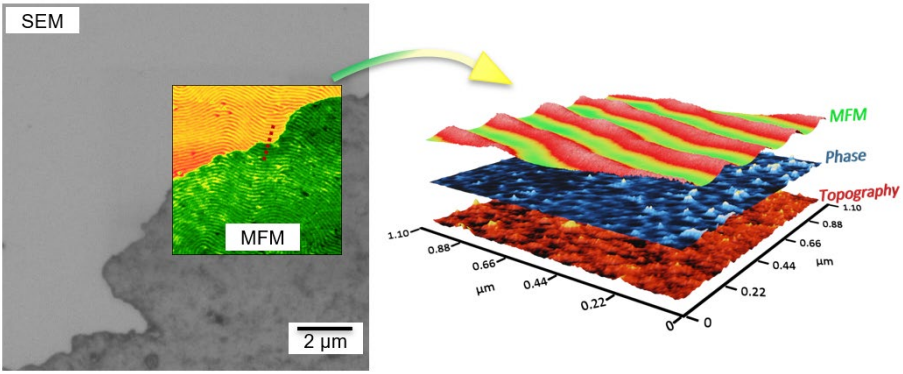

Figure 1. (Left) SEM image of a multilayer magnetic sample with correlative MFM image at a grain boundary. (Right) AFM data overlay of topography, phase, and MFM signals.

[1] D. Yablon, et al., Microscopy and Analysis, **31** (2), 14 (2017)
[2] S.H. Andany, et al., Beilstein J. Nanotechnol., **11**, 1272 (2020)
[3] J.M. Prohinig, J. Hütner, K. Reichmann, S. Bigl, Scripta Materialia, **214**, 114646 (2022)

* Corresponding author: frerichs@qd-microscopy.com

Quantum Design
EUROPE

qd-europe.com

Electron microscopy

Sample preparation and measurement

- AFSEM – correlative AFM and SEM
- High-resolution compact & tabletop SEM
- In situ sample management solutions for TEM/REM/µXCT
- Sputter & carbon coaters
- Cryo preparation system
- Comprehensive accessories

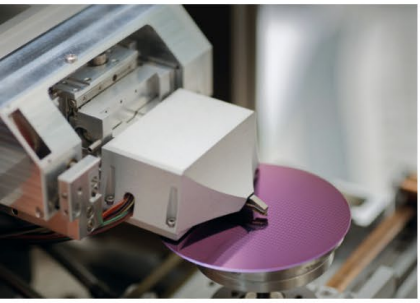

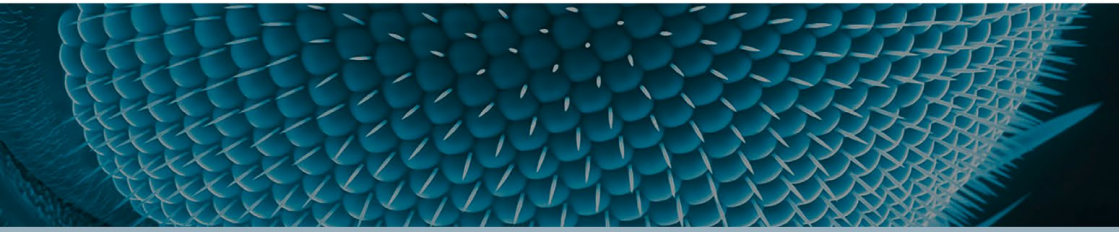

Quantum Design GmbH +49 6151 8806 0

em@qd-europe.com

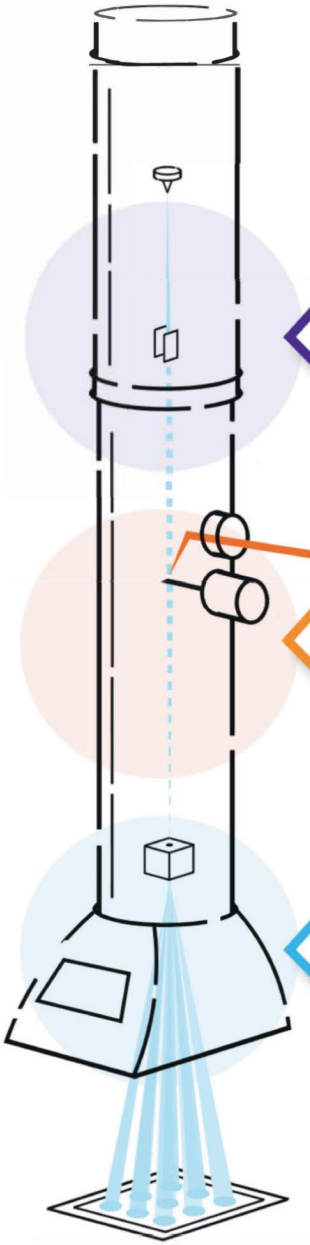

ILLUMINATING NANOSCALE DYNAMICS

EDM + SYNCHRONY® 1

Electron dose modulation via electrostatic beam blanking. Programmable dose management for beam-sensitive specimens.

LUMINARY® MICRO 2

Laser illumination of specimens with compact, column-mounted optics. Precise, localized laser heating with any sample holder.

RELATIVITY® 3

Multiply camera framerate with electrostatic sub-framing. Access kHz frame rates with any camera.

JEOL | IDES
INTEGRATED DYNAMIC ELECTRON SOLUTIONS

GET MORE INFO NOW
sales@jeol.de · +49 8161 9845 0

JEOL (Germany) GmbH
Gute Änger 30 · D-85356 Freising · www.jeol.de

Friday, April 22nd, 2022

SESSION 5

13:15	*Fritz Grasenick Laureate:* **Ederer Manuel** / TU Wien *Imaging the Spatial Distribution of Electronic States in Graphene Using Electron Energy-Loss Spectroscopy: Prospect of Orbital Mapping*
13:30	**Postl Andreas** / University of Vienna *Indirect measurement of the carbon adatom migration barrier on graphene*
13:45	**Preimesberger Alexander** / TU Wien *Discrimination of coherent and incoherent cathodoluminescence using temporal photon correlations*
14:00	**Kastenmüller Andreas** / AMETEK GmbH *Latest Development in EELS*
14:15	**Raggl Georg** / JEOL (Germany) GmbH *Integrated lasers and ultra-fast electrostatic beam blanking systems – Pathways to new experiments in modern transmission electron microscopy*

Imaging the Spatial Distribution of Electronic States in Graphene Using Electron Energy-Loss Spectroscopy: Prospect of Orbital Mapping

M. Ederer[1*], M. Bugnet[2,3,4], V. K. Lazarov[5], L. Li[6], Q. M. Ramasse[2,3], D. M. Kepaptsoglou[2,5], S. Löffler[1]

[1]TU Wien (Austria), [2]SuperSTEM (UK), [3]University of Leeds (UK), [4]Université de Lyon (France), [5]University of York (UK), [6]University of West Virginia (USA)

Electronic states are responsible for the majority of macroscopic properties of the materials in our everyday life. From the electrical characteristics to the type of chemical bonding, everything is ultimately determined by the specific state of the electronic orbitals. While models exist describing the electronic states in bulk materials, directly observing them in real space has proven impossible until recently [1]. We contribute to this still very elusive goal by presenting spatial distributions of graphene orbitals experimentally mapped with STEM-EELS and their remarkable agreement with theoretical simulations.

Electrons that inelastically interact with sample electrons can trigger a transition from an initial core state to the conduction band. Information about the transition to a specific final electronic state is contained in the EELS fine structure and can, thus, be mapped when a suitably small energy window is chosen. Using the K-edge of graphene provides a twofold advantage: firstly, the initial electron orbital with s-like angular momentum makes interpretation of the map straightforward and secondly, the two relevant final orbitals, π* and σ*, are sufficiently different in their spatial extent to make the maps distinguishable. While the antibonding σ* orbital is composed of sp^2 hybrid orbitals and mostly confined within the graphene sheets, the antibonding π* orbital is composed of p_z orbitals and, thus, stronger delocalized out-of-plane. In order to make use of this spatial distinction, a side view is necessary, i.e. parallel to the carbon planes. The sample was synthesized by epitaxially growing graphene on a 6H-SiC substrate resulting in a buffer layer directly on top of the SiC substrate and five "free-standing" layers of graphene.

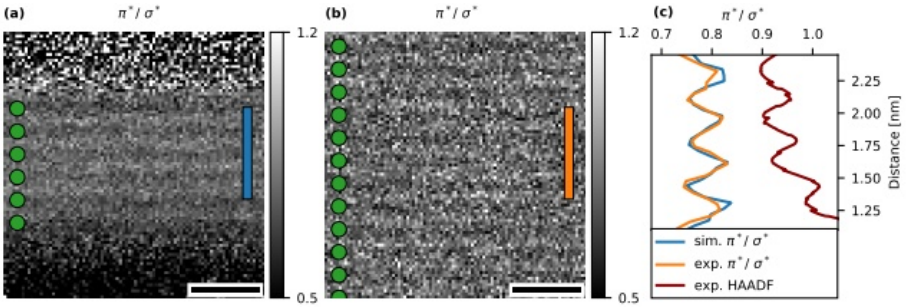

Figure 1. Ratio of π^* to σ^* orbital maps. The graphene layers (marked by green disks) are oriented in the [2 1 3 0] zone axis. The specimen thickness is approximately 25 nm and the acceleration voltage 60 kV. The scalebars indicate 0.5 nm. **(a)** Experimental map. **(b)** Simulated map with shot noise. **(c)** π^*/σ^* profiles from (a) and (b), integrated in the range indicated by the blue and orange bars, together with the experimental HAADF signal.

*Corresponding author: manuel.ederer@tuwien.ac.at

However, the energy filtered STEM-EELS maps show intensity maxima at the positions of the atomic columns for both orbitals. In order to explain this discrepancy to the theoretical model of the π* electron density, we employed extensive simulations. Elastic propagation of the probe electrons through the sample was calculated using the multislice algorithm. Inelastic scattering was calculated using the mixed dynamic form factor formalism with density functional theory data obtained with WIEN2k [2]. The resulting maps with shot noise and instrumental broadening reaffirm the experimental findings due to their excellent agreement. Performing the simulations for a number of different sample thicknesses, it becomes evident that the intensity increase of the π* maps at the atomic column positions is a result of elastic channeling. This effect is significant already for a projected sample thickness of 5 nm. Nevertheless, as channeling is present for both orbitals, the difference in extent of the orbitals between the atomic columns can be made visible by taking the ratio of the π* to the σ* map (**Figure 1**). The profile of the ratio clearly shows maxima between the atomic columns and minima at the columns when compared to the HAADF signal, thus visualizing the spatial distribution of both orbitals. Future planned steps for this system concern the buffer layer and the influence of the interface on the orbitals.

[1] Löffler et al., Ultramicroscopy, **26**, 177 (2017)
[2] Blaha et al., The Journal of Chemical Physics, **152**, 074101 (2020)

The authors gratefully acknowledge funding from FWF under grant nr. I4309-N36. Experiments were performed at the SuperSTEM Laboratory (UK) with support from the Engineering and Physical Science Research Council (EPSRC).

Curriculum Vitae

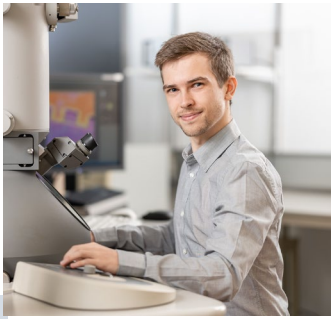

Manuel Ederer

Date of Birth: 03.02.1994
Address: Wiedner Hauptstraße 8-10, 1040 Wien
Telephone: +43 1 58801-45228
E-Mail: manuel.ederer@tuwien.ac.at
Nationality: Austria
ORCID: 0000-0002-8441-9778

Education History

since Feb 2020	TU Wien, Doctoral programme in Engineering Sciences Technical Physics at the University Service Centre for Transmission Electron Microscopy
Apr 2017 – Jan 2020	TU Wien, Master programme Technical Physics, completed with distinction
Oct 2013 – Apr 2017	TU Wien, Bachelor programme Technical Physics, completed with distinction
Sep 2004 – Jun 2012	BG and BRG Waidhofen an der Thaya

Scientific Interest

- STEM-EELS and EFTEM imaging
- Orbital mapping
- Simulation of inelastic scattering events (WIEN2k, multislice method, MDFF)
- Image processing

Indirect measurement of the carbon adatom migration barrier on graphene

A. Postl[1,2]*, P. Hilgert[1], A. Markevich[1], J. Madsen[1], K. Mustonen[1], J. Kotakoski[1], T. Susi[1†]

[1]*University of Vienna, Faculty of Physics, Boltzmanngasse 5, 1090 Vienna, Austria*
[2]*University of Vienna, Vienna Doctoral School in Physics, Boltzmanngasse 5, 1090 Vienna, Austria*

Surface diffusion is crucial for many physical and chemical processes, including epitaxial growth of crystals and heterogeneous catalysis. Although the phenomenon is common [1] and theoretically understood, measuring adatom migration barriers on 2D materials remains a daunting challenge. We are able to estimate the carbon adatom migration barrier on freestanding monolayer graphene, which has theoretically been predicted to be in the range of 350–500 meV [2,3], by quantifying the temperature-dependence of its electron knock-on damage.

To measure damage and healing rates as accurately as possible, we use 90 keV electrons and choose the fastest possible time for image acquisition with our aberration-corrected scanning transmission electron microscope. Contrary to expectations, the damage rate decreases with increasing temperature, which is due to the fast healing of vacancies by recombination with diffusing adatoms. By comparing the predicted and observed damage rates at 300–1073 K and using a model describing knock-on damage, vacancy healing, and our finite scanning probe, we find a barrier of (0.33 ± 0.03) eV, which is the first measurement reported (see **Figure 1**).

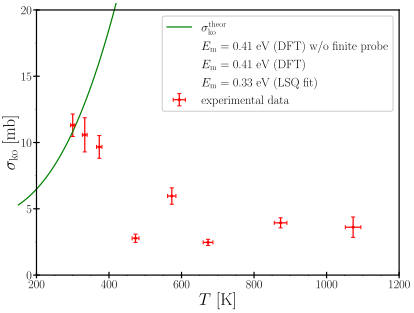

Figure 1. Knock-on damage cross section as a function of temperature: experimental observations (red points), theoretical model (green line), and an extended model describing the damage rate with counteracting vacancy healing (orange line for a least-squares fitted migration barrier and purple for the DFT barrier).

[1] R. Zan, et al., Nano Letters, **12**, 3936–3940 (2021)
[2] A. Krasheninnikov, et al., Physical Review B, **69**, 073402 (2004)
[3] O. Lehtinen, et al., Physical Review Letters, **91**, 017202 (2003)
[4] M. Tripathi, et al., Nano Letters, **18**, 5319–5323 (2018)
[5] C. Su, et al., Science Advances, **5**, eaav2252 (2019)

We gratefully acknowledge funding from the European Research Council (ERC) under the European Union's Horizon 2020 research and innovation program (Grant agreement no. 756277-ATMEN) and the Vienna Doctoral School in Physics.

* Corresponding author: andreas.postl@univie.ac.at
† Corresponding author: toma.susi@univie.ac.at

Discrimination of coherent and incoherent cathodoluminescence using temporal photon correlations

M. Scheucher[1,2], T. Schachinger[3,4], A. Preimesberger[1,*], T. Spielauer,[1]
M. Stöger-Pollach[3,4], and P. Haslinger[1,†]

[1]*Vienna Center for Quantum Science and Technology, Atominstitut, TU Wien, Vienna, Austria,*
[2]*IQOQI Vienna, Austrian Academy of Sciences, Vienna, Austria*
[3]*University Service Centre for Transmission Electron Microscopy (USTEM), TU Wien, Vienna, Austria*
[4]*Institute of Solid State Physics, TU Wien, Vienna, Austria*

We recently [1], developed a novel method to separate coherent and incoherent contributions of cathodoluminescence (CL) by using temporal correlations. This technique allows us to unveil different photon generation mechanisms by investigating the arrival time of consecutive photons. While incoherent CL (e.g. resulting from excitation of quantum systems within the sample) exhibits a certain lifetime, coherent CL is produced within the electron – sample interaction time (on the order of femtoseconds). By using a fiber-based Hanbury Brown and Twiss interferometer we recorded the temporal correlations of the photons. Since coherent CL generation is a probabilistic process, each electron has a certain probability to generate one, two or more photons as it interacts with the sample. The strong temporal constraint for coherent CL, posed by the electron – sample interaction time, leads to a pronounced peak in the second order correlation function $g^{(2)}(\tau)$ at $\tau = 0$. This bunching peak can be attributed to coherent interaction mechanisms, as we have confirmed for Cherenkov radiation via an additional measurement (high-tension scanning).

In the here presented data, we studied Cherenkov radiation, which is generated by electrons exceeding the speed of light in the nearby sample. This type of coherent CL exhibits many interesting features. Its emission characteristics can be modified, if we produce these photons in mode-selected geometries [2] such as tinniest Fabry-Pérot cavities or optimized 3D- printed microstructures. Furthermore, electron-photon pairs which are produced by the Cherenkov effect are strongly correlated by energy/momentum conservation, which we will exploit in future experiments.

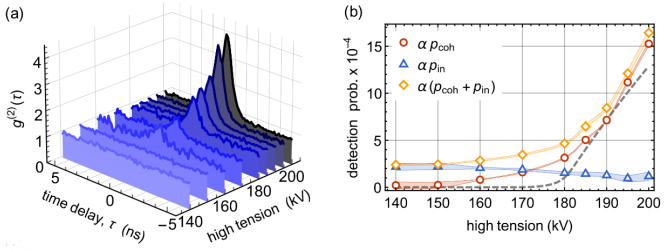

Figure 1. a) Second order correlation function $g^{(2)}(\tau)$ for different settings of the high tension. A pronounced peak appears as the electron energy surpasses the Cherenkov threshold. b) Coherent, incoherent and total photon detection probability, αp_{coh}, α_{pin} and $\alpha(p_{coh} + p_{in})$, respectively, as a function of the applied high tension.

[1] Scheucher M., et al., *arXiv preprint arXiv:2110.05126* (2021)
[2] Auad Y., et al., Nano letters **22**(1) 319 (2021)

* Corresponding author: alexander.preimesberger@tuwien.ac.at
† Corresponding author: philipp.haslinger@tuwien.ac.at

Latest Development in EELS

A. Kastenmüller[1], A.M. Thron[2], L. Spillane[2], R. Twesten[2], A. Pakzad[2], M. Pan[2]

[1]Ametek GmbH, BU EMT (Gatan / EDAX), Unterschleissheim, Edisonstr. 3, Germany
[2]Gatan Inc., Pleasanton, 5794 W Las Positas Blvd., USA

With the advent of aberration-correction, the modern scanning transmission electron microscope (STEM) can routinely achieve sub-Ångstrom resolution. Aberration corrected STEM, in conjunction with electron energy loss spectroscopy (EELS) cannot only resolve compositional changes atom-by-atom, but also changes in the projected unoccupied density of states across an atomic layer. The type and quality of the detector used at the end of energy filter is a key to realizing the full potential of EELS analysis in the TEM. The characteristics of an ideal detector include single electron sensitivity (Quantum efficiency), knowing the spatial location of each electron, elimination of background and readout noise, and a high dynamic range. Previously, detectors in electron microscopy have been based on indirect (scintillator) detection technology with a fiber-coupled CCD or CMOS sensor. In an indirect detector, the scintillator converts an incident electron into photons which are coupled through optic fibers onto the image sensor. The photons are then converted to an electrical charge and read out as a signal. Multiple scattering in the scintillator broadens the point spread function (PSF) of the detector, photon scattering in the optical fiber reduces the signal incident on the sensor, and read-out and noise of the CCD or CMOS sensor further reduces the DQE.

The alternative is a direct detection system in which electrons are directly incident on a radiation-hardened sensor, eliminating the inefficiency of electron-photon conversion process, resulting in an increase in the sensitivity of localized electron detection. Gatan's K3 camera is an example of a monolithic direct detector, with a very thin low-Z material that produces a very sharp point spread function at or above 80kV. However, the PSF in monolithic detectors starts to degrade below 80 kV. To address this, we introduced an integrated hybrid pixel detector (Gatan Stela), optimized for low kV experiments, in the GIF Continuum K3 system. Stela utilizes Dectris' hybrid pixel electron counting technology with single electron sensitivity, excellent PSF ≤ 80kV, extremely high dynamic range owing to the on-the-fly digitization, and high-speed electron counting (>16000 fps). **Figure 1** shows the GIF Continuum system equipped with both K3 and Stela cameras that covers the whole range of TEM voltages from 30 to 300 kV, suitable for a large variety of materials (batteries, polymers, bio- and 2D materials to metals, semiconductors and ceramics).

Here we demonstrate, with selected application examples, how a GIF Continuum K3 and Stela, fully integrated with DigitalMicrograph software, allows for seamless high-quality data acquisition and analysis across all kVs, not only for EELS but also for energy-filtered imaging, diffraction and 4D-STEM experiments.

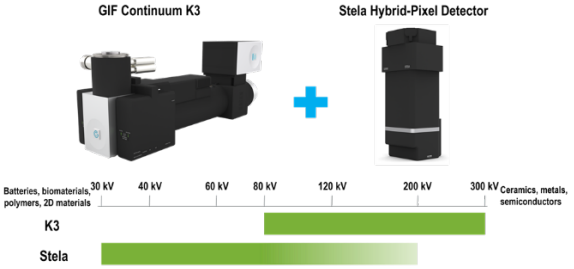

Figure 1. Integrated GIF Continuum K3 system with Stela Camera. Energy-filtered imaging and diffraction for the entire range of 30-300 kV.

Integrated lasers and ultra-fast electrostatic beam blanking systems – Pathways to new experiments in modern transmission electron microscopy

G. Raggl*, P. Wachsmut**

JEOL (Germany) GmbH, Gute Änger 30, 85356 Freising, Germany

In situ TEM is a powerful tool for revealing fundamental nanoscale processes in physics, biology, and materials science. This talk will explore the possibilities for studying laser-driven processes with the help of electrostatic deflection systems that can switch states on the nanosecond scale. In addition, we will highlight new developments involving electrostatic beam blankers, programmable high-speed timing systems, and advanced automation and data analysis.

A recently developed laser module, “Luminary Micro” (JEOL/IDES), facilitates direct focused laser-sample interaction. This has previously successfully been used to show dewetting of gold on a surface, sintering of nanoparticles and more [1]. Two electrostatic optical systems have been developed that can be precisely synchronized with the laser. The first of these, a pre specimen electrostatic dose modulator (EDM), works with a timing control system, “Synchrony” (JEOL/IDES), to enable nanosecond precision definition of electron beam temporal profiles. The second, a post specimen camera subframing system, “Relativity”, (JEOL/IDES) has previously been shown to provide kHz scale fame rates with similarly precise timing control [3].

Together the systems described here, a compact sample laser, a pre-specimen EDM, a post specimen camera subframing deflector, and a precision timing controller enable users to craft scriptable experiment definitions to control all timing aspects of a laser driven *in situ* experiment. From dose rate to heating profiles to camera frame rate, users can decide how their experimental conditions will evolve with nanosecond precision.

[1] B. W. Reed, A. A. Moghadam, R. S. Bloom, S. T. Park, A. M. Monterrosa, P. M. Price, C. M. Barr, S. A. Briggs, K. Hattar, J. McKeown, and D. J. Masiel, Struct. Dyn. **6**, 054303 (2019)

[2] https://www.jeol.co.jp/en/products/detail/LuminaryMicro.html

[3] B. W. Reed, S. T. Park, R. S. Bloom, and D. J. Masiel, Microsc. Microanal. **23** (S1), 84 (2017)

* Corresponding author: raggl@jeol.de

** Corresponding author: wachsmuth@jeol.de

EDAX + GATAN

Refine and sharpen your EBSD results

See how the high-speed EBSD detectors from EDAX, when combined with the specimen preparation capabilities of Gatan, can provide EBSD results that will lead to improved flexibility of magnesium alloys to be used more frequently and economically in automotive applications. A refined EBSD analysis permits statistical data on grain size and grain texture, both of which are essential parameters in determining crystalline materials' strength.

To discover more about EBSD detectors and specimen preparation, visit EDAX.com and Gatan.com, respectively.

AMETEK®

Friday, April 22nd, 2022

SESSION 6

14:45	*Fritz Grasenick Laureate*: **Noisternig Stefan** / University of Vienna *In situ STEM analysis of electron beam induced chemical etching of an ultra-thin amorphous carbon foil by oxygen during high resolution scanning*
15:00	**Åhlgren E. Harriet** / University of Vienna *Electron microscopy in gas atmospheres: exploring the role of oxygen in the degradation of 2D materials*
15:15	**Šimić Nikola** / FELMI- ZFE Graz *Phase Analysis of (Li)FePO4 by Selected Area Electron Diffraction in Transmission Electron Microscopy*
15:30	**Huang Yong** / Erich Schmid Institute of Materials Science Leoben *Stacking faults dominant strengthening mechanism behind the anomalous hardness variation of TaN/TiN multilayer films*
15:45	Closing Ceremony and Farewell

In situ STEM analysis of electron beam induced chemical etching of an ultra-thin amorphous carbon foil by oxygen during high resolution scanning

S.N. Noisternig[1,2*], C. Rentenberger[1], H.P. Karnthaler[1]

[1]*Physics of Nanostructured Materials, University of Vienna, Boltzmanngasse 5, 1090 Vienna, Austria*
[2]*Erich Schmid Institute of Materials Science, Austrian Academy of Sciences, Jahnstrasse 12, 8700 Leoben, Austria*

State of the art imaging methods using corrected (scanning) transmission electron microscopy ((S)TEM) make it possible to carry out high resolution studies at low acceleration voltages (of 80 kV and below) with low electron fluxes which is especially of advantage for beam sensitive materials. The latter are often carbon based and to be able to achieve ultimate resolution ultra-thin amorphous carbon foils (thickness < 5 nm) are frequently used as support foil. In our study we analyze *in situ* the effect of chemical etching of a 2 nm amorphous carbon foil by leaking in oxygen into the microscope column at different electron fluxes for 55 and 80 kV acceleration voltages, respectively [1].

The Nion STEM used in this study operates normally at ultra high vacuum (UVH) of $\sim 5 \times 10^{-10}$ mbar. It is equipped with a leak valve for leaking in gases. It was used for cleaning of graphene from carbon based contamination by chemical etching [2]. In the present study we leak in O_2 at three different pressures (P1 – P3) between 0.7 x 10^{-7} and 7.0 x 10^{-7} mbar while operating at high resolution scanning conditions for electron irradiation of the amorphous carbon foil at three mean electron flux conditions (F1 – F3) between 3.0 x 10^6 and 13.5 x 10^6 e/nm^2 (set by the size of the scan area). The mean thickness of the amorphous carbon foil is then calculated from high angle annular dark field (HAADF) images in dependence of the irradiation time using the linear relation between HAADF intensity and sample thickness (c.f. **Figure 1**). To obtain a reference sample thickness for HAADF intensities we apply a Kramers–Kronig analysis of electron energy loss spectra [3] acquired in a FEI Titan 80-300 TEM.

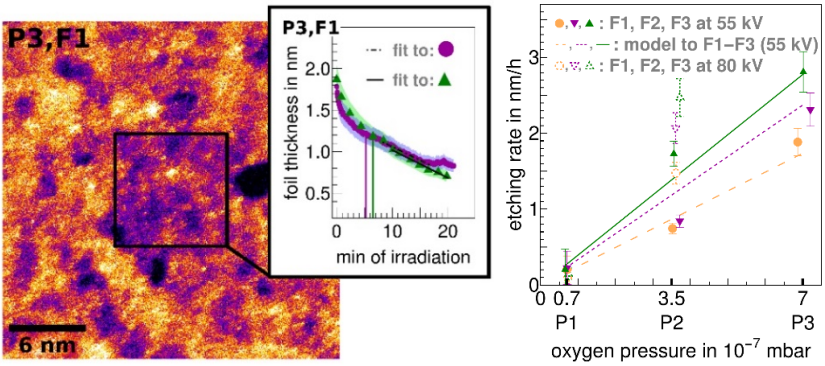

Figure 1. HAADF image of the ultra-thin amorphous carbon foil showing a continuously irradiated region (marked) and its time dependent thickness reduction in an overlay. In the diagram on the right the etching rates of all experimental conditions are displayed after subtraction of the sputtering contributions as resulting from UHV data. They are compared to the model (three lines). [1]

*Corresponding author: stefan.noisternig@univie.ac.at

During our chemical etching experiments we observe a linear decrease in foil thickness with irradiation time; this occurs after an initial rapid thickness decrease by residual bound oxygen [2] is subsided (c.f. overlay in **Figure 1**). The effect of chemical etching is distinguished from sputtering by knock-on damage using irradiation series acquired at UHV conditions. We generate a scanning etching model by combining an electron beam induced etching model from literature including adsorption and thermal desorption of O_2 [4] with the scanning routine of the Nion STEM. In this continuous model the observed weak dependency of the etching rate on electron flux is explained by the fact the depletion of adsorbed O_2 is already caused by the tails of the electron beam before it dwells on the considered scan position.

The resulting etching rates displayed in **Figure 1** showing that electron beam induced chemical etching is the dominant process of removing carbon atoms from an ultra-thin amorphous carbon foil at acceleration voltages of 80 kV and below. The O_2 concentration in the column and residual oxygen on the sample surface play a significant role for the lifetime of the foil. By introducing a scanning etching model we emphasize the importance of scan routines and scan parameters for processes that can be triggered at low electron fluxes.

[1] S.M. Noisternig, C. Rentenberger, H.P. Karnthaler, Ultramicroscopy, **235**, 113483 (2022)
[2] G.T. Leuthner, S. Hummel, C. Mangler, T.J. Pennycook, T. Susi, J.C. Meyer, J. Kotakoski, Ultramicroscopy, **203**, 76–81 (2019)
[3] R.F. Egerton, Energy-Loss Spectroscopy In The Electron Microscope, Plenum Press, New York(1996)
[4] M.G. Lassiter, P.D. Rack, Nanotechnology, **19** (45), 455306 (2008)

Curriculum Vitae

Stefan Manuel Noisternig, born on 21.02.1989, Villach, Austria

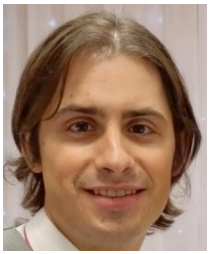

Education: Physics of Nanostructured Materials,
University of Vienna:
2016-ongoing PhD candidate, supervised: Christian Rentenberger
17.06.2016 MSc Physics: *Structural and elemental analysis of individual nanocrystals embedded in an amorphous matrix by transmission electron microscopy*, supervised: Christian Rentenberger

Academic work experience
project collaborator in the FWF projects:
2021-ongoing Nanoscale strain mapping of metallic glass composites
project lead: Christoph Gammer
Erich Schmid Institute of Materials Science, Austrian Academy of Sciences
2013-2018 Structural inhomogeneities in bulk metallic glasses
project lead: Christian Rentenberger
Physics of Nanostructured Materials, University of Vienna
2019-2020 teaching assistant at the University of Vienna

International conference presentations
MSE 2018 Darmstadt, ISCoC 2018 Erice, DPG spring meeting 2018 Berlin, MCM 2017 Rovinj

Poster Awards: ISCoC 2018 Erice, MCM 2015 Eger, MC 2013 Regensburg

Electron microscopy in gas atmospheres: exploring the role of oxygen in the degradation of 2D materials

E. H. Åhlgren*, A. Markevich, S. Scharinger, C. Mangler, J. Kotakoski

Faculty of Physics, University of Vienna, Boltzmanngasse 5 1090 Wien, Austria

Oxidation in ambient conditions can cause serious degradation in materials affecting their structure and properties. Understanding this behavior is important when planning the use of new materials. We study the chemical effects of oxygen in 2D transition metal dichalcogenides *in situ* in aberration corrected Nion UltraSTEM 100 electron microscope operated at controlled low pressure oxygen environments [1]. By directly observing the atomic scale dynamics, we show clear evidence of the oxidation related structural changes in 2D materials.

In $MoTe_2$ the interactions with oxygen lead to vacancy and pore formation at pressures above $1x10^{-7}$ torr. The damage is observed outside of the continuous imaging area. The process is accelerated by amorphous hydrocarbon contamination that is common on all surfaces. In comparison, MoS_2 is inert in all the measured oxygen partial pressures and any observed structural changes are caused by the interactions with the electron beam.

Our computational analysis reveals a possible mechanism for the oxygen mediated degradation in $MoTe_2$, and explores the role of the carbon based contamination in the etching process.

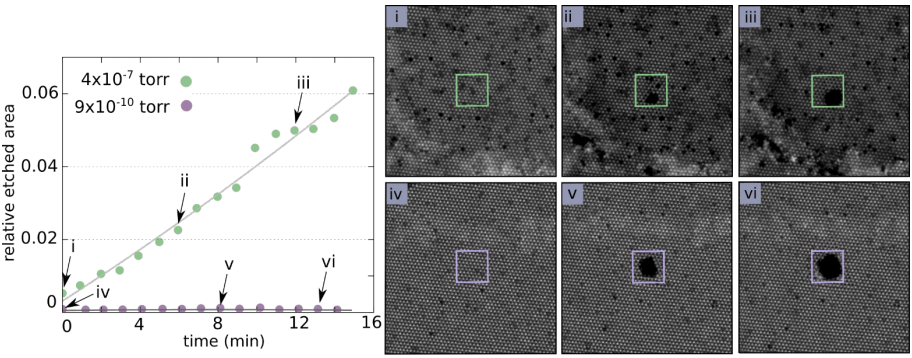

Figure 1. Relative etched area in $MoTe_2$ when oxygen is introduced into the microscope objective area (green) and without oxygen (purple). STEM HAADF images of the sample surface correspond to the points marked with arrows in the plot. The green and purple squares denote the continuous imaging area excluded from the analysis. Surrounding area (20x20 nm) is scanned once per minute to minimise the effects caused by the electron beam.

[1] G.T. Leuthner, S. Hummel, C. Mangler, T.J. Pennycook, T. Susi, J.C. Meyer, J. Kotakoski, Ultramicroscopy, **203,** 76-81 (2019)

* Corresponding author: harriet.ahlgren@univie.ac.at

Phase Analysis of (Li)$FePO_4$ by Selected Area Electron Diffraction in Transmission Electron Microscopy

N. Šimić[1*], D. Knez[2], I. Hanzu[3], W. Grogger[2]

[1]*Graz Centre for Electron Microscopy (ZFE), Graz, Austria*
[2]*Institute of Electron Microscopy and Nanoanalysis, Graz University of Technology, Graz, Austria*
[3]*Institute for Chemistry and Technology of Materials, Graz University of Technology, Graz, Austria*

Lithium iron phosphate ($LiFePO_4$) is a well-studied compound with a lot of promise as cathode material in rechargeable batteries. Due to its low cost, low toxicity, safety and the abundance of iron LFP is considered a very attractive energy storage option for the automotive industry.

$LiFePO_4$ has an orthorhombic crystal structure with Pnma space group [1]. During the discharge process lithium intercalates from a graphite anode into the $FePO_4$ cathode, where it is stored in between FeO_6 octahedra and PO_4 tetrahedra, thus slightly changing the lattice vector length of the unit cell while maintaining the same crystal structure as seen in figure 1.

To better understand the lithium deintercalation process various studies were performed with methods such as x-ray diffraction [2], precession diffraction [3] and transmission x-ray microscopy (TXM) [4] to identify charged and discharged (L)FP particles by measuring lattice spacings.

This work shows the identification process of (Li)$FePO_4$ particles via selected area electron diffraction (SAED) with comparison of theoretical calculations of respective crystal models. SAED patterns have been recorded for numerous particles with size of approximately 200 nm in either lithiated ($LiFePO_4$) or delithiated ($FePO_4$) samples with results matching expectations. Through rigorous experiments the presented methodology has been deemed reliable, therefore these results pave the way for future comparisons of (L)FP materials with differing synthetization methods.

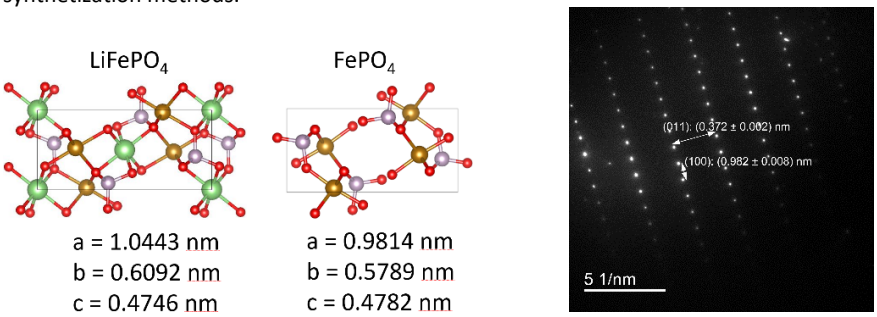

Figure 1. Showing the $LiFePO_4$ and $FePO_4$ models in a). Identifying a particle as $FePO_4$ by comparing lattice spacing of vector a in b). The vector matches the expected theoretical value within error estimates.

[1] T.V.S.L. Satyavani, A. Srinivas Kumar, P.S.V. Subba Rao, et. al., Engineering Science and Technology, an International Journal, **19** (1), 178-188 (2016)
[2] C. Delmas, M. Maccario, L. Croguennec, et. al., Nature Materials, **7** (1), 665–671 (2008)
[3] G. Brunetti, D. Robert, P. Bayle-Guillemaud, et. al., Chem. Mater., **23** (20), 4515-4524 (2011)
[4] W.C. Chueh, F. E. Gabaly, J. D. Sugar, et. al., Nano Lett., **13** (3), 866-872 (2013)

* Corresponding author: nikola.simic@felmi-zfe.at

Stacking faults dominant strengthening mechanism behind the anomalous hardness variation of TaN/TiN multilayer films

Y. Huang[1,2], Z. Chen[1], V. Terziyska[2], C. Mitterer[2], Z. Zhang[1,2*]

[1]*Erich Schmid Institute of Material Science, Austrian Academy of Sciences, Jahnstraße 12, 8700 Leoben, Austria*
[2]*Department of Materials Science, Montanuniversität Leoben, Franz-Josef-Straße 18, 8700 Leoben, Austria*

Multilayered materials, which consist of the periodic alternation of different layers, can realize drastic hardness enhancement when the individual layer thickness decrease to nanoscale. Numerous literatures suggested that bilayer period plays a key role in determining the enhancement of hardness and elastic modules for multilayer films. Extensive investigations also reveal several commonly accepted strengthening mechanisms including dislocation pile-ups, coherent stresses, misfit dislocations, elastic moduli mismatch or Koehler stress and the confined layer slip (CLS) model [1–4]. Among superlattice transition metal nitrides systems TaN/TiN show great potential due to their high hardness and good wear resistance.

In this work, TaN/TiN superlattice films with four bilayer periods Λ were synthesized by reactive magnetron sputtering. The hardness measurement by nanoindentation and X-ray diffraction (XRD) patterns both show that these TaN/TiN multilayer films exhibit an inverse trend in hardness and interfacial coherency compared to previous studies. These thin films were then characterized by spherical aberration-corrected (Cs-corrected) transmission electron microscopy (TEM, JEOL 2100F). Detailed high-resolution TEM (HRTEM) studies revealed that high density of stacking faults appeared in Λ= 20 nm sample (**Figure 1**a) and abundant stacking faults cannot only enhance the hardness but also relieve the interfacial stress.

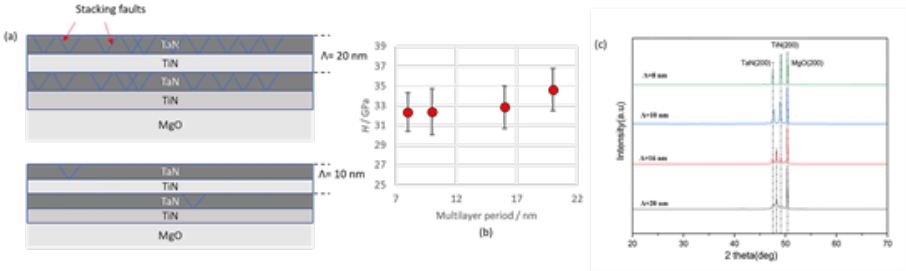

Figure 1. (a) Schematic of TaN/TiN multilayer films with Λ= 20 nm and Λ= 10 nm (b) nanoindentation hardness and (c) XRD patterns of TaN/TiN films with different bilayer period.

[1] N. Patel, S. Wang, A. Inspektor, P.A. Salvador, Surface and Coatings Technology **254**, 21 (2014)
[2] R. Daniel, M. Meindlhumer, J. Zalesak, W. Baumegger, J. Todt, T. Ziegelwanger, J.F. Keckes et al., Materials & Design **196** (2020)
[3] H. Wang, X. Zhang, A. Gupta, A. Tiwari, J. Narayan, Applied physics letters **83**, 3072 (2003)
[4] M. Nordin, F. Ericson, Thin Solid Films **385**, 174 (2001)

* Corresponding author: zaoli.zhang@oeaw.ac.at

POSTER PRESENTATIONS

HR-(S)TEM Sample Preparation of Semiconducting Materials

A. Alatrash*, W. Grogger, E. Fisslthaler, M. Dienstleder

Graz Centre for Electron Microscopy (ZFE) & Institute for Electron Microscopy and Nanoanalysis (FELMI), Graz University of Technology, Steyrergasse 17, 8010 Graz, Austria

High-resolution scanning transmission electron microscopy (HR-STEM) samples are mostly prepared using Focused Ion Beam (FIB) milling. The aim of this work is to provide an alternative preparation routes for semiconducting materials using mechanical and ion thinning techniques. Samples of silicon, silicon germanium and gallium nitride are prepared. A general route is applied to understand the materials, and an alternative route (using the MultiPrep™ Polishing System from Allied High Tech) has been implemented based on the type and the characteristics of the sample material. Filtered and unfiltered bright field images are recorded from each sample, and t/λ graphs are extracted. These graphs provide an estimate of the sample thickness in relation to the mean-free path using the Log-Ratio-Method [1]. Based on the recorded t/λ maps, a conclusion and an optimal preparation route is recommended for each material prepared.

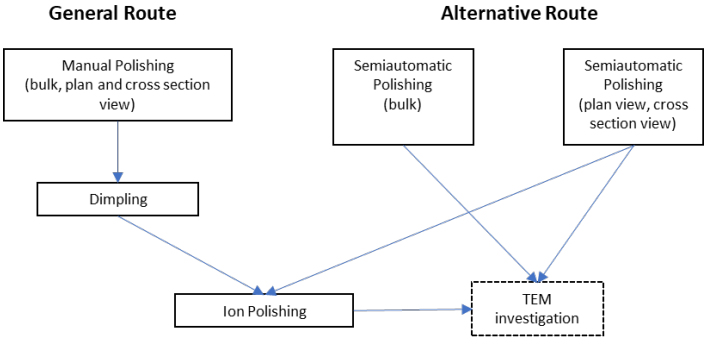

Figure 1. Overview of preparation routes implemented

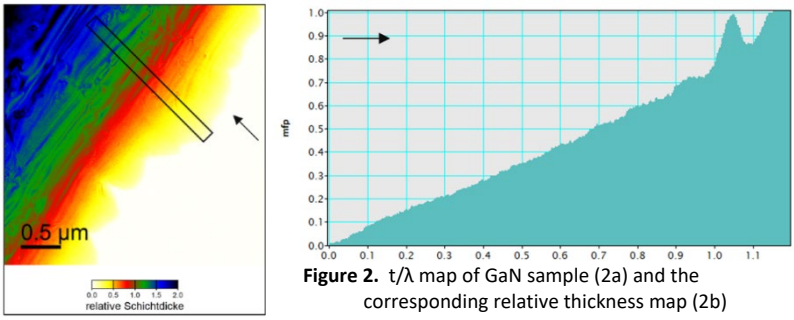

Figure 2. t/λ map of GaN sample (2a) and the corresponding relative thickness map (2b)

[1] R. F. Egerton, "TEM Applications of EELS," in *Electron EnergyLoss Spectroscopy in the Electron Microscope*, Springer, 293 (2011)

* Corresponding author: anas.alatrash@felmi-zfe.at

Strain engineering in GaδFeN / $Al_{0.1}Ga_{0.9}N$ heterostructures

A. Brozyniak[1]*, T. Truglas[1], A. Bonanni[2], A. Navarro-Quezada[2], H. Groiss[1]

[1]*Christian Doppler Laboratory for Nanoscale Phase Transformations, Center for Surface and Nanoanalytics, Johannes Kepler University Linz, Altenberger Str. 69, 4040 Linz, Austria*
[2]*Institute of Semiconductor and Solid State Physics, Johannes Kepler University Linz, Altenberger Str. 69, 4040 Linz, Austria*

Threading dislocations (TDs) in III-nitrides originate from a considerable lattice mismatch with the common single-crystal substrates, *e.g.* sapphire. Over the last years, much attention was paid to enhance the crystalline film quality by reducing the number of dislocations. However, for some applications a deliberate increase and control over the TDs through strain engineering can be desirable. An example is the hybrid material system Fe_yN nanocrystals (NCs) embedded in phase-separated GaδFeN layers, combining semiconductors and magnetic nanostructures (**Figure 1**). The magnetic easy axis orientation of these cubic Υ'-$Ga_yFe_{4-y}N$ and hexagonal ε-Fe_3N NCs differ in respect to the GaN matrix. As the TDs act as NCs nucleation sites, the strain-related TD density influences the ratio of the cubic and hexagonal NCs and allows to control the magnetic properties of the entire system [1].

In this work, transmission electron microscopy (TEM) investigations are presented that reveal these influences of the strain on the Fe_yN NC precipitation and the final NC density and ratios for samples where the strain-related TD density is controlled by the Al concentration in $Al_xGa_{1-x}N$ buffer layers. An outlook of a possible detailed analysis of the underlying strain by precession electron diffraction (PED) is given. Additionally, the dislocations can be influenced by an additional AlN interlayer, acting as a dislocation stopping barrier. This could lead to an even better controllability of the dislocation precipitation sites. First results of a detailed TEM dislocation analysis in such samples are presented.

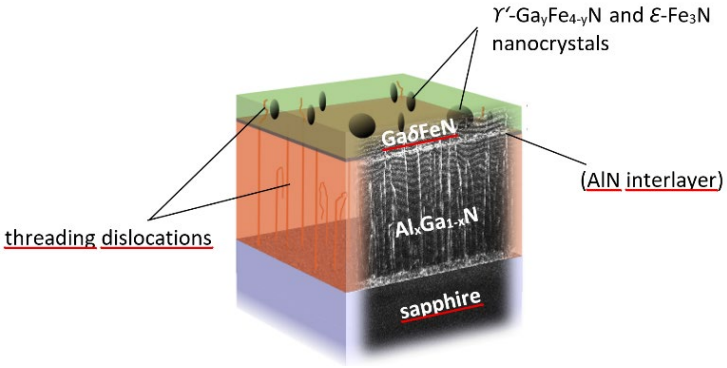

Figure 1. Structure of the investigated system: $Al_xGa_{1-x}N$ buffer layers grown on sapphire. An optional AlN interlayer can further influence the dislocation density, affecting the nanocrystals in the topmost GaδFeN layer. A **g**-3**g** weak-beam dark field image features the dislocations stopped by the AlN interlayer.

[1] A. Navarro-Quezada, K. Gas, T. Truglas, V. Bauernfeind, M. Matzer, D. Kreil, A. Ney, H, Groiss, M. Sawicki, A. Bonanni. *Materials*, **13**, 3294 (2020)

* Corresponding author: aleksander.brozyniak@jku.at

Electron beam shaping using light

M.C. Chirita Mihaila[1,2,3*], M. Schneller[1,3], L. Grandits[1,3], P. Weber[1,3], S. Nimmrichter[4], and T. Juffmann[1,3]

[1]*University of Vienna, Faculty of Physics, VCQ, A-1090 Vienna, Austria*
[2]*University of Vienna, Vienna Doctoral School in Physics, A-1090 Vienna, Austria*
[3]*University of Vienna, Max Perutz Laboratories, Department of Structural and Computational Biology, A-1030 Vienna, Austria*
[4]*Naturwissenschaftlich-Technische Fakultät, Universität Siegen, Walter-Flex-Straße 3, 57068 Siegen, Germany*

The precise control of electron wave functions is at the heart of high resolution electron microscopy, where complex multipole lenses [1] have enabled sub-A spatial resolution. Electron wave-front shaping techniques have been demonstrated mostly based on transmission through thin film materials [2] or through optical fields in the vicinity of matter [3]. Limiting factors are associated with inelastic scattering and beam-induced deterioration. Recently, single pixel phase shifting of electrons was realized in free space [4], which offers unity transmission, adjustability and no inelastic scattering.

Here we show programmable electron beam shaping in free space by using intense laser patterns, which we shape using a spatial light modulator (SLM) [5]. We realize the experiment in a modified scanning electron microscope where the electron beam interacts with a counter-propagating laser pulse. We demonstrate both positive and negative pondemorotive lensing, achieving focal lengths of a few millimeters, similar to those in state of the art traditional electromagnetic lenses.

[1] H. H. Rose, Journal of electron microscopy **58**, 77 (2009)
[2] D. Roitman, R. Shiloh, P. H. Lu, R. E. Dunin-Borkowski, and A. Arie, ACS Photonics **8**, 3394 (2021).
[3] O. Reinhardt and I. Kaminer, ACS Photonics **7**, 2859 (2020).
[4] O. Schwarz, J. J. Axelrod, S. L. Campbell, C. Turnbaugh, R. M. Glaeser, and H. Müller, Nature methods **16**, 1016 (2019).
[5] https://arxiv.org/abs/2203.07925

* Corresponding author: marius.chirita@univie.ac.at

Imidazole-Osmium mediated Freeze Substitution conserves Lipid Structures in Rat Hepatic Tissue

S. Dürr[1]*, S. Reipert[2], C. Fürnsinn[1], N. Cyran[2], D. Gruber[2]

[1]*Department of Medicine III, Medical University of Vienna, Spitalgasse 23, 1090 Vienna, Austria*
[2] *Core Facility Cell Imaging and Ultrastructural Research, University of Vienna, Djerassiplatz 1, 1030 Vienna, Austria*

Sample preparation for semi-correlative TEM (transmission electron microscopy) -NanoSIMS (Nanoscale Secondary Ion Mass Spectrometry) studies in animal tissue requires minute handling and an elaborate protocol. Structures of interest, such as lipid droplets, have to stay intact and elution of intracellular substances has to be avoided. Our initial approach resulted in samples with electron-lucent lipid droplets as a result of the elution of lipids. Therefore, we developed a hybrid protocol in combination with cryopreparation techniques.

Imidazole, a highly polar heterocyclic compound, has been shown to enhance the binding ability of osmium tetroxide to lipids and thereby improving their visualization in TEM [1]. However, a supplementary step of osmium-imidazole (1% OsO_4 in 0.1M imidazole) osmification before high-pressure freezing (HPM100, LEICA Microsystems) and freeze substitution (AFS2, LEICA Microsystems) with sample agitation [2] was not sufficient for preservation of the homogeneous content of lipid droplets in rat hepatic tissue **(Figure 1A)**.

To overcome this problem, we added 1% OsO_4 in 0.1M imidazole to the substitution medium, acetone, and developed an appropriate freeze-substitution protocol. By doing so, a significant improvement in preservation was achieved, resulting in homogeneously osmificated lipid droplets **(Figure 1B)**. We suggest that osmium-imidazole prevented the elution of lipid content during the warm-up phase of the freeze substitution protocol. Further investigations including NanoSIMS will be conducted to confirm this hypothesis.

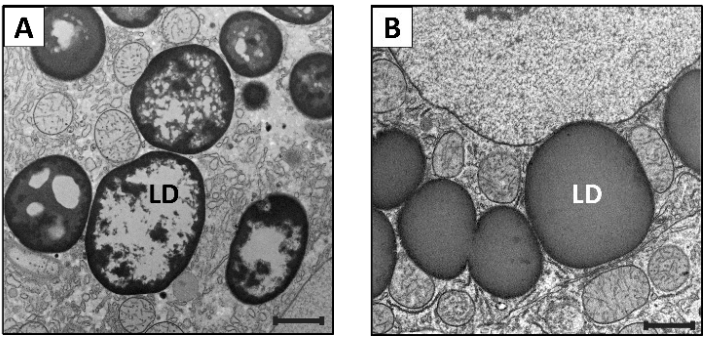

Figure 1. Steatotic rat hepatic tissue A) Lipid droplets (LD) after conventional freeze substitution exhibiting heterogeneous, holey content. B) Entirely homogenous lipid droplets after osmium-imidazole mediated freeze substitution. Scale bar indicates 1 µm.

[1] S. Angermüller, H. D. Fahimi, The Histochemical journal, **14** (5), 823 (1982)
[2] S. Reipert, H. Goldammer, et al., J Histochem Cytochem, **66** (12), 903 (2018)

* Corresponding author: sabine.duerr@meduniwien.ac.at

Tomography of surface phonon polariton fields by electron energy loss spectroscopy

R. Hauer[1]*, U. Hohenester[2], G. Kothleitner[1,3], G. Haberfehlner[1]

[1]*Institute of Electron Microscopy and Nanoanalysis, Graz University of Technology 8010 Graz, Austria*
[2]*Institute of Physics, University of Graz, Universitätsplatz 5, 8010 Graz, Austria*
[3]*Graz Centre for Electron Microscopy, Steyrergasse 17, 8010 Graz, Austria*

Surface phonon polaritons are coupled photon-phonon excitations that emerge at the surfaces of dielectric ionic nanostructured materials. Using a highly monochromated electron beam in a scanning transmission electron microscope, EEL spectrum images from a nanoscale MgO bipyramid are recorded as a function of tilt angle. This tilt series can be used as the basis for tomographically reconstructing the complete three-dimensional (3D) vectorial picture of the local photonic density of states (LDOS) [1]. To back up the obtained experimental results, a detailed examination of the reconstruction process using simulations is necessary. Knowing the full 3D LDOS promises insights into nanoscale physical phenomena and is invaluable to the design and optimization of nanostructures for fascinating new uses.

In this work, we perform a thorough examination of the tomography scheme introduced in [1]. Tomographic reconstruction of the LDOS is done by means of minimizing the difference between reprojected EELS maps of a reference structure and the simulated (or measured) EELS maps of the real structure (**Figure 1**). The reprojected maps are calculated based on an eigenmode decomposition, dependent on the used reference structure. In simulation studies, we consider the impact of the choice of reference structure and the type of eigenmodes used. Finally, we apply these findings to the 3D reconstruction of experimental EELS data [2].

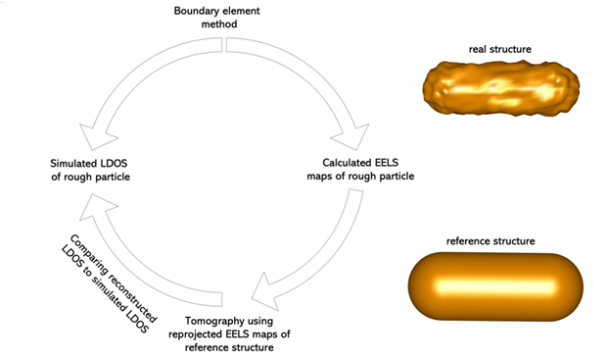

Figure 1. We use the boundary element method to calculate EEL spectrum images and the LDOS. To examine the reconstruction process, we compare the simulated LDOS to the reconstructed LDOS.

[1] X. Li, G. Haberfehlner, U. Hohenester, et al. Science, **371** (6536), 1364 (2021)

We thank X. Li and M. Kociak from Université Paris-Saclay, CNRS-LPS Orsay, France for providing experimental data. This project has received funding from the European Union's Horizon 2020 Research and Innovation Program under grant agreements 823717 (ESTEEM3)

* Corresponding author: raphael.hauer@felmi-zfe.at

Sub-nm defect patterning of graphene with a STEM

D. Imrich*, M. Längle, J. Kotakoski

Faculty of Physics, University of Vienna,
Boltzmanngasse 5, 1090 Vienna, Austria

Defects are typically introduced into monolayer graphene without spatial control by irradiating the sample with ions [1], or as a result of electron irradiation damage [2]. While patterning of defects can also be achieved with a focused ion beam [3] or a helium ion microscope [4], the electron probe in an aberration-corrected scanning transmission electron microscope provides the possibility for down to sub-nanometer accuracy.

In this study, we use the Nion UltraSTEM 100 in Vienna at 100keV to pattern defects into monolayer graphene. To do this, we develop and test a software plug-in based on an earlier imaging plug-in [5] written for Nion Swift [6] that allows us to precisely control the electron beam following a pre-determined pattern to "write" structures consisting of vacancies into the graphene lattice. In further work, we would like to try introducing heteroatoms into these vacancies, similar to Ref. [7, 8].

[1] A. Trentino, J. Madsen, A. Mittelberger, C. Mangler, T. Susi, K. Mustonen and J. Kotakoski, Nano Letters, **21** (12), 5179 (2021)
[2] J. Kotakoski, A. V. Krashennikov, U. Kaiser and J. C. Meyer, Physical Review Letters, **106**, 105505 (2011)
[3] J. Kotakoski, C. Brand, Y. Lilach, O. Cheshnovsky, C. Mangler, M. Arndt and J. C. Meyer, Nano Letters, **15** (9), 5944 (2015)
[4] D. Emmrich, A. Beyer, A. Nadzeyka, S. Bauerdick, J. C. Meyer, J. Kotakoski and A. Gölzhäuser, Applied Physics Letters, **108**, 163103 (2016)
[5] A. Mittelberger, C. Kramberger, C. Hofer, C. Mangler and J. Meyer, Microscopy and Microanalysis, **23** (4), 809 (2017)
[6] https://github.com/nion-software/nionswift, accessed March 24th, 2022.
[7] H. Inani, K. Mustonen, A. Markevich, E-X. Ding, M. Tripathi, A. Hussain, C. Mangler, E. Kauppinen, T. Susi and J. Kotakoski, Journal of Physical Chemistry C, **123**, 13136 (2019)
[8] A. Trentino, K. Mizohata, G. Zagler, M. Längle, K. Mustonen, T. Susi, J. Kotakoski and E. H. Åhlgren, 2D Materials, **9**, 020511 (2022)

*Corresponding author: daniel.imrich@univie.ac.at

Atom by Atom analysis of complex oxide materials

D. Knez[1*], A. Kobald[1], F. Hofer[1,2], G. Kothleitner[1,2]

[1]*Institute of Electron Microscopy and Nanoanalysis, Graz University of Technology, Graz, Austria*
[2]*Graz Centre for Electron Microscopy, Graz, Austria*

Complex oxide materials are of high technological relevance due to their wide range of electronic and magnetic properties. These properties are often determined by strong correlation effects of the d or f orbital electrons and can be tailored by introducing already small amounts of dopants and/or vacancies.

Information about the structural/electronic configuration of such defects is, therefore, vital for the understanding of the properties of these materials.

In this context, aberration-corrected scanning transmission electron microscopy (STEM) has proven to be a valuable tool for the characterization of the crystal structure of oxide materials [1,2]. Direct access to the position and electronic behavior of point defects is, however, still challenging, especially at low dopant concentrations and with the presence of vacancies.

On the example of **Ta doped (0.01 wt.%) STO**, we develop a methodology for the detection of individual atoms and point-defect structures in oxides by **quantitative analysis of STEM HAADF** images (**Figure 1**) and comparison with multislice simulations based on atomistic simulations. Due to the low thickness of the sample (< 5 nm), assessed by position averaged convergent electron beam diffraction (PACBED), even surface steps and defects can be discerned from the images and the sample surface morphology needs to be considered [3].

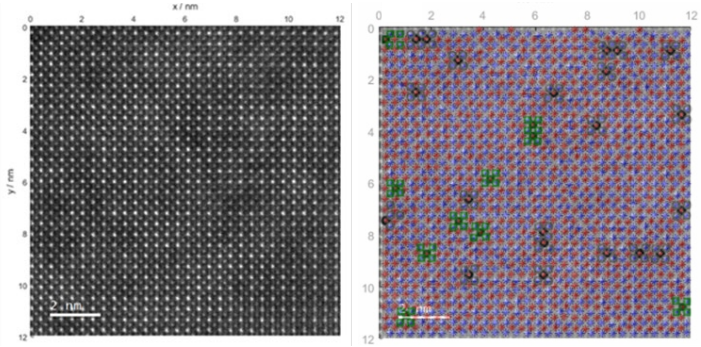

Figure 1. STEM HAADF image of STO:Ta (left) with corresponding intensity analysis of atomic columns (right). Columns with lower intensity are marked green (A site vacancies) and with higher intensity black (dopants at B sites).

[1] D. Knez et al., Nano letters, **20** (9) 6444 (2020)
[2] J. Hwang et al., Physical review letters, **111** (26) 266101 (2013)
[3] T. Furnival et al., Appl. Phys. Lett, **113** (18), 183104 (2018)

The authors acknowledge financial support by the European Union's Horizon 2020 research and innovation program under Grant 823717-ESTEEM3.

* Corresponding author: daniel.knez@felmi-zfe.at

Characterization of platinum diselenide thin films using STEM

C. Kofler[1]*, M. Sojková[2], V. Skakalova[1], J. Kotakoski[1]

[1]*Physics of Nanostructured Materials, University of Vienna, Boltzmanngasse 5, 1090 Vienna, Austria*
[2] *Institute of Electrical Engineering, Slovak Academy of Sciences, Dúbravská cesta 9, 84104 Bratislava, Slovakia*

In this work a platinum diselenide ($PtSe_2$) thin film was analyzed according to its atomic structure, polycrystallinity and surface coverage.

The sample was synthesized by one zone selenization of pre-deposited platinum on a SiO_2 substrate with reduced graphene oxide [1] and then transferred to a *Quantifoil* TEM grid and images of different magnifications were recorded using high-angular annular dark field transmission electron microscopy (HAADF-STEM) at an aberration corrected Nion *UltraSTEM 100* at 60 keV. The atomic resolution images were compared to simulations created using the python environment *abTEM* [2] and the *Atomic Simulation Environment* [3].

The octahedral 1T phase was found to be predominant in the material with approximately 82% of the images showing this structure. Additionally, parts of the sample showed 3R and N phases, all of which corresponded well to the respective simulations. The sample showed polycrystalline character with grain sizes ranging between 50 nm^2 and 1780 nm^2 and a mean grain size of about 355 nm^2. The surface coverage of the sample lies at about 83 %.

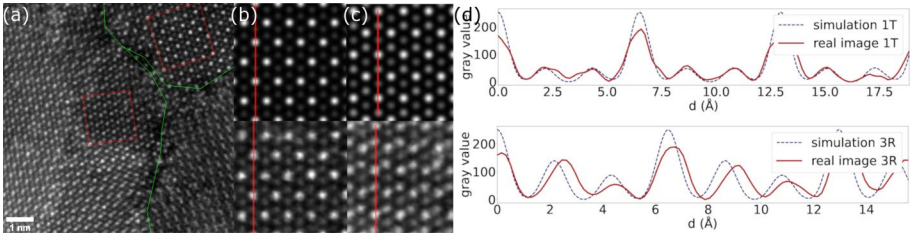

Figure 1. Comparison of simulated and observed 3R and 1T structure. (a) Image with 3R and 1T structure on the left and right side of the green line respectively; (b) simulated and real 3R structure; (c) simulated and real 1T structure; (d) comparison of the line scans indicated in red in (b) and (c) of the simulated and the observed structure.

[1] Sojková, M. et al., Appl. Surf. Sci., **538**, 147936 (2021)
[2] J. Madsen, T. Susi, Open Research Europe, **1**, *13015* (2021)
[3] Larsen, A. H. et al., Journal of Physics: Condensed Matter, **29**, 273002 (2017)

*Corresponding author: clara.kofler@univie.ac.at

Electron Tomography in a correlative approach to multimodal characterization of human bone

T. Kormilina[1,2*], S. Englisch[1], D. Drobek [1], T. Kochetkova[3], J. Schwiedrzik [3], E. Spiecker [1]

[1]*Institute of Micro- and Nanostructure Research (IMN) and Center for Nanoanalysis and Electron Microscopy (CENEM), FAU Erlangen-Nürnberg, Cauerstr.3, 91058 Erlangen, Germany*
[2]*Graz Centre for Electron Microscopy (ZFE) & Institute for Electron Microscopy and Nanoanalysis (FELMI), Graz University of Technology, Steyrergasse 17, 8010 Graz, Austria*
[3]*Empa, Swiss Federal Laboratories for Materials Science and Technology, Laboratory for Mechanics of Materials & Nanostructures, Feuerwerkerstr. 39, 3603 Thun, Switzerland*

Researches are often interested in materials with complex hierarchal 3D structure. One such familiar and abundant material is mammal cortical bone. For most of the bone investigation history, the conclusions about the 3D arrangement of its constituents were drawn from 2D slices. 3D imaging techniques can give a direct and illustrative answer to the inquiry that can be further adopted in subsequent medical procedures and biotechnological projects. One characterization trend that has emerged in the last years is extending and connecting the 3D structural study with that of a connected bone property [1]. On the other hand, the use of several complementary techniques in one study is gaining precedents [2].

We have reported a multimodal correlative approach for investigation of collagen fibril orientation combining quantitative polarized Raman spectroscopy (qPRS) with nanoscale X-ray computed tomography (nano-CT) and 360° HAADF STEM tomography (ET) [3]. ET plays a key role connecting micro- and nanostructure, resolving both the complex mineral crystal organization and MCF orientation from the collagen molecule d-spacing pattern.

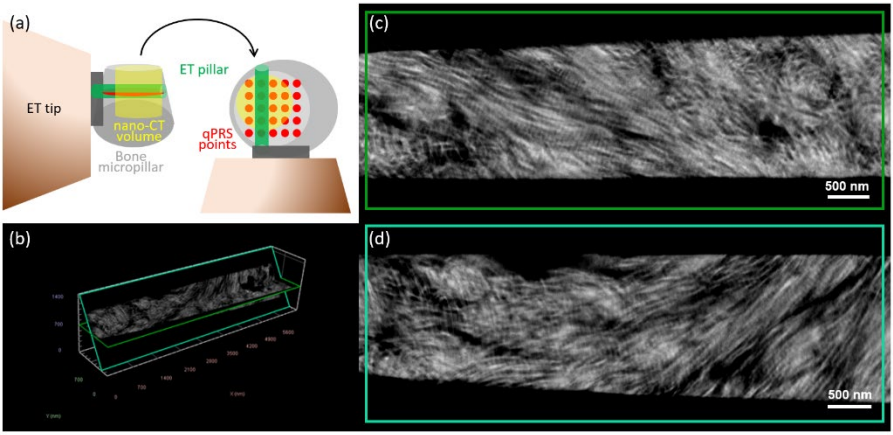

Figure 1. Correlative electron tomography – a) multimodal characterization scheme showing the position of ET volume, b) ET volume featuring c,d) - two slices through the reconstructed separated by 58° angle.

[1] A. Faingold et al., Acta biomaterialia, **9** (4), 5956 (2013)
[2] N. Reznikov et al., Science, **360**, 6388 (2018)
[3] T. Kormilina et al., Microscopy and Microanalysis, **27**(S1), 96 (2021)

*Corresponding author: tatiana.kormilina@felmi-zfe.at

In situ structural analysis of AlSi10Mg for additive manufacturing – from powder to thermally treated parts

R. Krisper[1,2*], M. Albu[1], J. Lammer[1,2], M. Dienstleder[1],
E. Fisslthaler[1], G. Kothleitner[1,2], W. Grogger[1,2]

[1]*Graz Centre for Electron Microscopy (ZFE), Steyrergasse 17, 8010 Graz, Austria*
[2]*Institute of Electron Microscopy and Nanoanalysis (FELMI), Graz University of Technology, Steyrergasse 17, 8010 Graz, Austria*

In situ STEM heating experiments allow us to characterize the process of laser melting-based 3-D printing of metal alloys, their structure and elemental composition – from pristine printing powders to as-built structures and thermally treated materials.

Printing 3-D, robust metallic structures via laser beam melting of alloy powders is a rapidly growing industry branch. Manufacturers of such parts optimize their processes to improve material properties, as well as to enhance the interchangeability of building platforms and thus, their economic flexibility. The number of critical parameters for 3-D printing is large and most simulations or macroscopic tests do not sufficiently predict the outcome of a recipe. Parts from the same powder alloys with slightly different building parameters do not possess the same mechanical properties due to the grade of intrinsic thermal treatment that they experience in the respective laser-melting process. Differential scanning calorimetry (DSC) and X-ray diffraction (XRD) are prominent techniques used to provide information on transitions and crystallinity in the material before and after additional treatments, but the results are often inconclusive with respect to morphological changes [1,2]. AlSi10Mg is a high-hardness lightweight alloy with well-known casting properties which is of great interest for additive manufacturing. We studied its micro- and nanostructure through *in situ* thermal treatments in the TEM: Our correlated EDXS and EELS results for structural and elemental analysis of feedstock powders and 3-D printed parts explain data obtained from DSC and XRD; they aid in improving production processes and the tuning of materials, that would otherwise be based on trial-and-error approaches [3].

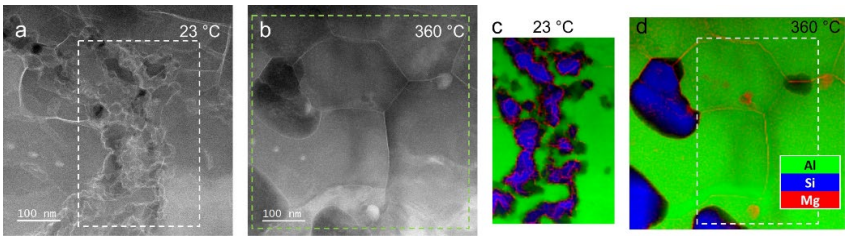

Figure 1. Elemental distribution of Si (blue) and Mg (red) in the Al (green) matrix acquired through STEM-EELS in an *in situ* heating experiment of an AlSi10Mg as-built specimen without prior thermal treatment. a, c) at 23 °C; b, d) at 360 °C. The spectrum image (c) is taken from the dashed white area in (a). The elemental map (d) is taken from the region in (b), bordered in dashed green and includes (c) (dashed white).

[1] S. Marola, D. Manfredi, G. Fiore, et al., J. Alloys Compd., **742**, 271-279 (2018)
[2] J. Fiocchi, A. Tuissi, P. Bassani, C.A. Biffi, J. Alloys Compd., **695**, 3402-3409 (2017)
[3] M. Albu, R. Krisper, J. Lammer, et al., Additive Manufacturing, **36**, 101605 (2020)

* Corresponding author: robert.krisper@felmi-zfe.at

Nanoscale investigation of liquid metal embrittlement in B-added TBF steels: revealing the role of grain boundaries

E. Akbari[1*], P. Kürnsteiner[1], G. Hesser[1], P. Oberhumer[1], H. Groiss[1], M. Arndt[2], M. Gruber[2], K. Steineder[2], R. Sierlinger[2]

[1]Christian Doppler Laboratory for Nanoscale Phase Transformations, Center for Surface and Nanoanalytics, Johannes Kepler University Linz, Altenberger Straße 69, 4040 Linz, Austria
[2]voestalpine Stahl GmbH, voestalpine Straße 3, 4031 Linz, Austria

Automotive advanced high-strength steels such as third-generation transformation induced plasticity assisted bainitic ferritic (TBF) steels with a Zn coating are prone to a detrimental failure known as liquid metal embrittlement (LME) [1]. LME occurs for instance during resistance spot welding, while the steel is in contact with liquid Zn under external and thermal stress. Thus, the liquid Zn penetration toward the underlying steel can generate macroscopic cracks that cause premature brittle fracture [2]. Therefore, enormous research has been conducted so far to cast light on the effect of various alloying elements and the mechanism controlling LME in the Fe-Zn couple [3].

This study is aimed to systematically investigate the effect of B on LME behavior of electro-galvanized TBF steels. Hot tensile test results indicated that the presence of B reduces LME sensitivity. Therefore, electron backscatter diffraction (EBSD) was conducted to reconstruct the prior austenitic matrix to study the high temperature microstructure present when LME occurs. The results verified an intergranular penetration of Zn along high-angle prior austenite grain boundaries (PAGBs). In addition to this microstructural evaluation, transmission electron microscopy in conjunction with energy dispersive X-ray spectroscopy was carried out to analyze grain boundary chemistry, specifically the influence of B on the alloy element segregation at PAGBs. **Figure 1** demonstrate the identification of a PAGB with a misorientation angle of 52.5˚ for the TEM investigation and selected area diffraction patterns of the two neighboring grains of the selected PAGB.

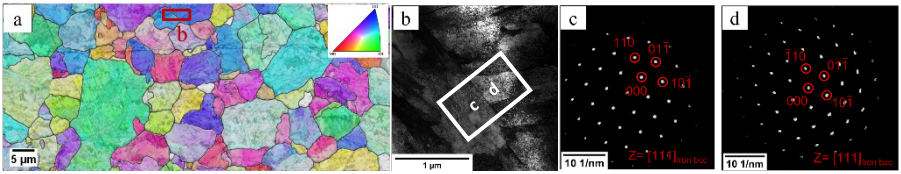

Figure 1. Grain boundary investigation in B-added TBF steel (a) EBSD IPF map of reconstructed PAG overlaid with EBSD band contrast image of bainitic-martensitic as-received sample, (b) TEM image of the PAGB marked in (a), (c) and (d) SAD patterns of the neighboring grains at the sides of the PAGB marked in (b)

[1] N. Fonstein, Advanced High Strength Sheet Steels, Springer, (2015)
[2] J.H. Kang, D. Kim, D. H. Kim, and S.J. Kim, Coatings Technol, **357**, 1069 (2019)
[3] H.E. Emre and R. Kaçar, Metals, **6**(12), 299 (2016)

* Corresponding author: elahe.akbari@jku.at

Noble gas clusters in a graphene sandwich

M. Längle[1,3*], C. Pesenhofer[1], K. Mizohata[2], A. Trentino[1,3], C. Mangler[1], K. Mustonen[1], E.H. Åhlgren[1], J. Kotakoski[1]

[1]*Faculty of Physics, University of Vienna, Boltzmanngasse 5 1090 Vienna, Austria*
[2]*Department of Physics, University of Helsinki, P.O. Box 43, FI-00014 Helsinki, Finland*
[3]*University of Vienna, Vienna Doctoral School in Physics, Boltzmanngasse 5, 1090 Vienna, Austria*

Due to their chemical inertness, noble gases do not condense under normal conditions. When trapped between two graphene sheets, however, the atoms are forced together by the external pressure that leads into formation of clusters [1]. We create such clusters by implanting singly charged low energy ions into suspended bi- and double layer graphene, which allows their direct imaging through (scanning) transmission electron microscopy (**Figure 1**) inside the graphene sandwich [2]. While all small clusters (up to at least 14 atoms) remain solid, larger clusters exhibit either solid- or liquid-like structures depending on their size, chemical element and possibly local microscopic environment. As a general observation, Xe clusters appear more solid than Kr ones (**Figure 2**).

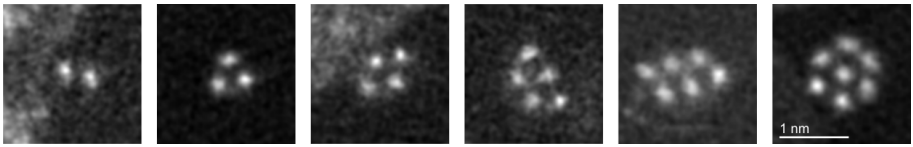

Figure 1: Filtered annular dark field scanning transmission electron microscopy images of Xe clusters to up to seven atoms.

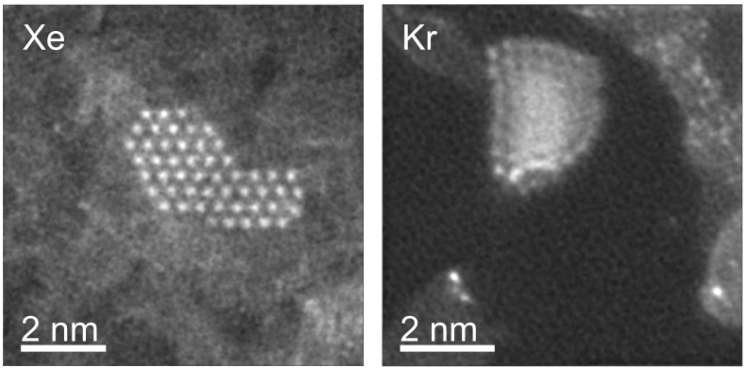

Figure 1: Filtered annular dark field scanning transmission electron microscopy images of a Xe51 cluster and a Kr cluster of a comparable size.

[1] Längle, M., Mizohata, K., Åhlgren, E., Trentino, A., Mustonen, K., & Kotakoski, J., Microscopy and Microanalysis, **26**(S2), 1086 (2020)
[2] Rasim Mirzayev, Kimmo Mustonen, Mohammad R. A. Monazam, Andreas Mittelberger,Timothy J. Pennycook, Clemens Mangler, Toma Susi, Jani Kotakoski, Jannik C. Meyer, Science Advances **3**, e1700176 (2017)

*Corresponding author: manuel.laengle@univie.ac.at

CANVAS: A System for Controlled Alteration of Nanomaterials in Vacuum Down to the Atomic Scale

C. Mangler[1*], J.C. Meyer[1,2], A. Mittelberger[1,3], K. Mustonen[1], T. Susi[1], J. Kotakoski[1]

[1]*University of Vienna, Faculty of Physics, Physics of Nanostructured Materials, Boltzmanngasse 5, 1090 Vienna, Austria*
[2]*Currently: Institute for Applied Physics, University of Tuebingen, Auf der Morgenstelle 10, 72076 Tuebingen, Germany*
[3]*Currently: Nion Co., 11511 NE 118th St., Kirkland, WA 98034, USA*

To get a true understanding of materials' properties, one has to assess their structure down to the atomic level. The next step is to enhance these properties by controlled and atomically precise alterations. While investigations of materials are usually carried out in high-resolution electron microscopes, their alteration typically has to be done in separate devices in controlled atmospheres, often ultra-high vacuum (UHV). This leads to the problem of sample transfer, where a major issue is their contamination. This is especially critical for low-dimensional materials due to their high surface-to-volume ratio.

To overcome this drawback, we have built **one** vast UHV system for the controlled alteration of nanomaterials in vacuum down to the atomic scale (CANVAS). The CANVAS system spans over two floors and consists of an aberration-corrected UHV scanning transmission electron microscope Nion UltraSTEM 100 [1] with a specially modified stage [2], an atomic force microscope (AFM), and a manipulation chamber equipped with a plasma source, a 6W diode laser and various thermal and electron-beam evaporators. Insertion of samples is done via a fully computer-controlled loadlock which is attached to a glovebox under argon atmosphere. The individual parts of the system are all connected via a novel arbitrary-length UHV transfer system consisting of magnetically coupled transfer cars and a new sample-holder design, which can be accommodated by all devices in the system (cf. **Figure 1** for an overview).

The CANVAS system allows the controlled alteration of materials and even the growth of new ones by utilizing various parts of the apparatus and quickly moving samples between them. Typical workflows include experimental steps like the alteration of a materials by thermal evaporation or plasma irradiation augmented by quick checks at atomic resolution at the STEM.

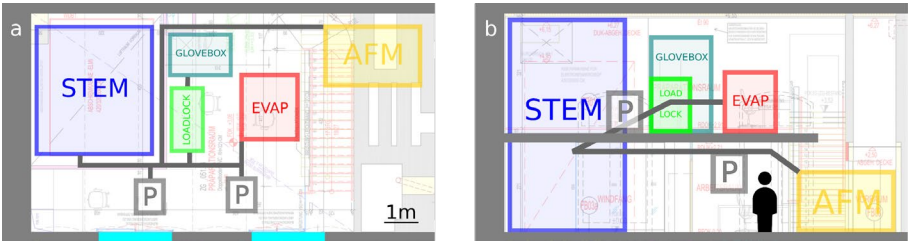

Figure 1. Top-view (a) and cross-section (b) of the Vienna lab showing the CANVAS system: scanning transmission electron microscope (STEM), loadlock and glovebox, evaporation chamber (EVAP), atomic force microscope (AFM) and sample storage (P).

[1] O.L. Krivanek, G.J. Corbin, N. Dellby, et al., Ultramicroscopy, **108** (3), 179 (2008)
[2] M.T. Hotz, G. J. Corbin, N. Dellby, et al., Microscopy and Microanalysis, **22** (S3), 34 (2016)

* Corresponding author: clemens.mangler@univie.ac.at

In situ TEM annealing of thin GeSn layers grown by MBE

K. Martínez[1*], A. Minenkov[1], J. Aberl[2], L.Vukušić[2], M. Brehm[2] and H. Groiss[1]

[1]*Christian Doppler Laboratory for Nanoscale Phase Transformations, Center for Surface and Nanoanalytics, Johannes Kepler University Linz, Altenberger Str. 69, 4040 Linz, Austria.*
[2]*Institute of Semiconductor and Solid-State Physics, Johannes Kepler University Linz, Altenberger Str. 69, 4040 Linz, Austria*

In situ Transmission Electron Microscopy (TEM) is a powerful technique that allows the observation of dynamic processes in materials under external stimuli. Temperature is one of the most important factors affecting materials' structure and behavior. To track real-time changes during annealing, micro-electro-mechanical system (MEMS) devices are used [1].

By this technique, the thermal stability of epitaxially-grown GeSn layers with a constant thickness of 50 nm and various Sn content of 10 and 14 at% was systematically studied. The interest in the study of this system is motivated by its great potential in high-performance Si-based electronics and optoelectronics. However, the low eutectic temperature and a very restricted Sn solubility of 1% in a bulk Ge, make the GeSn substitutional solid solutions dramatically nonequilibrium, resulting in phase separation and decomposition processes [2,3]. To trace the samples' structural evolution upon annealing, cross-sectional lamellae were cut from specimens and installed on MEMS heating chips (DENS-solutions) with a focused ion beam FIB. Heating experiments were carried out from 25 to 600°C. Combining complementary TEM techniques and energy dispersive X-ray (EDX) spectroscopy, it was shown that $Ge_{0.9}Sn_{0.1}$ has a higher thermal stability than $Ge_{0.86}Sn_{0.14}$. The $Ge_{0.9}Sn_{0.1}$ alloy is stable up to 460°C, at 470°C Pt diffusion from the capping layer induces a decomposition. The $Ge_{0.86}Sn_{0.14}$ sample is stable up to 300°C. At 350°C a clear Sn segregation was observed, resulting in the emergence of Sn-rich precipitates (**Figure 1**).

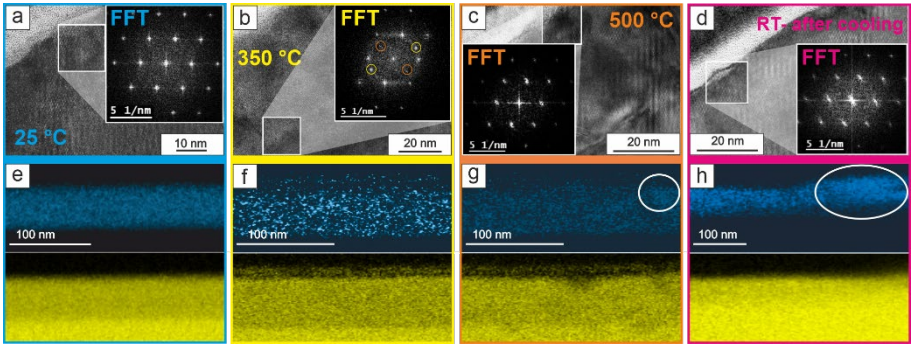

Figure 1. Thermal evolution of a $Ge_{0.86}Sn_{0.14}$ layer. (a-d) High resolution (HR) TEM images and FFT patterns of highlighted areas. At 350°C, extra reflexes appear in the FFT. (e-h) EDX maps of Ge, in yellow, and Sn, in blue. Sn precipitates at 500°C and at RT-after cooling are highlighted with white ovals.

[1] J. T. van Omme et al, Ultramicroscopy, **192**, 14 (2018)
[2] H. Groiss et al., Sci. Rep., **7**(1), 1 (2017)
[3] A. Minenkov, H. Groiss, J. Alloys Compd., **859**, 157763 (2021)

* Corresponding author: kari.martinez_reyna@jku.at

Mysterious electron beam induced hole growth in amorphous carbon

S.M. Noisternig[1,2*], C. Rentenberger[1], H.P. Karnthaler[1]

[1]*Physics of Nanostructured Materials, University of Vienna, Boltzmanngasse 5, 1090 Wien, Austria*
[2]*Erich Schmid Institute of Materials Science, Jahnstrasse 12, 8700 Leoben, Austria*

Thin foils of amorphous carbon are widely used in electron microscopy as supporting materials for both, biological and inorganic samples. Carbon foils are commercially available and can be as thin as 2 nm only. In this study we demonstrate that a well focused electron beam placed in the middle of a hole of the carbon foil can lead to a growth of the hole although the beam is not touching the rim of the hole, at least not visibly. The experimental setup is as follows: We use our dedicated STEM (Nion UltraStem 100) at two different vacuum conditions, as normally with ultra high vacuum (UHV) working at $< 10^{-9}$ mbar and with leaked-in O_2 at 7×10^{-7} mbar, respectively [1]. The later corresponds to the vacuum condition of standard STEM/TEM instruments. Due to the cold field emission gun and the corrector lenses the diameter of the probe is only ~ 0.1 nm and it is placed in the middle of a nm sized hole (5– 100 nm²). At UHV the size of the hole does not change. In contrast when using the vacuum condition with leaked-in O_2 the electron beam placed in the middle of the hole leads to hole growth. In this context it is interesting to note that when the beam is deflected from the hole no growth of the hole is encountered. To document these results it is necessary to take micrographs and as shown in recently published studies [2,3] thinning of the amorphous carbon sample is expected to occur by chemical etching. Therefore, the hole growth occurring during the exposure time of the documentation micrographs has to be subtracted.

In contrast to the well documented findings of this unexpected hole growth by a non touching beam a quantitative explanation remains mysterious. Still, we have some suggestions providing a qualitative interpretation. As suggested by Jani Kotakoski and co-workers the electron beam on its way through the vacuum above and below the sample is expected to interact with O_2 molecules and dissociate them into O [4]. In case the O atoms hit the foil of amorphous carbon they could react and form CO, thus reducing the foil thickness. But the amount of thickness reduction is not enough to explain the findings. An additional explanation could be the occurrence of beam tails; this means that the focused beam has weak extensions reaching much further than the tails corresponding to a Gaussian profile. Aberrations are corrected, but chromatic ones could give rise to very weak beam tails that interact with the rim of the hole. This could also explain the long time needed to observe hole growth. Another suggestion is that the O_2 molecules are dissociated by the X-rays present in the microscope column. This would increase their adsorption time on the amorphous foil and reduce the activation energy needed to form CO.

[1] G.T. Leuthner, S. Hummel, C. Mangler, T.J. Pennycook, T. Susi, J.C. Meyer, J. Kotakoski, Ultramicroscopy, **203**, 76 (2019)
[2] G.T. Leuthner, T. Susi, C. Mangler, J.C. Meyer, J. Kotakoski, 2D Materials, **8**, 035023 (2021)
[3] S.M. Noisternig, C. Rentenberger, H.P. Karnthaler, Ultramicroscopy, **235**, 113483 (2022)
[4] J. Kotakoski and co-workers, private communication (2021)

* Corresponding author: stefan.noisternig@univie.ac.at

Remote PACBED Thickness Determination by CNNs

M. Oberaigner[1]*, D. Weber[2], A. Clausen[2], D. Knez[1], G. Kothleitner[1,3]

[1]*Institute of Electron Microscopy and Nanoanalysis, Graz University of Technology, Graz, Austria*
[2]*Ernst Ruska-Centre for Microscopy and Spectroscopy with Electrons, Forschungszentrum Jülich, Jülich, Germany*
[3]*Graz Centre for Electron Microscopy, Graz, Austria*

Accurate thickness determinations of specimens are important for many STEM-applications. A convenient method for crystalline samples is the position averaged convergent-beam electron diffraction (PACBED) method [1]. The thickness is determined by finding the best match of the recorded PACBED pattern with a series of simulated PACBED, calculated at different crystal thickness. This is a time-consuming process and is not practical during a microscope session.

Xu and LeBeau showed the automatization of such PACBED analysis by convolutional neural networks (CNNs) [2]. Although, this enables fast analysis, simulating a large training dataset of PACBEDs and training the CNNs has high computational costs and these CNNs are only valid for the simulated system. Since many scientists are working with the same materials, the scientific community would benefit of a shared database of trained CNNs to predict the thickness of the specimen without having to simulate PACBEDs and train CNNs by themselves.

Therefore, we propose a server-based PACBED thickness determination by CNNs, which is integrated in GMS to enable an easy and fast PACBED analysis during a microscope session. The system parameters and the recorded PACBED will be uploaded to the server by a GUI in GMS. If the requested system is available, the specimen thickness and mistilt will be predicted by CNNs (**Figure 1**a). Additionally, a visual feedback is returned to the user for validating the results (**Figure 1**b). Here, we will present a proof of concept with a working prototype.

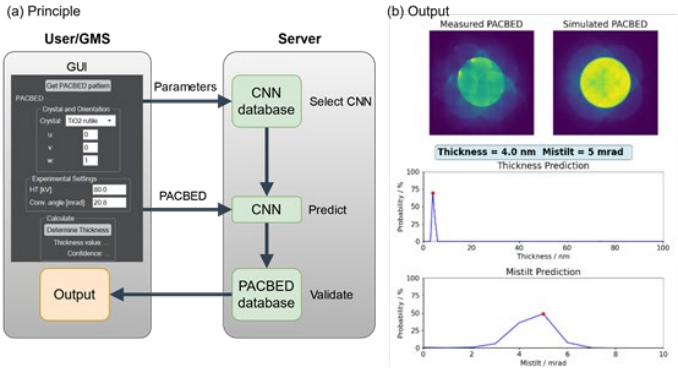

Figure 1. (a) Data flow chart of the remote PACBED analysis. **(b)** Output, given to the user to validate the prediction.

[1] J. M. LeBeau, S. D. Findlay, L. J. Allen, and S. Stemmer, Ultramicroscopy, **110**(2) (2010)
[2] W. Xu and J. M. LeBeau, Ultramicroscopy, **188** (2018)

The authors acknowledge financial support by the Austrian Science Fund (FWF) under grant nr. I4309-N36 and European Union's Horizon 2020 research and innovation program under Grant 823717-ESTEEM3.

* Corresponding author: michael.oberaigner@felmi-zfe.at

Defect formation in graphene using noble gas irradiation

C. Pesenhofer*, M. Längle, C. Mangler, J. Kotakoski

Faculty of Physics, University of Vienna, Boltzmanngasse 5 1090 Vienna, Austria

Material properties can be controlled via defect creation in traditional materials. Recently our group has shown that defect engineering of graphene can be brought to near macroscopic scale combining sample cleaning via laser, noble gas irradiation with a plasma source, and automated atomic-resolution imaging [1]. Here we characterize the energy distribution of the ions from the plasma source and investigate defect formation as a function of irradiation energy and ion species for mono- and multilayer graphene samples. With this we expect to gain high control over the kind of defects introduced and their concentration. The goal is to find parameters that allow us to deliberately create graphene samples with the desired vacancy defects. The defects are investigated using a Nion UltraSTEM 100 aberration corrected scanning transmission electron microscope.

[1] A. Trentino, J. Madsen, J. Kotakoski, et al., Nano Lett. **21**, 5179 (2021)

* Corresponding author: a01612537@unet.univie.ac.at

Correlative Raman-SEM-EDX analysis of corroded components

In particular microbiologically induced corrosion (MIC) of steel and chlorid corrosion of concrete

T. Planko[1*], H. Fitzek[1], S. Eichinger[3], J. Rattenberger[1], G. Koraimann[4], H. Zeitlhofer[5], M. Peyerl[5] and H. Schroettner[1,2]

[1]*Graz Centre for Electron Microscopy, Steyrergasse 17, Graz, Austria*
[2]*Institute of Electron Microscopy and Nanoanalysis, NAWI Graz, Graz University of Technology, Steyrergasse 17, Graz, Austria*
[3]Institute of Applied Geosciences, Graz University of Technology, Rechbauerstraße 12, 8010 Graz, Austria
[4]*Institute of Molecular Biosciences, University of Graz, Humboldtstraße 50,8010 Graz, Austria*
[5]*Science Center, Smart Minerals GmbH, 1030 Vienna, Franz-Grill-Straße 9, Austria*

Direct cost due to corrosion is estimated to be between 3-5 % of gross domestic product (GDP) [1] and represents a safety risk. We investigate two specific kinds of corrosion, Microbiologically influenced corrosion (MIC) of steel, where the presents of microbes alters the corrosion process, and Chloride-induced corrosion of concrete and rebar steel, which is often caused by de-icing salt. For our analysis we use a novel technique that combine Raman imaging with scanning electron microscopy (SEM) and energy dispersive X-Ray spectroscopy (EDX) [2], where Raman contributes additional information about chemical bonds and oxidation states. An example measurement of a MIC corroded steel sample is shown below.

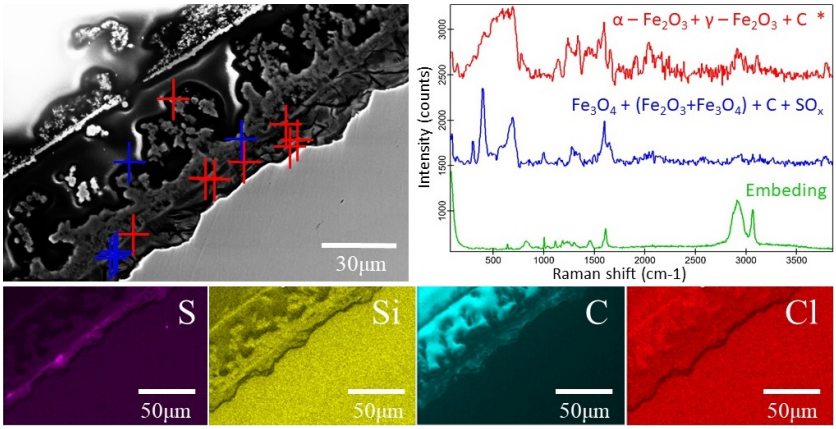

Figure 1. Left (top): Cross section of steel MIC sample (SEM). Raman measuring points marked. Right (top): Fe-oxides were identified with Raman spectroscopy as hematite, amorphous maghemite (red spectrum), raw sienna and magnetite (blue spectrum). Graphite (red and blue spectrum) was also found. The band at 1000 cm-1 indicates a sulfur oxide. Bottom: Edx measurements with most important elements: iron, carbon, chlorine, sulfur, and silicon.

[1] G.F. Hays, Now is the Time. In: World Corrosion Organization (2010)
[2] Schmidt R, Fitzek H, Nachtnebel M et al. The combination of electron microscopy, Raman microscopy and energy dispersive x-ray spectroscopy for the investigation of polymeric materials. In: Macromolecular Symposia. Wiley Online Library, 1800237

* Corresponding author: thomas.planko@felmi-zfe.at

STEM analysis of freestanding monolayer h-BN irradiated with slow highly charged ions

D. Propst[1*], C. Speckmann[1], A. Niggas[2], R.A. Wilhelm[2], J. Kotakoski[1]

[1]*Physics of Nanostructured Materials, University of Vienna, Boltzmanngasse 5, 1090 Vienna, Austria*
[2]*Institute of Applied Physics, TU Wien, Wiedner Hauptstraße 8-10/E134, 1040 Vienna, Austria*

Two-dimensional (2D) materials and their applications play a large role in the development of new technologies. However, the manufacturing of specific features on such limited scales is a challenge that requires precise, definite and reproducible methods of fabrication. Novel and well-known strategies are being employed to produce certain well-defined defects in 2D materials. Perforations of few to single atomic layers are of high interest, due to their applications in the fields of DNA-sequencing [1] and water desalination [2]. Slow highly charged ions (HCIs) have shown to produce well defined pores of regular density in 2D materials, such as MoS_2 [3] and carbon nanomembranes [4]. The pore sizes can be tuned by the charge state of the ions. This is a relatively young field of research, due to the only recent advent of monolayer synthesis methods. It also offers new insights of ion-matter interactions, where the energy exchange and neutralization dynamics can be studied in just one atomic layer, which differs from the multitudes of interlayer effects in the bulk. Hexagonal boron nitride (h-BN) has been proposed as a suitable 2D material for the applications mentioned above, due to its favorable properties of chemical stability and oxidation resistance [5]. It also has many similarities to graphene, being considered its non-conducting counterpart. But the research on freestanding ion-irradiated h-BN is lacking, partially due to difficulties in the preparation of a suitable sample. Therefore, the effects of slow highly charged xenon ions with charge states 20 and 38 impinging on freestanding monolayer h-BN are investigated by Scanning Transmission Electron Microscopy (STEM), in regard to nanoscopic pore formation in the material. The CCD and MAADF detectors are used for the analysis, collecting a multitude of images. Two monolayer h-BN samples prepared on Quantifoil Transmission Electron Microscopy (TEM) grids are pre-characterized by STEM, then irradiated with the highly charged ions. After irradiation the samples are then characterized by STEM again. From the STEM images the post-irradiation pore sizes are collected and the mean pore radius for both charge states is determined. The samples exhibit pore formations with a larger mean pore size for the higher charge state, showing that monolayer h-BN is susceptible to perforation by HCI irradiation.

[1] Qiu, H., Zhou, W. & Guo, W., ACS Nano **15**, 18848 (2021)
[2] Safaei, J., Xiong, P. & Wang, G., Materials Today Advances **8**, 100108 (2020)
[3] Kozubek, R. et al., The Journal of Physical Chemistry Letters **10**, 904 (2019)
[4] Ritter, R. et al., Applied Physics Letters **102**, 63112 (2013)
[5] Liu, Z. et al., Nature Communications **4**, 2541 (2013)

*Corresponding author: diana.propst@univie.ac.at

Atomic-scale investigation of LSCO-STFO multilayer grown on a (001) YSZ with a GDC buffer layer

S. Ražnjević[1], M. Kubicek[3], M. Čeh[4], S. Drev[4], M. Siebenhofer[3], C. Böhme[3], C. Reidl[3], Z. Zhang[1,2]

[1]*Erich Schmid Institute of Materials Science, Austrian Academy of Sciences, Leoben, 8700, Austria*
[2]*Montanuniversität Leoben, Franz-Josef-Straße 18, 8700 Leoben, Austria*
[3]*Institute of Chemical Technologies and Analytics, Getreidemarkt 9/164EC, 1060 Vienna, Austria*
[4]*Jozef Štefan Institute, Jamova 39, 1000 Ljubljana, Slovenia*

Cobalt-based oxides have attracted a lot of attention in the scientific community due to their interesting optical and electrical transport properties [1]. Lanthanum cobaltite ($LaCoO_3$) have a rhombohedral structure at room temperature. However, doping by Strontium atoms can change its structure to cubic [2]. Substitution of the Lanthanum La^{3+} ions with Strontium Sr^{2+} changes the Cobalt valence thus introducing metallic ferromagnetism [1]. $La_{1-x}Sr_xCoO_{3-\delta}$ has a good electrical and oxygen conductivity, making it interesting for electrochemical applications such as solid oxide fuel cell [3].

In this study a multilayer of $La_{0.6}Sr_{0.4}CoO_{3-\delta}$ and $SrTi_{0.3}Fe_{0.7}O_{3-\delta}$ was deposited on (100) Yttria-stabilized Zirconia substrate on which, first, 10nm of $Ce_{0.8}Gd_{0.2}O_{2-\delta}$ buffer layer was deposited.

XRD results show that STFO have a slightly larger lattice parameter and thus it introduces tensile strain in the LSCO layers. In previous works, it has been shown that the strain in the LSCO layer can induce Brownmillerite phase.

Structural characterization will be determined using probe-corrected JEOL ARM200F operated at 200kV. Additionally, intermixing across interface will be investigated using Z-contrast analysis. For this study cross-section sample was prepared by mechanical grinding, polishing and ion milling.

[1] J. Gazquez et al., APL Mater. **1**, 012105 (2013).
[2] K. Kleveland et al., J. Am. Ceram. Soc. **84**(9), 2029 (2001)
[3] S. Stemmer et al., J. Appl. **90**, 3319 (2001).

We kindly acknowledge the financial support by the Austrian Science Fund (FWF): No. 031654.
Our gratitude also goes to the ESTEEM3 project, which enabled sample investigation in Ljubljana.

A single quantum bit free-electron logic gate in a TEM

T. Schachinger[1,2]*, P. Hartel[3], P.-H. Lu[4], M. Obermair[5], M. Dries[5], D. Gerthsen[5], R. E. Dunin-Borkowski[4], S. Löffler[1], P. Schattschneider[1,2]

[1]*USTEM, TU Wien,Wiedner Hauptstraße 8-10/E057-02, 1040 Wien, Austria*
[2]*Institute of Solid State Physics, TU Wien, Wiedner Hauptstraße 8-10/E138-03, 1040 Wien, Austria*
[3]*CEOS Corrected Electron Optical Systems GmbH, Englerstraße 28, 69126 Heidelberg, Germany*
[4] *ER-C and Peter Grünberg Institute, Forschungszentrum Jülich, 52425 Jülich, Germany*
[5] *Laboratorium für Elektronenmikroskopie (LEM), Karlsruher Institut für Technologie (KIT), Engesserstraße 7, 76131 Karlsruhe, Germany*

For the successful implementation of quantum computing devices, Di Vincenzo and later Ladd et al. formulated fundamental criteria [1]. Besides, e.g., system scalability and quantum error correctability, quantum gates are essential building blocks [1]. So far, these were realized in the form of ion traps, quantum dot confined electrons, SQUIDS and photons. However, modern TEMs also represent a highly versatile platform to coherently shape the electron wavefront. We show the realization of a single qubit gate, namely a $\sqrt{NOT} - gate$, using free-floating electrons inside a TEM [2], **Fig. 1** (a). A Hilbert phase plate prepares the input qubit, **Fig. 1** (b), which is sent to the manipulating quantum gate, a mode converter (MC) implemented in the probe forming aberration corrector of the TEM [3]. The output qubit is then detected on a 2D-electron detector for two arbitrary input qubits, **Fig. 1** (b). So far, the gate action was compared to numerical simulations, but future directions will concentrate on reliable hardware readout mechanisms, e.g., a second MC or an orbital angular momentum sorter device.

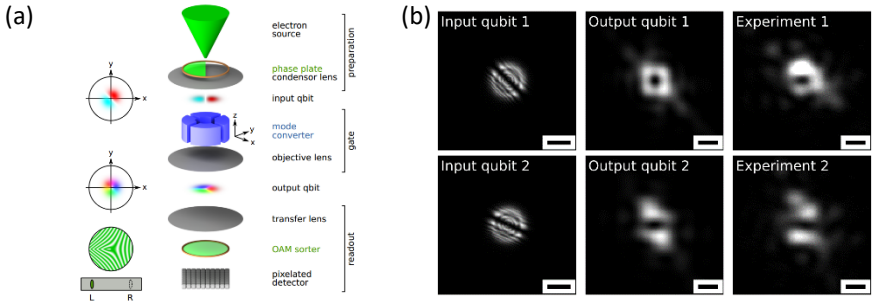

Figure 1. a) Experimental setup of qubit preparation, manipulation and readout on a TEM platform. b) Simulated input/output qubit as well as its experimental realization in the PICO microscope for two distinct input qubit states (upper/lower row). The scale bars in the first column represent 500 nm, all other scale bars denote 2 nm.

[1] T. D. Ladd et al., Nature, **464**, 45 (2010)
[2] S. Löffler et al., A quantum logic gate for free electrons, (2022), submitted
[3] T. Schachinger et al., Ultramicroscopy, **229**, 113340 (2021)

We acknowledge financial support by the FWF (P29687-N36, I4309-N36), EU Horizon 2020 research and innovation programme (No. 823717-ESTEEM3, No. 856538 "3D MAGiC") and the DFG (Ge 841/26).

*Corresponding author: thomas.schachinger@tuwien.ac.at

Theory of Ponderomotive Transverse Electron Beam Shaping

M.C. Chirita Mihaila[1,2,3], P. Weber[1,3], M. Schneller[1,3*], L. Grandits[1,3], S. Nimmrichter[4], T. Juffmann[1,3]

[1]*University of Vienna, Faculty of Physics, VCQ, A-1090 Vienna, Austria*
[2]*University of Vienna, Vienna Doctoral School in Physics, A-1090 Vienna, Austria*
[3]*University of Vienna, Max Perutz Laboratories, Department of Structural and Computational Biology, A-1030 Vienna, Austria*
[4]*Naturwissenschaftlich-Technische Fakultät, Universität Siegen, Walter-Flex-Straße 3, 57068 Siegen, Germany*

Electron-Photon interactions are limited to second order effects and commonly described by the ponderomotive potential. The problem at hand is a pulsed electron beam in a SEM set-up modulated by a high intensity pulsed laser light field in parallel propagation. Considering a relativistic electron in paraxial approximation, we derive the transverse phase modulation realized by an effective scattering phase $\varphi_v(x,y)$. This is done by reducing the Dirac equation to an effective Schrödinger equation [1] and using a pulsed light field within the ponderomotive potential to get:

$$\varphi_v(x,y) = -\frac{\alpha}{2\pi(1 \pm \beta)} \frac{E_L}{E_e} \frac{\lambda_L I(x,y)}{\int dx dy\, I(x,y)}$$

Furthermore, we implemented a ray as well as wave optics simulation to compare our theoretical description to experimental data [2]. For the ray optics simulation, a simple ray tracing scheme (ABCD matrices) combined with classical deflection of the electrons was used. Due to resolution limitations in the experimental set-up, this classical ansatz worked and was computationally fast. The wave optics simulation however relies, due to memory issues, on the radial symmetry of the light field in our set-up. Ponderomotive wave front shaping may enable aberration correction, the creation of exotic electron beams and the realization of adaptive electron microscopy.

[1] F.J. Garcia de Abajo and A. Konečna, Phys. Rev. Lett., **126**, 123901 (2021)
[2] M.C. Chirita Mihaila, P. Weber, M. Schneller, L. Grandits, S. Nimmrichter, T. Juffmann, arXiv:2203.07925 (2022)

* Corresponding author: matthias.schneller@univie.ac.at

Surface Corrugation in 2D Materials

R. Singh*, J. Kotakoski

Physics of Nanostructured Materials (PNM), University of Vienna, Boltzmanngasse 5, Wien, Austria

Nanoscale corrugation is a ubiquitous property of 2D materials in both free-standing state as well as when placed on a smooth surface such as hBN [1–3]. Generally, surface corrugation is characterized by three parameters namely corrugation height (R_{rms}), angular deviation (γ_{rms}) and the wave vector (κ_{rms}) [2]. Transmission electron microscopy (TEM) is the ideal method for characterizing the structure of 2D materials because of their intrinsically thin structure. Apart from revealing structure of materials with atomic precision, including defects and impurity atoms, it also offers the possibilities of studying the surface corrugation through electron diffraction patterns, as was first demonstrated in Ref. [3]. Indeed, by recording a series of electron diffraction patterns at different specimen tilt angles, the surface roughness in graphene and graphene-hBN heterostructure have been determined [1,3]. This method uses the change in reciprocal lattice vector (***G***) and diffraction spot intensity to probe the order of surface corrugation in 2D materials as shown in **Figure 1**.

Despite a handful of experimental studies, no quantitative data have been reported on some of the key factors affecting the roughness in 2D materials. Here, we provide a statistical analysis of surface corrugation in graphene for different sample types (mechanically exfoliated vs. samples grown via chemical vapor deposition) and as a function of the size of the suspended sample area and as a function of disorder introduced by electron irradiation. In addition to graphene, we also report similar results for other 2D materials and their heterostructures.

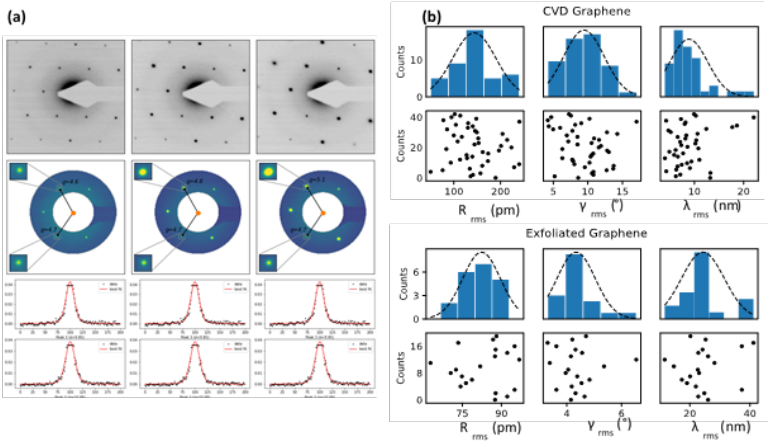

Figure 1. (a) Method of measuring Surface corrugation in 2D materials. (b) Experimentally measured roughness parameters for mechanically exfoliated and CVD grown graphene.

[1] J. D. Thomsen et al., Phys. Rev. B, **96**, 014101 (2017)
[2] U. Ludacka et al., npj 2D Materials and Applications, **2**, 25 (2018)
[3] J. C. Meyer et al., Solid State Communication, **143** (2007)

*Corresponding author: rajendra.singh@univie.ac.at

Electron-irradiation induced sulphur displacement cross section in MoS_2

C. Speckmann*, J. Lang, J. Madsen, T. Susi, J. Kotakoski

University of Vienna, Faculty of Physics, Boltzmanngasse 5, 1090 Wien, Austria

Atomic-resolution imaging of 2D materials allows investigating electron-irradiation effects with unprecedented accuracy, as has been demonstrated for graphene [1,2] and MoS_2 [3]. While the measured displacement cross section in graphene can be explained by a knock-on process caused by elastic scattering of electrons from carbon nuclei of the material at its ground state, the situation with semi-conducting MoS_2 is more complicated. Specifically, Kretschmer et al. [3] showed that there is a peak in the displacement cross section at energies close to 30 keV, which the authors explained to arise from an excited state knock-on event whose probability increases with decreasing electron energy. They also predicted that at energies above 80 keV the cross section should again increase due to displacements from the ground state. However, experimental data at the higher energy range is still lacking. Very recently, Yoshimura et al. established a more elaborate theoretical model [4] based on quantum electrodynamics to calculate from first principles the probabilities of excitations and displacement events related to them. However, their results only agree with the experimental data of Kretschmer et al. if single and double excitations do not contribute to observed displacements, but only higher ones. Overall, it is clear that more experimental data is needed to be able to properly test these theoretical models. Here, we combine aberration-corrected scanning transmission electron microscopy and computational assisted image analysis to extend the experimental data set for MoS_2 between 55 and 90 keV. Several hundred image sequences were recorded to provide statistically significant data. Examples of the first two frames from one recorded image sequence are shown in **Figure 1**, where a sulphur vacancy (red circle) was created in the second frame. Our results hint at another peak at electron energies close to 70 keV, and a significant increase at higher energies.

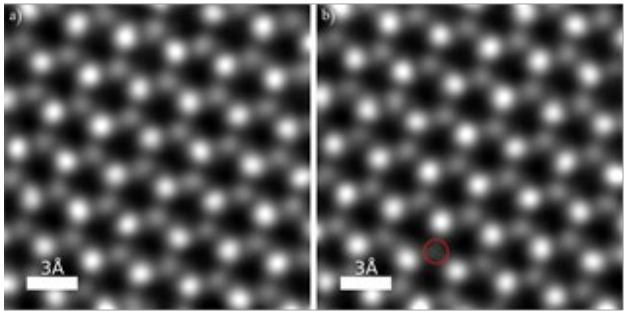

Figure 1. Filtered scanning transmission electron microscopy high-angle annular dark field images of monolayer MoS_2 recorded at 75 keV (frame time ca. 0.86 s).

[1] J. C. Meyer et al., Phys. Rev. Lett., **108**, 19 (2012)
[2] T. Susi et al., Nat. Commun. **7**, 13040 (2016)
[3] S. Kretschmer et al., Nano Lett., **20**, 2865 (2020)

* Corresponding author: carsten.speckmann@univie.ac.at

Carbon mapping and quantification by UHV-EDXS

G. Säckl[1,2*], M. Arndt[5], J. Duchoslav[2,3], H. Groiss[4], K. Steineder[5], G. Wallner[1,6], D. Stifter[2]

[1] *Christian Doppler Laboratory for Superimposed Mechanical-Environmental Ageing of Polymeric Hybrid Laminates (CDL-AgePol), Johannes Kepler University Linz, Altenberger Straße 69, 4040 Linz, Austria*
[2] *Center for Surface and Nanoanalytics (ZONA), Johannes Kepler University Linz, Altenberger Straße 69, 4040 Linz, Austria*
[3] *Centre for Electrochemistry and Surface Technology GmbH (CEST), Stahlstraße 2-4, 4020 Linz, Austria*
[4] *Christian Doppler Laboratory for Nanoscale Phase Transformations, Center for Surface and Nanoanalytics (ZONA), Johannes Kepler University Linz, Altenberger Straße 69, 4040 Linz, Austria*
[5] *voestalpine Stahl GmbH, voestalpine-Straße 3, 4031 Linz, Austria*
[6] *Institute of Polymeric Materials and Testing (IPMT), Johannes Kepler University Linz, Altenberger Straße 69, 4040 Linz, Austria*

The detection and quantification of carbon by conventional energy dispersive X-ray spectroscopy (EDXS) performed under standard conditions is not feasible due to occurring contaminations in common electron microscopes. In contrast, novel ultra high vacuum EDXS (UHV-EDXS) was used to acquire elemental mappings of carbon on dual phase (DP) steel, which exhibits a microstructure consisting of ferrite and martensite. These phases differ in hardness, local dislocation density and, most importantly, in their carbon content.

Since the UHV conditions in combination with a customized windowless EDXS detector ensured a minimization of hydrocarbon contamination during the measurements and a maximization of the sensitivity for the detection of light elements, UHV-EDXS carbon mappings could successfully be obtained, which clearly reflect the ferrite and martensite microstructure of the investigated DP steels, as confirmed by electron back scatter diffraction (EBSD). Most importantly, it was possible to quantify the carbon content of individual grains with concentrations as low as 0.2 wt.%. Furthermore, nano-hardness tests were performed on the very same grains which were characterized by UHV-EDXS and EBSD. It is shown that the hardness of the martensite grains is correlated to their carbon content, as directly determined by UHV-EDXS. With this new method an additional tool for advanced material characterization of multiphase materials on the level of individual grains is now available.

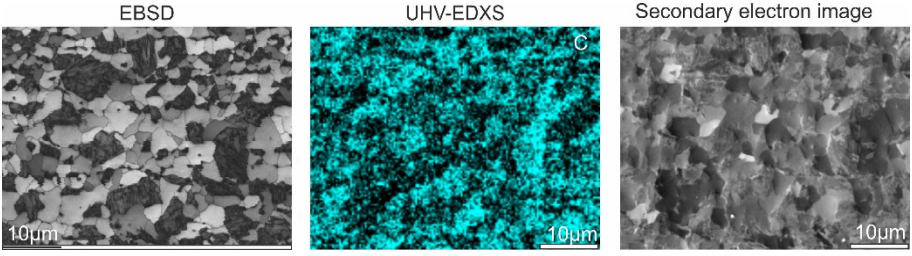

Figure 1. EBSD, UHV-EDXS carbon mappings and secondary electron image in comparison. The UHV-EDXS carbon mapping clearly reflects the microstructure of the investigated DP steel.

*Corresponding author: gary.saeckl@gmail.com

Towards Driving Quantum Systems with the Non-Radiating Near-Field of a Modulated Electron Beam

T. Weigner[1]*, M. Kolb[1], T.Spielauer[1], J. Toyfl[1], G. Boero[2], P. Haslinger[1]

[1]*VCQ, Technische Universität Wien, Atominstitut*
Stadionallee 2, 1020 Vienna, Austria
[2]*EPFL, BM 3110 Station 17, CH-1015 Lausanne, Switzerland*

Coherent manipulation of quantum systems generally relies on electromagnetic radiation as produced by lasers or microwave sources. In the experiment presented here we attempt a novel approach to drive quantum systems, as it was recently proposed [1]. This method utilizes the non-radiating near-field of a modulated electron beam to coherently drive quantum systems, leading to new possibilities for controlling quantum states. For instance, one can locally address subsystems far below the diffraction limit of electromagnetic radiation or paint potentials at atomic scales.

In this proof of concept experiment (see Figure 1), we want to couple the oscillating near-field of a spatially modulated electron beam to the unpaired spins of a solid, organic radical sample (BDPA). The electron beam is generated with a cathodic ray tube from a fast analog oscilloscope. The decaying spins couple to a micro-coil around the sample, which is read out by a standard measurement setup with a lock in amplifier.

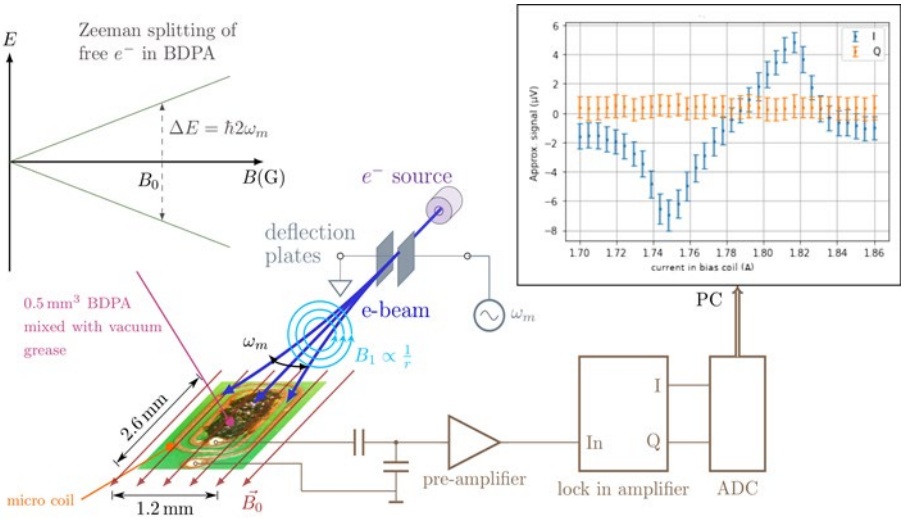

Figure 1. Experimental setup: The blue electron beam is spatially modulated next to the sample with ω_m, which produces a magnetic field B_1 varying at $2\omega_m$ in the sample, exciting the Zeeman levels. The spins populating these levels couple to a micro coil around the sample. The signal picked up by the coil is then demodulated and detected with a lock in amplifier. Via an ADC the data is send to a PC for analysis.

[1] D. Rätzel, D. Hartley, O. Schwartz, P. Haslinger. Phys. Rev. Research **3**, 023247 (2021)

* Corresponding author: thomas.weigner@tuwien.ac.at

Expanding High-fidelity 3D-Nanoprinting - From Meshes toward Closed Structures

A. Weitzer[1*], M. Huth[2], G. Kothleitner[1,3] and H. Plank[1,3,4]

[1]*Institute of Electron Microscopy and Nanoanalysis, Graz University of Technology, 8010 Graz, Austria*
[2]*Physics Institute, Goethe Universität Frankfurt, 60438 Frankfurt am Main, Germany*
[3]*Graz Centre for Electron Microscopy, Steyrergasse 17, 8010 Graz, Austria*
[4]*Christian Doppler Laboratory - DEFINE, Graz University of Technology, 8010 Graz, Austria*

High-fidelity additive manufacturing of 3-dimensional objects on the nanoscale is a very demanding task. Among the few capable techniques, 3D nanoprinting via Focused Electron Beam Induced Deposition (3D-FEBID) is an increasingly relevant technology due to its additive direct-write capabilities with feature sizes below 100 nm on a regular basis and below 20 nm under optimized conditions and its flexibility in terms of substrate materials and morphology as well as available precursors. The working principle relies on the localized immobilization of surface adsorbed precursor molecules, injected into a vacuum chamber in gaseous states, via a dissociation process triggered by an electron beam. Although this technique has been around for a few years, in the past, most fabricated structures were meshed, meaning a combination of differently oriented, individual nanowires, connected at specific points in 3D space according to the target application. To leverage this technology to the next level, we here report about the expansion of 3D-FEBID capabilities from mesh-like toward closed structures with a high degree of precision.

The main challenge and source of most deviations from target shapes is based on local beam heating and its implications on local growth rates. While well understood in meshed structures, closed objects revealed additional dependencies on the dimensions of built objects and the XY pixel position within the structures. Furthermore, electron trajectories are more complex in closed objects, introducing additional proximity effects. To tackle this problem, we combined finite-difference simulations with 3D-FEBID experiments and developed a python-based compensation tool, capable of stabilizing the growth in each patterning plane by pre-determined parameter adaptions. The gained insight allowed further expansion, now being applicable for different element-widths and -heights, as demonstrated by more advanced structures. By that, the new model crucially expands FEBID-based 3D nanoprinting by opening up design possibilities for closed and consequently mixed objects for novel applications in various fields of research and development.

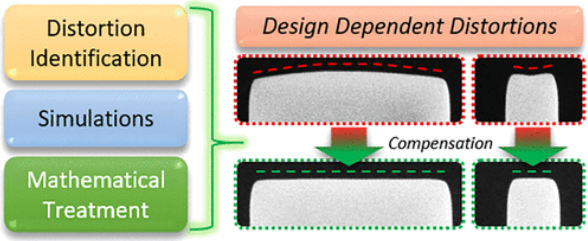

Figure 1. Schematic of design improvements due to our compensation tool on the example of a wall [1].

[1] A. Weitzer, M. Huth, G. Kothleitner, and H. Plank, ACS Appl. Electron. Mater., **4** (2), 744 (2022)

*Corresponding author: anna.weitzer@felmi-zfe.at

LIST OF PARTICIPANTS

A	**Åhlgren Harriet** / University of Vienna / harriet.ahlgren@univie.ac.at	**50**,65
	Alatrash Anas / FELMI-ZFE / anas.alatrash@felmi-zfe.at	**54**
B	**Bellapianta Alessandro** / JKU – ZMF alessandro.bellapianta@jku.at	
	Bernardi Johannes / TU Wien bernardi@ustem.tuwien.ac.at	17
	Bichler Bernhard / Videko GmbH bernhard.bichler@videko.at	19
	Brandstetter Marlene / Vienna Biocenter Core Facilities GmbH marlene.brandstetter@vbcf.ac.at	
	Breitenmoser Reto / Systron EMV GmbH reto.breitenmoser@systronemv.com	
	Brozyniak Aleksander / Center for Surface and Nanoanalytics, JKU Linz aleksander.brozyniak@jku.at	**55**
C	**Cetkovic Ana** / Zentrum für Medizinische Forschung, JKU Linz ana.cetkovic@jku.at	
	Chen Zhuo / Erich Schmid Institute of Materials Science of the Austrian Academy of Sciences / zhuo.chen@stud.unileoben.ac.at	**16**,52
	Chirita Mihaila Marius Constantin / University of Vienna marius.chirita@univie.ac.at	**56**,75
D	**Drexler Nicole** / Vienna Biocenter Core Facilities GmbH nicole.drexler@vbcf.ac.at	
E	**Ederer Manuel** / USTEM, TU Wien manuel.ederer@tuwien.ac.at	**40**
F	**Frerichs Hajo** / Quantum Design Microscopy GmbH frerichs@qd-microscopy.com	**36**
G	**Groiß Heiko** / Center for Surface and Nanoanalytics, JKU Linz heiko.groiss@jku.at	55,64, 67,78
H	**Haberfehlner Georg** / Institute of Electron Microscopy and Nanoanalysis, Graz University of Technology / georg.haberfehlner@felmi-zfe.at	8, 58
	Haselgrübler Klaus / Center for Surface and Nanoanalytics, JKU Linz klaus.haselgruebler@jku.at	
	Haselmann Ulrich / Erich Schmid Institute of Materials Science haselmann.ulrich@gmail.com	**24**
	Haslinger Philipp / Atominstitut, Technische Universität Wien philipp.haslinger@tuwien.ac.at	43, 79
	Heuser Thomas / Vienna Biocenter Core Facilities thomas.heuser@vbcf.ac.at	

H	**Hingerl Kurt** / Center for Surface and Nanoanalytics, JKU Linz kurt.hingerl@jku.at	
	Horák Michal / CEITEC Brno University of Technology michal.horak2@ceitec.vutbr.cz	**34**
	Huang Yong / Austrian Academy of Science yong.huang@oeaw.ac.at	**52**
I	**Imrich Daniel** / Physik nanostrukturierter Materialien, Universität Wien daniel.imrich@univie.ac.at	**59**
J	**Jäpel Tom** / Tescan GmbH tom.jaepel@tescan.com	**12**
	Juffmann Thomas / Universität Wien thomas.juffmann@univie.ac.at	56,75
K	**Karnthaler Hans Peter** / Physik Nanostrukturierter Materialien, Universität Wien / hans-peter.karnthaler@univie.ac.at	48,68
	Kastenmüller Andreas / Ametek GmbH andreas.kastenmueller@ametek.com	**44**
	Kaufmann Walter / Institute of Science and Technology Austria (ISTA) walter.kaufmann@ist.ac.at	
	Knez Daniel / FELMI-ZFE / TU Graz daniel.knez@felmi-zfe.at	8,24,51, **60**,69
	Kolb Dagmar / Core Facility Ultrastructure Analysis dagmar.kolb@medunigraz.at	79
	Kormilina Tatiana / FELMI-ZFE tatiana.kormilina@felmi-zfe.at	**62**
	Kotakoski Jani / Universität Wien jani.kotakoski@univie.ac.at	35,42,50, 59,61,65, 66,70,72, 76,77
	Kotisch Harald / Vienna BioCenter Core Facilities harald.kotisch@vbcf.ac.at	
	Krisper Robert / FELMI-ZFE robert.krisper@felmi-zfe.at	**63**
	Käppeli Stephan / Systron EMV GmbH stephan.kaeppeli@systronemv.com	**11**
	Kürnsteiner Philipp / Center for Surface and Nanoanalytics, JKU Linz philipp.kuernsteiner@jku.at	**64**
L	**Lammer Judith** / FELMI-ZFE Graz judith.lammer@felmi-zfe.at	**8**,63
	Lang Julia / Universität Wien julia.lang@univie.ac.at	77
	Leitner Michael / Johannes Kepler University Linz michael.leitner_1@jku.at	

L	**Längle Manuel** / Physik Nanostrukturierter Materialien, Universität Wien manuel.laengle@univie.ac.at	**65**
	Löffler Stefan / USTEM, TU Wien stefan.loeffler@tuwien.ac.at	8,40,74
M	**Makat Andreas** / Ametek GmbH, Geschäftsbereich EMT (EDAX / Gatan) andreas.makat@ametek.com	
	Mangler Clemens / Physik Nanostrukturierter Materialien, Universität Wien / clemens.mangler@univie.ac.at	35,50,65, **66**,70
	Martínez Reyna Karí / Center for Surface and Nanoanalytics, JKU Linz kari.martinez_reyna@jku.at	**67**
	Minenkov Alexey / Center for Surface and Nanoanalytics, JKU Linz oleksii.minienkov@jku.at	67
	Minnich Bernd / Universität Salzburg bernd.minnich@plus.ac.at	**32**
N	**Nemeth Margit** / Johannes Kepler University Linz margit.nemeth@jku.at	
	Noisternig Stefan Manuel / Physik Nanostrukturierter Materialien, Universität Wien / stefan.noisternig@univie.ac.at	**48**,68
O	**Oberaigner Michael** / FELMI - TU Graz michael.oberaigner@felmi-zfe.at	69
P	**Pesenhofer Christian** / Fakultät für Physik, Physics of Nanostructured Materials, Universität Wien / a01612537@unet.univie.ac.at	65,**70**
	Phifer Daniel / Thermo Fisher Scientific daniel.phifer@thermofisher.com	**20**
	Planko Thomas / FELMI-ZFE thomas.planko@felmi-zfe.at	**71**
	Ploszczanski Leon / Inst. F. Physik u. Materialwissenschaften der Boku Wien / leon.ploszczanski@boku.ac.at	**18**
	Postl Andreas / University of Vienna andreas.postl@univie.ac.at	**42**
	Pum Dietmar / Universität für Bodenkultur Wien dietmar.pum@boku.ac.at	
R	**Ražnjev Sergej** / Erich Schmid Institute of Materials Science sergej.raznjevic@oeaw.ac.at	**73**
S	**Schachinger Thomas** / TU Wien, USTEM thomas.schachinger@tuwien.ac.at	43,**74**
	Schneller Matthias / University of Vienna matthias.schneller@univie.ac.at	56,75
	Schwalb Chris / Quantum Design Microscopy GmbH schwalb@qd-microscopy.com	36
	Seebauer Stefan / TU Wien, Siemens AG stefan.seebauer@student.tuwien.ac.at	**17**

	Singh Rajendra / University of Vienna rajendra.singh@univie.ac.at	**76**
	Smith Andrew Jonathan / Kleindiek Nanotechnik andrew.smith@kleindiek.com	**27**
	Stabentheiner Edith / Institut für Biologie, Universität Graz edith.stabentheiner@uni-graz.at	
	Steiger-Thirsfeld Andreas / TU Wien steiger@ustem.tuwien.ac.at	
	Steiner Philip / Institut für Pharmakologie, MED Fakultät, JKU Linz philip.steiner@jku.at	**10**
	Stöger-Pollach M. / Michael TU Wien stoeger@ustem.tuwien.ac.at	17,43
	Sunkara Sowmya / Medizinische Universität Graz sowmya.sunkara@medunigraz.at	**25**
	Susi Toma / Universität Wien toma.susi@univie.ac.at	**9**,42,66, 77
	Säckl Gary / Center for Surface and Nanoanalytics, JKU Linz gary.saeckl@jku.at	**78**
T	**Tollabimazraehno Sajjad** / Instrument Futurism tollaby@gmail.com	
W	**Weigner Thomas** / TU Wien, Atominstitut thomas.weigner@tuwien.ac.at	**79**
	Weis Serge / Kepler Universitätsklinikum serge.weis@kepleruniklinikum.at	
	Wojcik Tomasz / TU Wien tomasz.wojcik@tuwien.ac.at	
	Wolff Marion / Quantum Design Microscopy GmbH wolff@qd-microscopy.com	36
Z	**Zellnig Günther** / Institut für Biologie, Universität Graz guenther.zellnig@uni-graz.at	
	Zhang Zaoli / Erich Schmid Institute of Materials Science zaoli.zhang@oeaw.ac.at	16,24,52, 73
	Zheden Vanessa / Institute of Science and Technology Austria (ISTA) vanessa.zheden@ist.ac.at	
	Zierler Susanna / Institut für Pharmakologie, MED Fakultät, JKU Linz susanna.zierler@jku.at	10

YOUR NOTES

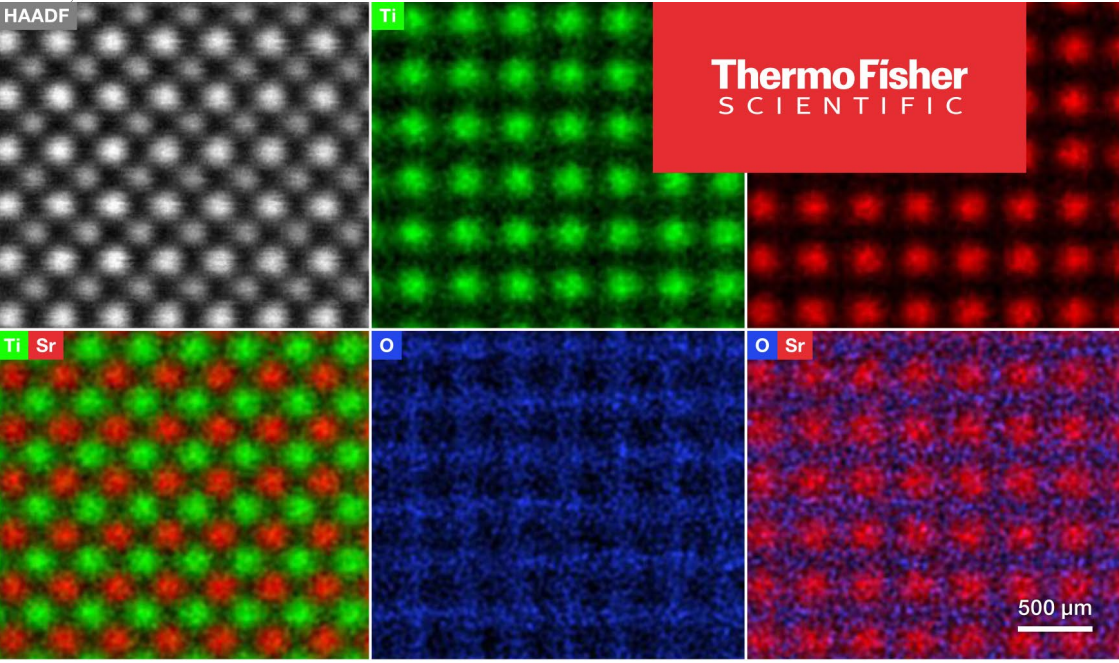

Best uncorrected EDS: Talos F200X G2 (S)TEM's X-Twin with X-CFEG.

Talos F200X G2 (S)TEM

Fast chemical analysis in multiple dimensions with ultimate EDS cleanliness

The Thermo Scientific™ Talos™ F200X G2 (S)TEM (scanning transmission electron microscope) delivers the most precise, quantitative characterization of nanomaterials in multiple dimensions.

With innovative features designed to increase throughput, precision, and ease of use, the Talos F200X G2 (S)TEM is ideal for advanced research and analysis across academic, government, and industrial research environments.

Learn more at **thermofisher.com/talos**

thermo scientific

CONFERENCE DINNER. Please, follow the indicated path to “Stiegl-Klosterhof”

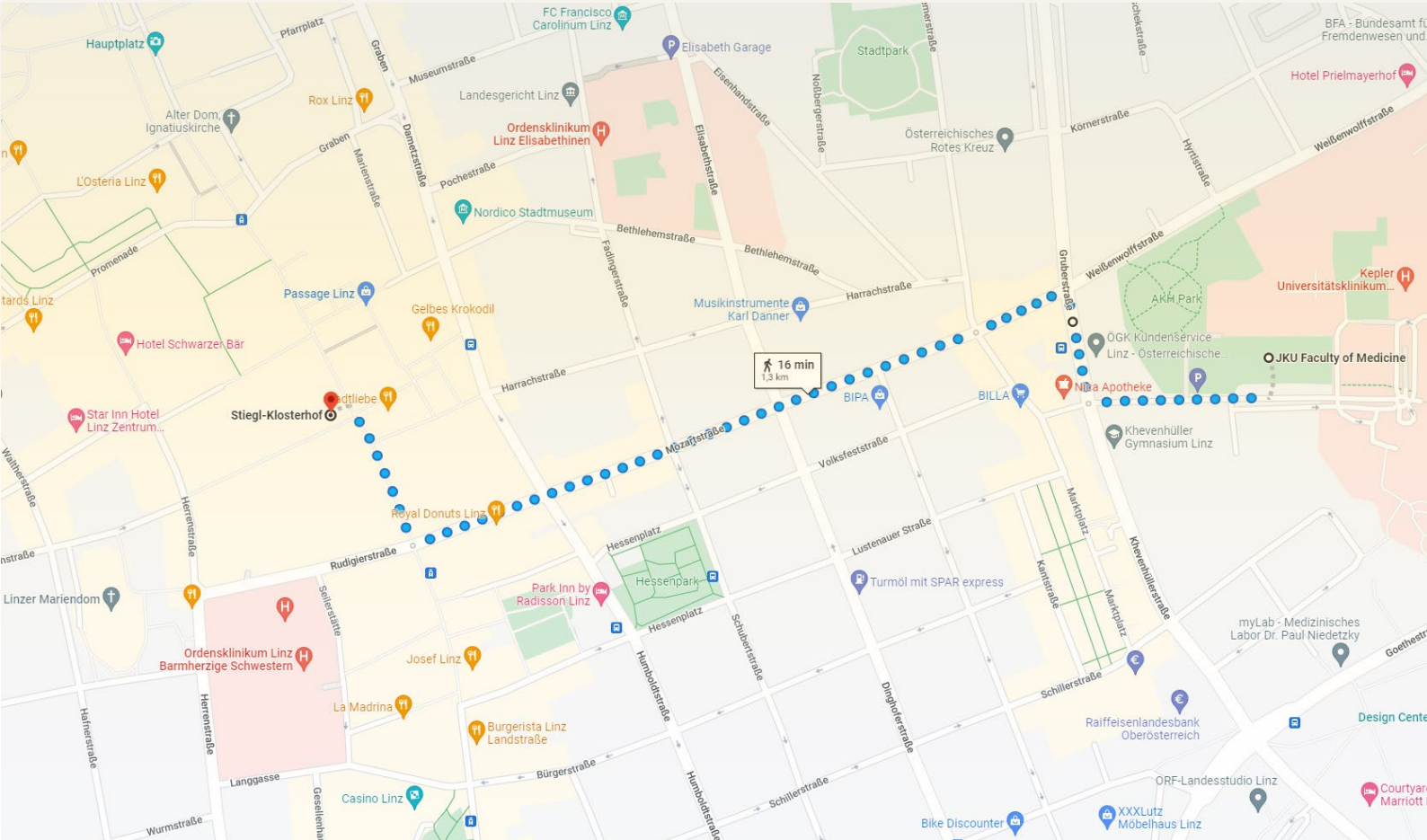

TESCAN

A unique combination of Plasma FIB and field-free UHR SEM for the widest range of multiscale materials characterization applications

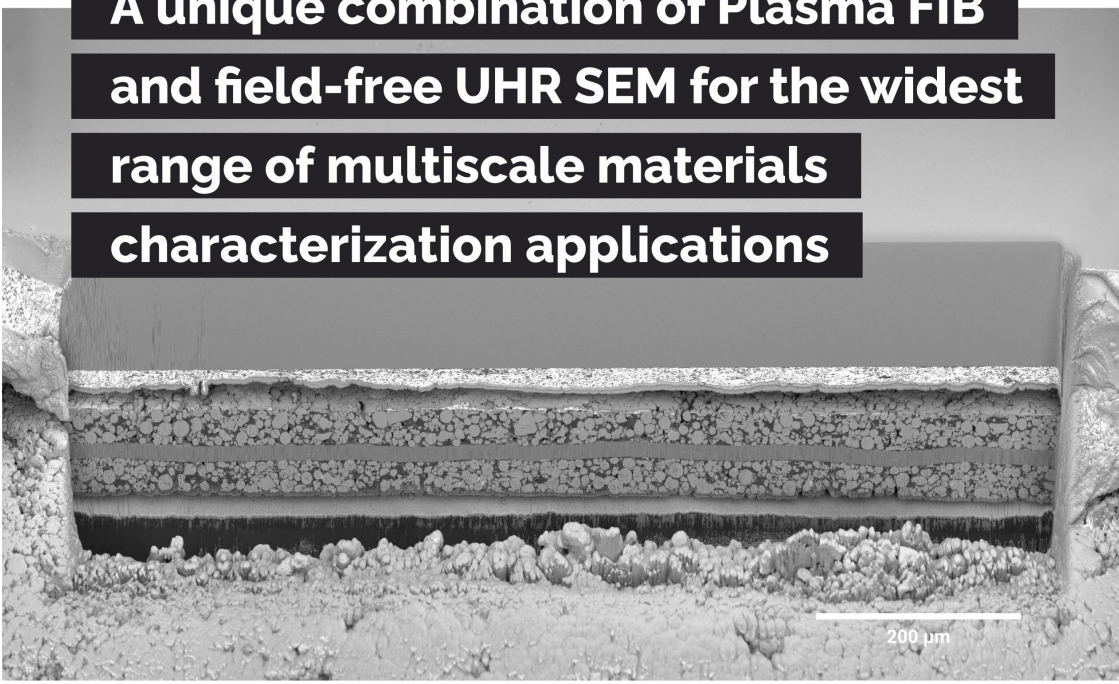

1 mm cross-section through a Li-ion battery electrode

TESCAN AMBER X

- ✓ High throughput, large area FIB milling up to 1 mm
- ✓ Ga-free microsample preparation
- ✓ Ultra-high resolution, field-free FE-SEM imaging and analysis
- ✓ In-column SE and BSE detection
- ✓ Spot optimization for high-throughput, multi-modal FIB-SEM tomography
- ✓ Superior field of view for easy navigation
- ✓ Essence™ easy-to-use, modular graphical user interface

For more information visit

www.tescan.com